Theoretical Investigation on Addition Reactions

For the Award of

Doctor of Philosophy

in

Chemistry

By

Sonali Sarkar

GUIDE

Dr. Anirban Misra

Department of Chemistry

University of North Bengal

May, 2014

Dedicated to My Parents

DECLARATION

I declare that the thesis entitled "Theoretical Investigation on Addition Reactions" has been prepared by me under the guidance of Dr. Anirban Misra, Associate Professor in the Department of Chemistry, University of North Bengal. No part of this thesis has formed the basis for the award of any degree or fellowship previously.

Sonali Sarkar

Sonali Sarkar

Department of Chemistry,
University of North Bengal,
Siliguri,
Dist. Darjeeling
PIN 734013
India

Date: 15.05.2014

CERTIFICATE

I certify that Sonali Sarkar has prepared the thesis entitled "Theoretical Investigation on Addition Reactions", for the award of PhD degree of the University of North Bengal, under my guidance. She has carried out the work at the Department of Chemistry, University of North Bengal.

Dr. Anirban Misra,
Associate Professor,
Department of Chemistry,
University of North Bengal,
Siliguri, Dist. Darjeeling
PIN 734013
India

Date: 15.5.2014

ABSTRACT

The first chapter is pervaded with a general introduction of this work based on the mechanistic study of addition reactions. The background of the present thesis is briefly described. This chapter also represents the different objectives of this thesis.

The second chapter is devoted to the theoretical background for the estimation of electronic energy and charge density and potential energy surface of different species involved in a reaction. Theoretical background for the prediction of reactivity of a molecule has also been discussed here.

In the third chapter we have investigated mechanistic pathways for four different electrophilic addition processes with benzene (monoprotonation, diprotonation, monomethylation and dimethylation) in DFT framework. In all the cases, transition states have been isolated and characterized through intrinsic reaction coordinate calculations. Fukui functions, local softness values, local charge densities, different electrophile affinities, thermochemical parameters have been calculated and correlated. Fukui functions and local softness values have been found to be reliable descriptors for kinetically controlled products; whereas, prediction of thermodynamically controlled products can be made through local charge density values. Electrophile affinities are found to be additive and correlate well with thermochemical parameters.

In the fourth chapter we have investigated the mechanism of an unexpected reaction between two molecules of 1, 3-dicarbonyl compound and one molecule of the aldehyde in presence of molecular iodine by density functional theory based approach. The geometries and the frequencies of reactants, intermediates and transition states are calculated using Becke three parameter exchange and Lee-Yang-Parr correlation functional. The vibrational analysis, intrinsic reaction coordinate (IRC) calculation and ESP analysis verify the authenticity of the transition states. Depending on substitution pattern of 1, 3-dicarbonyl compound, there may be two pathways, one leads to furan derivative and the other to cyclopropane derivative. The nucleus independent chemical shift (NICS) values have been calculated for the intermediates, products and the corresponding transition states to ensure the aromaticity contribution to the reaction pathway. The results are in good agreement with the experimental findings.

In the fifth chapter we have computed and investigated the performance of Minnesota density functionals especially the M05, M06 and M08 suite of complementary density

functionals for the prediction of the heat of formations (HOFs) and the ionisation potentials (IPs) of various benchmark complexes, which are formed by addition reactions between first row transition metals and different ligands. The eight functionals of M0X family, viz. the M05, M05-2X, M06-L, M06, M06-2X, M06-HF, M08-SO and M08-HX are taken for the computation of the above mentioned physical properties of such metal complexes along with popular Los Alamos National Laboratory 2 double-ζ (LANL2DZ) basis set. Total 54 benchmark systems are taken for HOF calculation, whereas the 47 systems among these benchmark complexes are chosen for the calculation of IPs due to lack of experimental results on rest of the 7 systems. The computed values of HOFs and IPs are compared with the experimental results obtained from the literature. The deviation of these computed values from the actual experimental results is calculated for each eight different M0X functionals to judge their performances in evaluating these properties. Finally, a clear relationship between the exchange correlation energy of eight M0X functionals and their efficiency are made to predict the different physical properties.

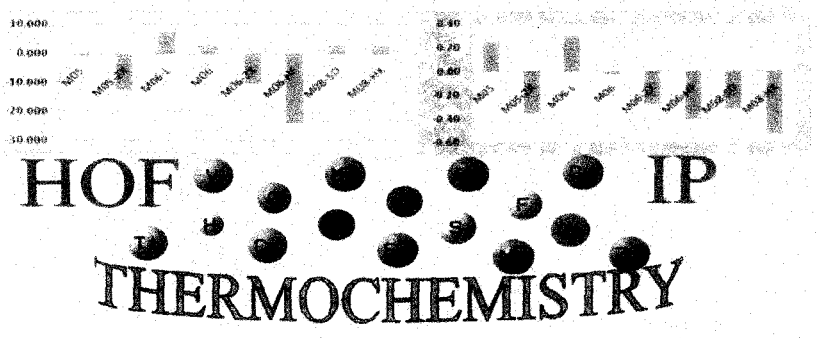

Figure 1. Thermochemistry with Minnesota Density Functionals.

In the sixth chapter, regio-controlled nitration of 4-quinolone, the highly privileged scaffold, has been investigated in density functional theory (DFT) based approach. Nitro group can selectively be introduced in diverse position simply by tuning the reactivity of the moiety. Discrimination is being achieved through the selective protection of free N-H group. The selection of protecting group is screened theoretically with the help of Fukui function and local softness calculations. Theoretical predictions are synchronized well with the experimental findings. Finally, this selective nitration allows the access of the structurally diverse 4-quinolones.

A comprehensive conclusion of this thesis is given at the last in chapter seven.

List of Publications

(1) **S. Sarkar**, S. Shil, S. Paul and A, Misra, On protonationa and methylation of benzene: a B3LYP DFT based study, *J. Mol. Struct. (THEOCHEM)* **916**, 154-158 (2009).

(2) S. Shil, D. Bhattacharya, **S. Sarkar** and A. Misra, Performance of the Widely Used Minnesota Density Functionals for the Prediction of Heat of Formations, Ionization Potentials of Some Benchmarked First Row Transition Metal Complexes, *J. Phys. Chem. A* 117, 4945-4955 (2013).

(3) **S. Sarkar**, S. Shil and A. Misra, DFT based study on the mechanism of an unexpected reaction of aldehydes with 1, 3-dicarbonyl compounds, *J. Ind. Chem. Soc.* (Accepted 2014).

(4) **S. Sarkar**, P. Ghosh, S. Das, Regio-controlled nitration of 4-quinolones: Convergence of theoretical and experimental findings (Communicated).

Table of Contents

Chapter 1

Addition reactions

A general introduction about the mechanistic aspects of various addition reactions is presented. A detailed survey of literature along with the objectives of this thesis is stated in this chapter.

1.1 Introduction

An accurate preview of the mechanistic pathway of any chemical reaction can be made possible through a deep insight into the chemical structures of the reactant, product, transition state and intermediate of that reaction. A precise knowledge of molecular structure can be obtained through quantum mechanical calculations. All such calculations are made possible through efficient computer programs and the credit of the development of such quantum computational packages goes initially to J. A. Pople. However chemical reactions take place at lightning speed. In a fraction of millisecond, electrons jump from one atom to another. It is virtually impossible to experimentally map every little step in a chemical process. Here comes the worth of theoretical study. Today the computer is an important device for chemists. A qualitative interpretation of any reaction mechanism can be bridged with an actual happening or experimental findings through a high-degree of accurate quantification of electronic structure parameters such as electronic energy, charge density, potential energy surface etc. Results of theoretical analysis is found complementary with the information obtained by chemical experiments in most of the cases, even it can in some cases predict hitherto unobserved chemical phenomena. Simulations are so realistic that they predict the outcome of traditional experiments. Even so it can be used to design synthetic pathways to new compounds.

1.2 Addition Reaction: Definition & Types

Among a variety of reactions, we choose to study the addition reactions. In an addition reaction two or more molecules combine to form a larger one. There are basically four ways by which addition reaction can take place and on that basis it can be categorized as (A) Electrophilic addition (B) Nucleophilic addition (C) Free radical addition (D) Concerted addition.

In electrophilic addition reaction first step involves the formation of an intermediate cation that arises from the reaction of a positively charged species or positively polarized reagent with a multiple bond and the second step is a combination of the resulting intermediate with a species carrying an electron pair and often bearing a negative charge. In nucleophilic addition reaction a

nucleophile brings its pair of electrons to one carbon atom of the double or triple bond, creating a carbanion in the first step and the second step is the combination of this carbanion with a positive species. Radical addition reactions involve the addition of a reactive species with an unpaired electron (radical or free radical) to a multiple bond to give an intermediate that also has an unpaired electron. Radical addition reactions are chain reactions. That feature makes them mechanistically unique from other addition reactions. In case of last one i.e., concerted addition reaction, the mechanism is somewhat different because here the addition of reagents to multiple bonds occur in a single step without ionic or radical intermediates. Representative examples of various addition reactions are given below:

(A) Electrophilic addition: Chlorination reaction

(B) Nucleophilic addition: Addition of Grignard reagent to carbonyl group

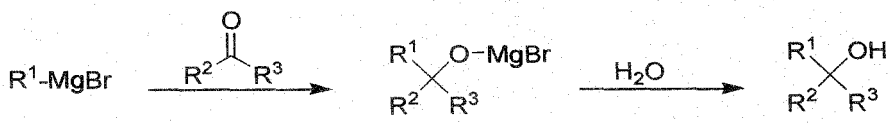

(C) Free radical addition: Paterno Buchi reaction

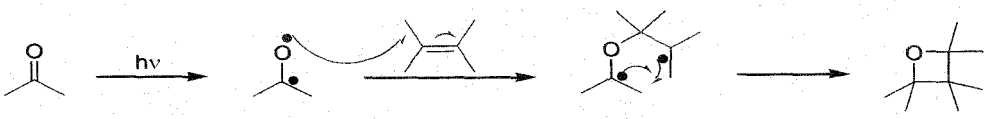

(D) Concerted addition: Diels-Alder reaction

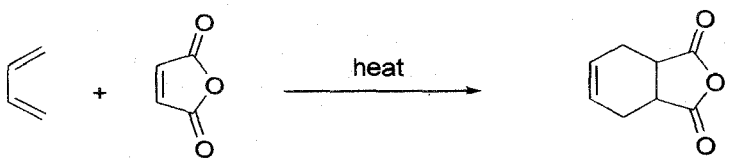

Figure 1.1: (A), (B), (C), (D) are the representative examples of addition reaction.

1.3 Background

Great deals of theoretical works in the investigation of the mechanistic aspects of various addition reactions are available in literature. Brief accounts of theoretical exertion are appended below.

1.3.1 Electrophilic Addition

Electrophilic addition across the olefinic double bond is a fundamental process in organic chemistry that has both theoretical value and far reaching synthetic applications. Oodles theoretical works have been performed on different electrophilic addition reactions.[1] Previously the mechanism of electrophilic addition of H^+, F^+, Cl^+, Br^+, ^+SR, ^+HgX, Ag^+ to ethylene was studied using extended Huckel molecular orbital calculations.[1a] The results correlate well with the experimental data and chemical intuition. Local hardness has been found to be a good selectivity descriptor for Markonikov addition to substituted alkenes.[1b] It is the only density functional descriptor which can predict the orientation of addition of hydrogen halides to mono substituted alkenes.

Control of regio- and stereo-chemistry, particularly in conformationally flexible acyclic systems, is of fundamental concern to rational synthesis design. Khan et.al.,[1c] have studied the regio- and stereo-chemistry of electrophilic attack on different allylic systems. They delineate the factors which control selectivity. The reactivity models have been found to provide a sensitive and unambiguous account of the preferred stereochemistry of electrophilic additions to double bonds. Assignment is based on direct evaluation of the relative affinities of diastereotopic olefin faces toward a test electrophile (H^+). From theoretical analysis it has been found that substitution of olefins with electron- releasing groups, e.g., methyl, not only enhances the overall activation toward electrophilic addition but also results in high regio- and stereo-selectivity. On contrary, electron-withdrawing substituents e.g., cyano deactivates the system and also reduces the selectivity.

The pyrimidine base, Cytosine (Cyt) is found both in DNA and RNA. In eukaryotic genomes, enzymatic methylation of cytosine results 5-methyl cytosine. Cytosine undergoes

protonation at one of the three plausible sites namely N3, O2 and N4 (Figure1.2) respectively. The mechanism for the effects of protonation and methylation of cytosine has been studied by Jin et.al, by means of CBS-QB3 and CBS-QB3/PCM methods.[1d]

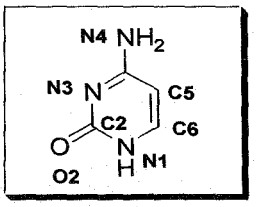

Figure 1.2 Structure of cytosine.

1.3.2 Nucleophilic Addition

Nucleophilic addition to carbonyl group is an elementary reaction in organic chemistry and biochemistry. Common examples include ester and amide hydrolysis, aldol condensation and numerous reactions of organometallic reagents and ylides. Plethora of theoretical investigations on various nucleophilic addition reactions are available in literature.[2] Among the earlier studies, important one is the exploration of the energy profiles for the nucleophilic addition of hydroxide ion to formaldehyde both in the in the gas and solution phase. The calculations were performed using ab initio method with the 6-31G* basis function and subsequently by Monte Carlo simulation.[2a] Later on, the effect of solvation was studied by integral equation theory.[2b]

Nitrile oxides are versatile reagents used in organic synthesis. These can undergo a series of reactions with nucleophilic agents as shown in (scheme 1.1).

Scheme 1.1

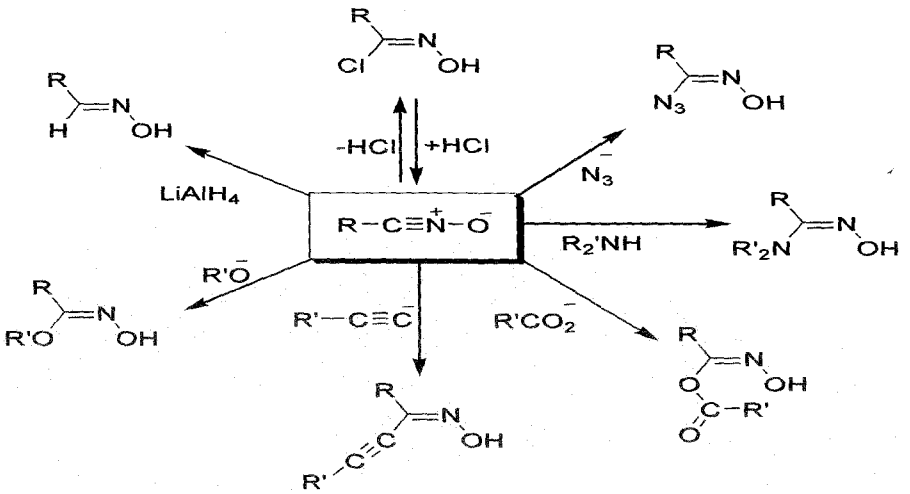

Nguyen et.al, made an attempt to rationalize the stereospecificity of addition of neutral nucleophiles to nitrile oxides using ab initio method.[2e] They used the simple model reactions of water with the formonitrile oxide (HCNO) and with acetonitrile oxide (CH_3NO). From simulations they concluded that the reactions are concerted but highly asynchronous in nature. Subsequent mechanistic studies on the addition reactions of fulminic acid (HCNO) to water, ammonia, and methanol (Scheme 1.2) also confirm the one step mechanism of these reactions.[2d]

Scheme 1.2

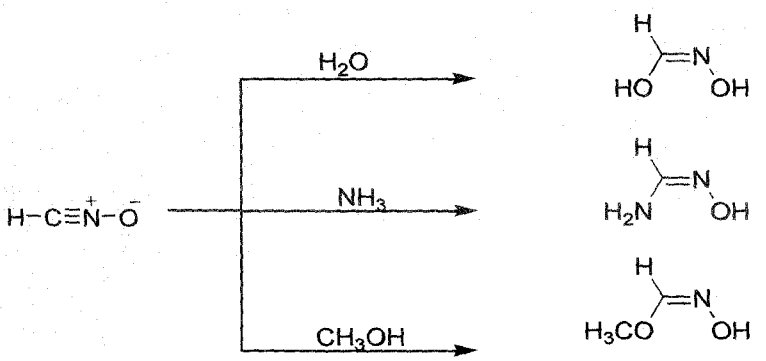

The mechanism of the intramolecular nucleophilic addition of N-alkylfurylacryl acetamide has been investigated in the DFT based approach.[2g] Three possible reaction channels have been considered based on the possible conformations of the reactant, which endures in three

stages hydrogen elimination, followed by the nucleophilic addition via an anti-Michael (Michael) mechanism and then proton transfer. The calculations show that the pathway corresponding to the reactant with the most stable conformation is the most favorable one and accordingly anti-Michael addition is more favorable than the Michael addition pathway (Scheme 1.3), considering the solvent effect.

Scheme 1.3

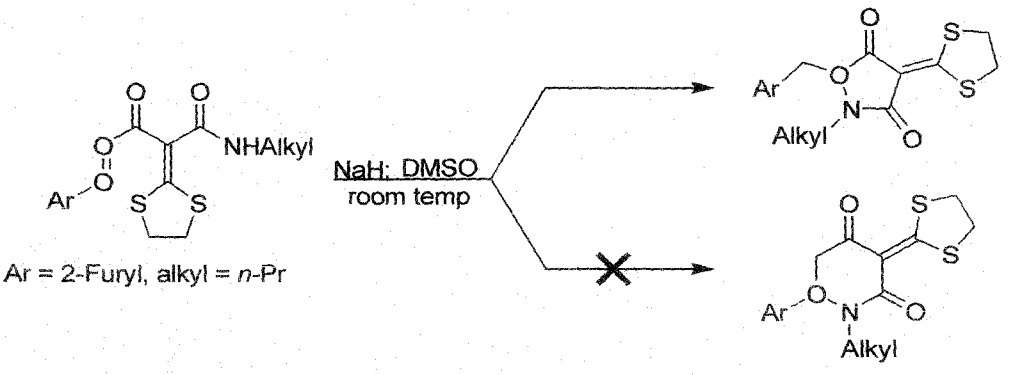

1.3.3 Radical Addition

The mechanism of radical addition to alkenes is a subject of great interest. In basic chemistry it represents a fundamental bond forming process and in applied chemistry it is interesting as many polymerization reactions go via radical mechanism. Carbon-centered radicals are nucleophilic or electrophilic species, depending upon the substituent at the radical center. Electron-donating substituents like alkyl or alkoxy groups increase the nucleophilicity whereas electron-withdrawing substituents like ester or nitrile groups swell their electrophilic behavior.[3,4] Investigations for a variety of cases have shown that nucleophilic radicals approach the olefinic carbon atoms at angles between 104° and 108 °. Geometry of transition states for the addition of the methyl radical to ethylene at the UHF/6-31G* level is shown in Figure 1.3.[5]

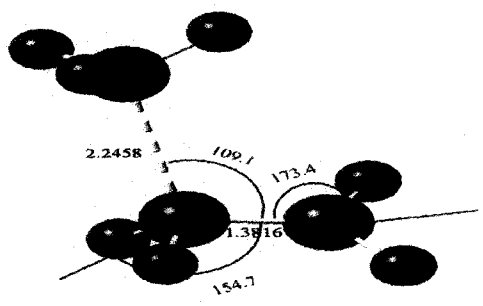

Figure 1.3 Geometry of transition state for the addition of the methyl radical to ethylene.

The rate of additions of radicals to alkenes is governed by a complex interplay of polar, enthalpy and steric effects.[6] However, establishing the relative importance of these factors in specific case is quite difficult.[7,8] Wong et.al., have performed theoretical investigation on the addition reactions of methyl radical with a series of substituted alkenes (Scheme 1.4).[9]

Scheme 1.4

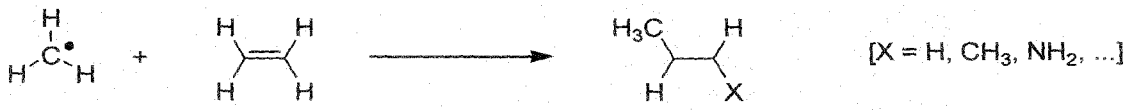

They reach the imperative conclusion that polar contributions to the reactivity of the methyl radical toward alkenes are insignificant and the reaction exothermicity is the foremost influencing factor. From the ab initio study (QCISD/6-311G*+ZPVE) on the addition of different radicals ($CH_3^{\cdot}$, $CH_2OH^{\cdot}$, $CH_2CN^{\cdot}$ and $(CH_3)_3C^{\cdot}$) to the substituted alkenes CH_2=CHX (X=H, NH_2, F, Cl, CHO, and CN) followed by curve crossing model analysis, it has been concluded that unlike the methyl radical, both polar and enthalpy effects are important for the latter three radicals.[10] The polar factor leads to tert-butyl radical displaying strong nucleophilic character which stabilizes the transition states by 20-25 KJ mol^{-1} compared with those for the relatively non polar reactions of methyl radical.

Natural emission of volatile organic compounds (VOCS) plays a major role in the atmospheric chemistry particularly in rural and remote areas. Vegetation is the most important source of these compounds. Terpenoids represent the most profuse VOCS emitted by plants.

Trans-geraniol (1), 6-methyl-5-hepten-2-one (2), and 6-hydroxy-4-methyl-4-hexenal (3) (Figure 1.4) are such worth mentioning terpenoids.

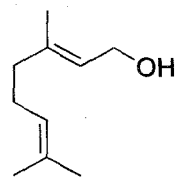

1
(*E*)-3,7-dimethylocta-2,6-dien-1-ol

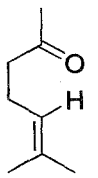

2
6-methylhept-5-en-2-one

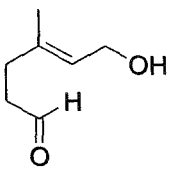

3
(*E*)-6-hydroxy-4-methylhex-4-enal

Figure 1.4 Structures of different terpenoids.

The primary degradation pathways of these terpenoids (1, 2 & 3) involve reaction with OH radicals, NO_3 radicals and ozone. A combined density functional and transition state theory approach has been employed to investigate the gas phase addition reaction of OH radical to trans geraniol (**1**), 6-methyl-5-hepten-2-one (**2**), and 6-hydroxy-4-methyl-4-hexenal (**3**).[11] All different possibilities for the addition of the OH radical to the C-C double bonds have been considered. The rate coefficients obtained from theoretical investigation are in good agreement with the available experimental data.

The addition reaction of alkyl radicals to multiple bonds is of fundamental importance as a carbon-carbon bond forming reaction. High level ab initio calculations have been performed for the addition of methyl radical to ethyne, propyne, ethane and propene.[12] These calculations confirm that these reactions are contra thermodynamic in nature, with addition to the alkenes being favored despite the alkyne addition having the greater exothermicity. It has been concluded that the greater barrier for addition to alkynes is primarily the result of larger singlet-triplet gap in the substrate. The barrier raising effect dominates the barrier lowering effect of the reaction exothermicity.

In recent years, epidemiological evidence has been reported which supports a protective effect of carotenoids in the development of chronic diseases, especially cardiovascular ones and in cancer. These diseases seem to have their origin in the oxidative damage of biological tissues

due to the action of free radicals. For this reason it has been suggested that antioxidant like β-carotene may play an important role in their prevention. A theoretical study of the reaction of β-carotene with nitrogen dioxide radical in solution was carried out using DFT method at the B3LYP/6-31G(D) level and polarizable continuum model (PCM) to account for the solvent effect.[13] Three feasible reaction mechanisms (Scheme 1.5) electron transfer, hydrogen abstraction and radical addition were considered. From these calculations it is apparent that in

Scheme 1.5

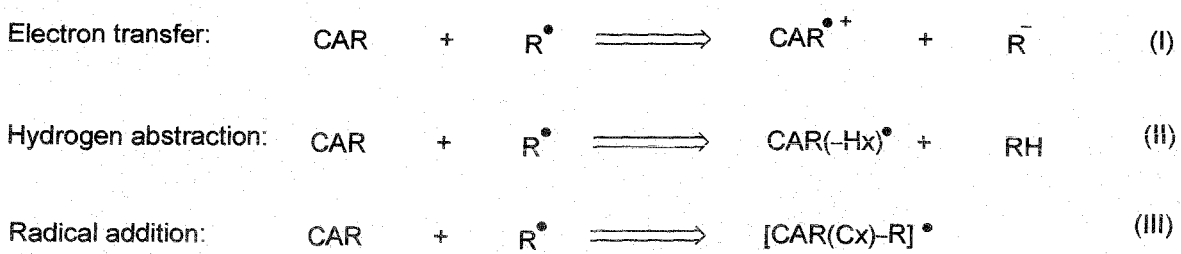

non polar solvents like heptanes, the reaction takes place simultaneously through hydrogen abstraction mechanism. This therefore supports on theoretical grounds the experimental observation of 4-nitro-β-carotene as an oxidation product of degradation of β-carotene by cigarette smoke in non polar environments.

1.3.4 Concerted Addition

Concerted addition is a class of chemical reaction where all bond breaking and bond making processes occur in a single step without any radical or ionic intermediate. Cycloaddition, a variety of pericyclic reaction is an important example of concerted addition. It is an excellent technique for the carbon-carbon bond forming process in synthetic organic chemistry. The reaction proceeds through cyclic transition state. The energy necessary to attain the transition state is usually provided externally either thermal or photochemical activation of the reactants. Theoretical explorations of these reactions are avowed categorically as follows:

1.3.4.1 (4+2) Cycloaddition

The Diels-Alder reaction remains one of the most useful approaches to cyclic organic compounds in terms of regio control and simplicity. Furthermore, the introduction of hetero atoms in the dienophile or diene or in both of them presents a powerful tool for the preparation of a wide variety of heterocyclic compounds. Extensive theoretical investigations have been performed on Diels-Alder reaction.[14] Ab initio calculations for the Diels-Alder reaction between 2-phenylcyclopentadiene and α-(methylthio)acrylonitrile (Scheme 1.6), show the existence of four transition structures on the potential energy surface corresponding to the formation of para/endo, para/exo, meta/endo and meta/exo adducts.[14d] The formation of the para adducts takes place with smaller energy barriers than the formation of the meta products. However the theoretical prediction correlates well with the observed experimental data.

Scheme 1.6

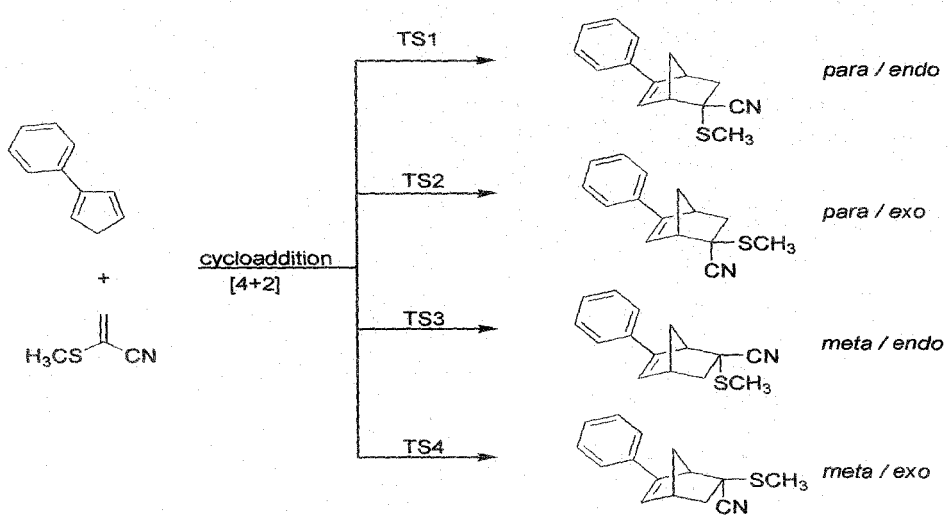

The Diels-Alder reaction of cyclopentadiene and acrolein in a model room temperature ionic liquid ([mmim][PF_6]) has been investigated with the help of KS-DFT/3D-RISM-KH theory.[14c] It has been calculated that the ionic liquid can distort noticeably the transition state geometry, inverting the order of frontier orbitals and leading to an enhancement of the asynchronicity of the reaction. This method of calculation has been found to be able to reproduce the experimental features, concerning the reaction rate and endo selectivity enhancement in ionic

liquids. The rate acceleration is attributed to the free energy of solvation, which promotes aggregation of non ionic molecules in solutions. On the other hand, the endo selectivity enhancement is ascribed to the most favourable $\pi-\pi$ interaction between the reactants in presence of ionic liquid.

1.3.4.2 (3+2) Cycloaddition

The cycloaddition of a 1, 3-dipolar species with dienophile for the synthesis of five membered rings is a classic reaction in organic chemistry. 1,3-dipolar cycloadditon (DC) is an important technique for the construction of five membered ring. This protocol is often used for the easy accesses of five membered heterocyclic compounds, complex natural products and bioactive molecules. Wide-ranging theoretical exertions have been performed on 1, 3-DC reactions. [15]

1, 3-DC reaction between trifluoromethyl thiomethyl azomethine ylide and acronitrile (Scheme 1.7) has been studied theoretically to explore the actual mechanistic pathway in DFT based approach.[15a] Relative rates, regioselectivity and endo stereoselectivity have been analyzed and discussed as a function of the substituents on dipole and dipolarophile fragments. Theoretical analysis shows that these reactions are single step processes having dissymmetric transition structures. Transition state energies are in full agreement with the stereochemical outcome.

Scheme 1.7

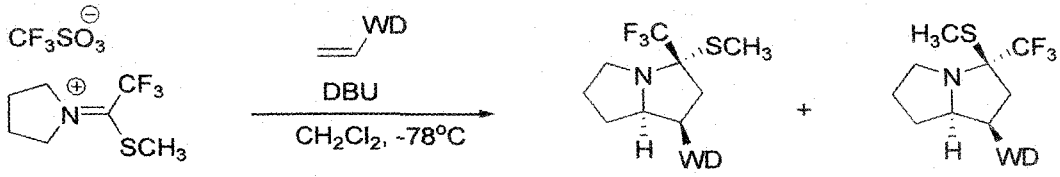

WD = -CN	96 : 4
$-CO_2CH_3$	95 : 5

DFT based study on the mechanism of electrophilically activated nitrile N-oxides with C-C double bonds show the existence of two competitive pathways (Scheme 1.8), one leading to

(3+2) cyclo-adducts and another to two isomeric (E)- and (Z)-oximes.[15c] The 1,3-dipolar cycloadditions take place through a concerted but highly asynchronous transition state, while the formation of the oximes is achieved through stepwise manner with the formation of zwitterionic intermediate. Both the 1, 3-DC reaction and oxime formation have effect through the nucleophilic attack of electron affluent C-C double bond of the dipolarophile to the electrophilically activated nitrile N-oxides. The electrophilicy index has been found to be an important tool in predicting the polar nature of the reactions.

Scheme 1.8

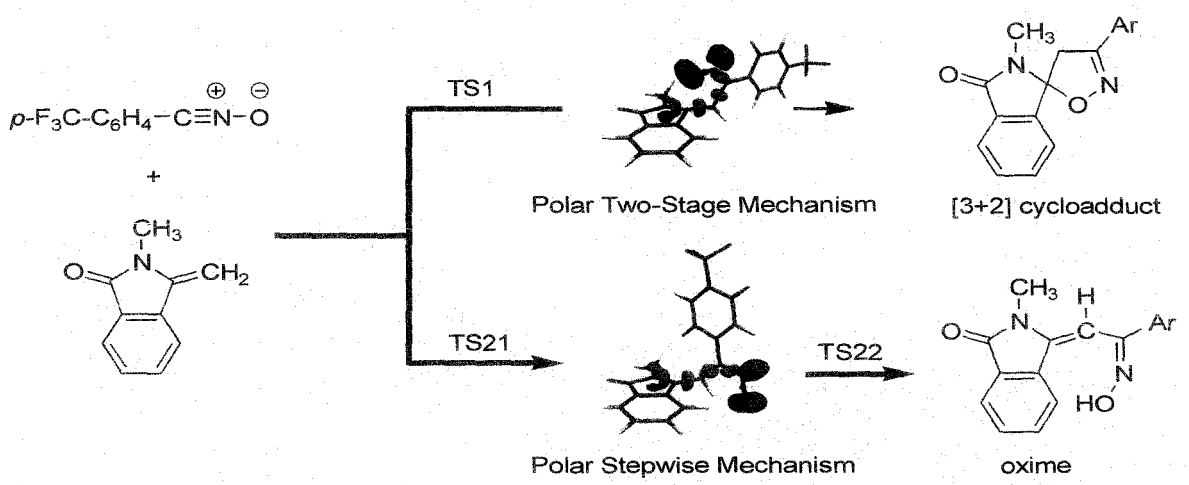

1.3.4.3 (2+2) Cycloaddition

The cycloaddition reaction between ketenes and olefins leading to cyclobutanones (Scheme 1.9) has been studied by means of both the semiemperical and ab initio methodologies.[16] The reaction is found to be concerted in all but in few cases, it takes place through twisted transition states with small charge transfer from the olefin to the ketene. Theoretical analysis shows that the reaction is of the 2+2+2 type rather than $[\pi 2_s + \pi 2_a]$ one. Effects of both ketene and olefin substituents on the energetic, regioselective and stereoselective aspects of the reaction have been studied thoroughly.

Scheme 1.9

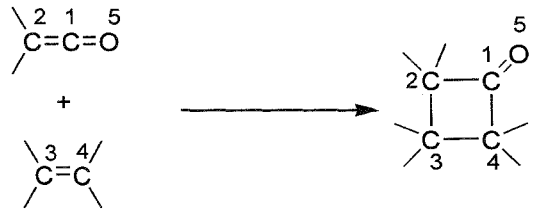

1.3.4.4 (1+2) Cycloaddition

Carbenes are mechanistically important as well as synthetically useful intermediates. They react with olefins to form cyclopropane. Theoretical analysis of the mechanistic aspects of (1+2) cycloaddition reactions have been performed in ab initio methodology.[17] The reaction between singlet and triplet methylene with benzene and related aromatic compounds has been investigated by kinetic isotope effects, solvent effects and product studies.[17c] Mechanistic study shows the existence of two distinct reaction pathways for the singlet and the triplet species. For the triplet reaction the proposed intermediate (Figure 1.5) has been detected by ab initio UMP2/6-31G*//UHF/6-31G* calculations, however no stable singlet intermediate has been found. These surveillances are consistent with other carbene addition reactions.

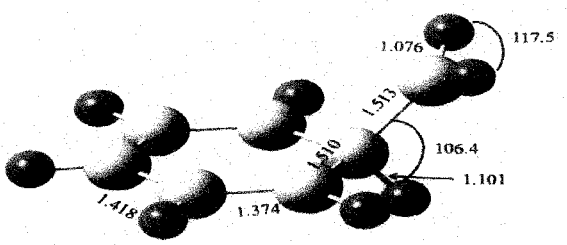

Figure 1.5 Intermediate calculated for the triplet reaction.

Careful investigation on the reaction pathway and transition state geometries of unsaturated carbene-olefin reactions [addition of unsymmetrical alkylidenecarbenes $R(CH_3)C{=}C{:}$, where R=Et, i-pr, t-Bu, to two unsymmetrical olefins, isobutylene and tert-butylethylene] reveals an interesting fact that in all cases, E adduct predominates over the Z

adduct, with increasing stereo-selectivity being observed upon going from R=Et to R=t-Bu in the carbene.[17b]

1.4 Objectives of the Thesis

Theoretical calculations are very helpful tools in understanding the chemistry of reactions. Careful use of computer modeling can help in predicting or optimizing various physical and chemical parameters which determine reaction conditions. Simulations are not a replacement for conventional experiments but it can be used to prop up the experimental results. However the most important role of computer simulations is their use as a predictive tool in a chemical reaction. The ability to predict the outcome of a reaction provides large savings in time and economy. Keeping these factors in mind, the present thesis is aimed to cultivate the objectives, which are affirmed as follows:

(1) We investigate the mechanistic pathway of diprotonation and dimethylation of benzene and predict the stability of the possible isomers (Chapter 3 On Protonation and Methylation of Benzene: A B3LYP DFT Based Study).

(2) We also investigate the mechanistic pathway of an unexpected reaction and correlate the results well with the reported experimental findings (Chapter 4 DFT Based Study on the Mechanism of an Unexpected Reaction of Aldehydes with 1, 3- Dicarbonyl Compounds).

(3) We explore the accuracy and reliability of different Minnesota density functionals for the prediction of heat of formations and ionization potential values of various benchmarked transition metal complexes formed by addition reaction (Chapter 5 Performance of the widely used Minnesota density functionals for the prediction of heat of formations, ionization potentials of some benchmarked first row transition metal complexes).

(4) We investigate the regioselective addition of nitronium ion to 4-quinolones using DFT based reactivity descriptors and validate the results by experimental surveillance (Chapter 6 Regio-

selective/Regio-controlled nitration of 4-quinolones: Convergence of theoretical and experimental findings).

1.1 References and notes

1. (a) Bach, D. B.; Henneike, H. F. *J. Am. Chem. Soc.* **1970**, *92*, 5589. (b) Meneses, L.; Araya, A.; Pilaquinga, F.; Espin, M.; Carrillo, P.; Sanchez, F. Int. J. Quantum Chem. **2010**, *110*, 2360. (c) Khan, S. D.; Pau, C. F.; chamberlin, A. R.; Hehre, W. J. *J. Am. Chem. Soc.* **1987**, *109*, 650. (d) Jin, L.; Wang, W., Hu, D., Min, S. *J. Phys. Chem. B* **2013**, *117*, 3. (e) Clavero, C.; Duran, M.; Liedos, A.; Ventura, O. N.; Bertran, J. *J. Am. Chem. Soc.* **1986**, *108*, 923. (f) Veszpremi, T.; Takahashi, M.; Hajgato, B.; Kira, M. *J. Am. Chem. Soc.* **2001**, *123*, 6629.
2. (a) Madura, J. D.; Jorgensen, W. L. *J. Am. Chem. Soc.* **1986**, *108*, 2517. (b) Yu, H. A.; Karplus, M. J. Am. Chem. Soc. 1990, *112*, 5706. (c) Williams, I. H.; Maggiora, G. M.; Schowen, R. L. *J. Am. Chem. Soc.* **1980**, *102*, 7831. (d) Nguyen, M. T.; Malone, S.; Hegarty, A. F.; Williams, I. I. *J. Org. Chem.* **2001**, *123*, 3683. (e) Nguyen, M. T.; Sana, M.; Leroy, G.; Dignam, K. J.; Hegarty, A. F. *J. Am. Chem. Soc.* **1980**, *102*, 573. (f) Sharma, K. K.; Aggarwal, A. K. *Int. J. Quantum Chem.* **1986**, *30*, 213. (g) Yuan, H.; Zheng, Y.; Zhang, J. *J. Org. Chem.* **2012**, *77*, 8744-8749.
3. (a) Citterio, A.; Minisci, F.; Porta, 0.; Sesana, G. J. Am. Chem. Soc. **1977**, *99*, 7960. (b) Giese, B. Angew. Chem. **1983**, *95*, 771. (c) Giese, B. Angew. Chem.; Int. Ed. Engl, **1983**, *22*, 753.
4. (a) Riemenschneider, K.; Bartels, H. M.; Dornow, R.; Drechsel-Grau, E.; Eichel, W.; Luthe, H.; Matter, Y. M.; Michaelis, W.; Boldt, P. J. Org. Chem. **1987**, *52*, 205. (b) Gleicher, G. J.; Mahiou, B.; Aretakis, A. J. *J. Org. Chem.* **1989**, 54, 308. (c) Giese, B.; He, J.; Mehl, W. Chem. Ber. **1988**, *121*, 2063.
5. Gonzalez, C.; Sosa, C.; Schlegel, H. B. J. Phys. Chem. **1989**, *93*, 2435.
6. (a) Giese, B. *Angew. Chem., Int. Ed. Engl.* **1983**, *22*, 753. (b) Tedder, J. M. *Angew. Chem., Int. Ed. Engl.* **1982**, *21*, 401. (c) Tedder, J. M.; Walton, J. C. *Adv. Free Radical Chem.* **1980**, *6*, 155. (d) Heberger, K.; Fischer, H. *Int. J. Chem. Kinet.* **1993**, *25*, 249.

7. (a) Munger, K., Fischer, H. *Int. J. Chem. Kinet.* **1985**, *17,* 809. (b) Beranek, I.; Fischer, H. *Free Radicals in Synthesis and Biology;* Minisci, F., Ed.; Kluwer: Dordrecht, **1989**. (c) Fischer, H. *Free Radicals in Synthesis and Biology;* Viehe, H. G., Janousek, Z., Merenyi, R., Eds.; Reidel: Dordrecht, **1986**. (d) Heberger, K.; Walbiner, M.; Fischer, H. *Angew. Chem., Int. Ed. Engl.* **1992**, *31*, 635. (e) Fischer, H.; Paul, H. *Acc. Chem. Res.* **1987**, *20*, 200. (f) Avila, D. V.; Ingold, K. U.; Lusztyk, J.; Dolbier, W. R.; Pan, H.-Q. *J. Am. Chem. Soc.* **1993**, *115,* 1577. (g) Citterio, A.; Sebastiano, R.; Marion, A.; Santi, R. *J. Org. Chem.* **1991**, *56*, 5328. (h) Riemenschneider, K.; Bartels, H. M.; Domow, R.; Drechsel-Grau, E.; Eichel, W.; Luthe, H.; Matter, Y. M.; Michaelis, W.; Boldt, P. *J. Org. Chem.* **1987**, *52, 205.* (i) Baban, J. A.; Roberts, B. P. *J. Chem. SOC., Perkin Trans. II* **1981**, 161.

8. (a) Zipse, H.; He, J.; Houk, K. N.; Giese, B. *J. Am. Chem.* Soc. **1991**, *113*, 4324. (b) Houk, K. N.; Paddon-Row, M. N.; Spellmeyer, D. C.; Rondan, N. G.; Nagase. S. *J. Org. Chem.* **1986**, *51*, 2874. (c) Fueno, T.; Kamachi, M. *Macromolecules* **1988**, *21,* 908. (d) Gonzales, C.; Sosa, C.; Schlegel, H. B. *J. Phys. Chem.* **1989**, *93*, 2435. (e) Amaud, R.; Vidal, S. *New J. Chem.* **1992**, *16,* 471. (f) Tozer, D. J.; Andrews, J. S.; Amos, R. D.; Handy, N. C. *Chem. Phys. Lett.* **1992**, *199,* 229. (g) Amaud, R.; Subra, R.; Barone, V.; Lelj, F.; Olivella, S.; Sole, A.; Russo, N. *J. Chem.* Soc., *Perkin Trans. II* **1986**, 1517. (h) Clark, T. *J. Chem. SOC., Chem. Commun.* **1986**, 1774. (i) Amaud, R. ***New.*** *J. Chem.* 1989, 13, 543. (i) Wong, M. W.; Pross, A.; Radom, L. *J. Am. Chem. Soc.* **1993**, *115,* 11050. (j) Wong, M. W.; Pross, A.; Radom, L. *Isr. J. Chem.* **1993**, *33*,415. (k) Wong, M. W.; Pross, A.; Radom, L. *J. Am. Chem. SOC.* **1994**, *116,* 6284.

9. Wong, M. W.; Pross, A.; Radom, L. *J. Am. Chem. Soc.* **1993**, *115*, 11050.

10. (a) Wong, M. W.; Pross, A.; Radom, L. *J. Am. Chem. Soc.* **1994**, *116*, 6284. (b) Wong, M. W.; Pross, A.; Radom, L. *J. Am. Chem. Soc.* **1994**, *116*, 11938.

11. Leonardo, T.; Baptista, L.; Silva, E. C.; Arbilla, G. *J. Phys. Chem. A* **2010**, *114*, 5468.

12. Gomez-Balderas, R.; Coote, M. L.; Henry, D. J.; Fischer, H.; Radom, L. *J. Phys. Chem. A* **2003**, *107*, 6082.

13. Ceron-Carrasco, J. P.; Bastida, A.; Requena, A.; Zuniga, J.; Miguel, B. *J. Phys. Chem. B,* **2010**, *114*, 4366.

14. (a) Bernardi, F.; Bottoni, A.; Field, M. J.; Guest, M. F.; Hillier, I. H.; Robb, M. A.; Venturini, A. *J. Am. Chem. Soc.* **1988**, *110*, 3050. (b) Bauld, N. L. *J. Am. Chem. Soc.*

1992, *114*, 5800. (c) Chiappe, C.; Malvaldi, M.; Pomeli, C. S. *J. Chem. Theory Comput.* **2010**, *6*, 179. (d) Domingo, L. R.; Picher, M. T.; Andres, J.; Safont, V. S. *J. Org. Chem.* **1997**, *62*, 1775. (e) Jursic, B. S.; Zdravkovski, Z. *J. Org. Chem.* **1994**, *59*, 7732. (f) Jursic, B. S. *J. Org. Chem.* **1997**, *62*, 3046. (f) Zhang, X.; Du, H.; Wang, Z.; Wu, Y-D.; Ding, K. J. Org. Chem. **2006**, *71*, 2862. (g) Regas, D.; Ruiz, J. M.; Afonso, M. M.; Palenzuela, J. A. *J. Org. Chem.* **2006**, *71*, 9153. (h) Silva, M. A.; Pellegrinet, S. C.; Goodman, J. M. *J. Org. Chem.* **2002**, *67*, 8203. (i) Pi, Z.; Li, Shuhua. *J. Phys. Chem. A* **2006**, *110*, 9225.

15. (a) Domingo, L. R. J. Org. *Chem.* **1999**, *64*, 3922. (b) Carda, M.; Portoles, R.; Murga, J.; Uriel, S.; Marco, J. A.; Domingo, L. R.; Zaragoza, R. J.; Roper, H. *J. Org. Chem.* **2000**, *65*, 7000. (c) Domingo, L. R.; Picher, M. T.; Arroyo, P.; Saez, J. A. J. Org. *Chem.* **2006**, *71*, 9319. (d) Mandez, F.; Tamariz, J.; Geerlings, P. J. Phys. Chem. A 1998, 102, 6292.
16. (a) Valenti, E.; Pericas, M. A.; Moyano, A. *J. Org. Chem.* **1990**, *55*, 3582. (b) Wang, X.; Houk, K. N. *J. Am. Chem. Soc.***1990**, *112*, 1754.
17. (a) Zurawski, B.; Kutzelnigg, W. *J. Am. Chem. Soc.* **1978**, *100*, 2654. (b) Apeloig, Y.; Karni, M.; Stang, P. J.; Fox, D. P. *J. Am. Chem. Soc.* **1983**, *105*, 4781. (c) Hartz, N.; Surya Prakash, G. K.; Olah, G. A. *J. Am. Chem. Soc.* **1993**, *115*, 901.

Chapter 2

Theoretical Insight

The theoretical background for the quantification of electronic energy, charge density has been discussed. Theoretical settings for the calculation of potential energy surface of a reaction and prediction of reactivity of a molecule have been conferred here.

2.1 Introduction

The theoretical foundation for modern chemistry was laid more than 80 years ago. Today it becomes possible to use this knowledge for understanding how electrons, molecules and atoms interact. A reaction mechanism is the step by step sequence of elementary reactions by which overall chemical change occurs. The study of reaction mechanisms is important for many reasons including the understanding and controlling chemical reactions. It is the theoretical analysis which makes possible to study each step of a reaction by exact computation of electronic structure parameters such as electronic energy, charge density and potential energy surface (PES). Theory plays an important role in the development of chemical concepts. An example is the idea of a transition state for a reaction. Molecular modeling is simply an art of representing molecular structures numerically and simulating their behavior with the equations of quantum and classical physics. The density functional theory (DFT) has strongly influenced the evolution of quantum chemistry. For its development, Prof. Walter Kohn was awarded the Nobel Prize in 1998. It is presently the most successful and also the most promising approach to compute the electronic structure of matter. Its applicability ranges from atoms, molecules and solids to nuclei and quantum, classical fluids.

This chapter gives a brief introduction to density functional theory along with a special deliberation to Conceptual density functional theory. Theoretical condition for the calculation of transition state has also been conferred using Born-Opponheimer approximation.

2.2 Overview on Hartrre-Fock and Post-Hartree-Fock Methods

Before going deep into DFT it will be useful to pay a little endeavor in discussing about the wave function based methods. The fundamental equation of quantum mechanics which describes any given chemical system is the Schrödinger equation. To get a physical property of a system from Schrödinger equation we have to solve it. In 1920 Hartree and Fock gave a solution for the Schrödinger equation of many electron system based on variational principle. They assumed that the exact N-body wave function of the system can be approximated by single Slater determinant of N spin orbitals. One can get Hartree-Fock (HF) wave function and energy of the

system by solving N-coupled equations for N spin orbitals using variational principle. The main short coming of the HF method is that it assumes the electrons are moving independently; i.e. they have no correlation. That is the main reason for poor performance of HF method. Taking HF as the starting point, several post-HF methods such as configuration interaction or coupled cluster methods are introduced. These post-HF methods provide eminent ways of recovering the correlation missing from HF method. Although, Post-HF methods are more accurate, they are not so popular due to their resource intensive nature.[1]

2.3 Density Functional Theory

Density functional theory (DFT) has allowed studying the physical properties and reaction energetics of compounds containing up to 100 or more heavy atoms. DFT provided a sound basis for the development of computational strategies for obtaining information about the energetic, structure, and properties of atoms and molecules at much lower computational cost than commonly used ab initio methods like Hartree-Fock. This makes DFT quite popular for calculating organic molecules. Computational efficiency and accuracy are the main benefits of DFT approaches. It is a powerful methodology for chemical simulation where the energy of the systems can be defined in terms of its electron probability density (ρ), that is, in DFT formalism the electronic energy E is treated as the functional of the electron density E (ρ). Modern DFT based on two basic theorems proposed by Hohenberg and Kohn in 1964.[2] These are as follows:

Theorem I

For any system of interacting particles in an external potential $v_{ext}(r)$, the density is uniquely determined (in other words, the external potential is a unique functional of the density).

Theorem II

A universal functional for the energy E [ρ] can be defined in terms of the density. The exact ground state is the global minimum value of this functional.

2.4 The Energy Functional

The energy functional contains three terms – the kinetic energy, the interaction with the external potential and the electron-electron interaction and can be written in the following form

$$E[\rho] = T[\rho] + V_{ext}[\rho] + V_{ee}[\rho]. \tag{2.1}$$

The interaction with the external potential is expressed as

$$V_{ext}[\rho] = \int \hat{V}_{ext}\, \rho(r) dr. \tag{2.2}$$

The kinetic and electron-electron functionals are unknown and they have a common form for every system. Direct minimization of the energy would be possible if good approximations to these functionals could be found.

These kinetic and electron-electron functional can be approximated by a popular approach due to Kohn and Sham.[3] The Kohn-Sham system is composed of N non-interacting, thus fictitious, electrons which can be described by a single determinantal wave function in N "orbitals" ϕ_i . In this system the kinetic energy and electron density are known exactly from the orbitals;

$$T_s[\rho] = -\frac{1}{2}\sum_{i}^{N}\langle\phi_i|\nabla^2|\phi_i\rangle \tag{2.3}$$

Here the suffix emphasizes that this is not the true kinetic energy but is that of a system of non-interacting electrons, which reproduce the true ground state density

$$\rho(r) = \sum_{i}^{N}|\phi_i|^2 \tag{2.4}$$

The acceptance of the methodology emerges from the construction of the density explicitly from a set of orbitals. This ensures that it can be constructed from any asymmetric wave function. The electron – electron interaction term in the energy functional is distinctly composed of the classical Coulomb interaction, which is known as the Hartree energy. This can be written in terms on density as

$$V_H[\rho] = \frac{1}{2}\int \frac{\rho(r_1)\rho(r_2)}{|r_1 - r_2|} dr_1 dr_2 . \tag{2.5}$$

Here we introduce *exchange – correlation functional*

$$E_{xc}[\rho] = (T[\rho] - T_s[\rho]) + (V_{ee}[\rho] - V_H[\rho]). \tag{2.6}$$

E_{XC} is simply the sum of the error made in using a non – interacting kinetic energy and the error made in treating the electron – electron interaction classically.
Now, the expression for the energy functional can be written as

$$E[\rho] = T_s[\rho] + V_{ext}[\rho] + V_H[\rho] + E_{xc}[\rho] \tag{2.7}$$

The non-interacting orbitals, from which the density was built in equation *2.7*, satisfy the following set of equations

$$\left[-\frac{1}{2}\nabla^2 + v_{ext}(r) + \int \frac{\rho(r')}{|r - r'|} dr' + v_{xc}(r)\right]\phi_i(r) = \varepsilon_i \phi_i(r). \tag{2.8}$$

Here we have introduced a local potential which is the functional derivative of the exchange correlation energy with respect to the density,

$$v_{xc}(r) = \frac{\delta E_{xc}[\rho]}{\delta \rho} . \tag{2.9}$$

This set of non-linear equations (the Kohn-Sham equations) describes the behavior of non-interacting "electrons" in an effective local potential. For an exact local potential, the "orbitals" yield the exact ground state density via equation *2.4* and exact ground state energy via equation *2.6*.

2.5 Born-Oppenheimer approximation, potential energy surface and transition state

The Schrodinger equation treats electrons and nuclei in the same way but in the Born-Oppenheimer approximation we make a compromise between classical and quantum mechanics. At this circumstance, we fairly accurate the nuclei (which are about 1000 times heavier than the electrons) as stationary classical point like particles. Thus, instead of solving the Schrodinger equation for a system of mobile electrons and nuclei, one solves the equation for the electronic motion for different fixed nuclear positions or conformations.

The Schrodinger equation for a molecule is given by

$$\hat{H}\psi(r,R) = (\hat{T}_e + \hat{T}_n + V_{en} + V_{ee} + V_{nn})\,\psi(r,R) = E\psi(r,R) \tag{2.10}$$

Since the electronic and the nuclear motions are assumed to be separable we can write

$$\psi(r,R) = \psi_R(r)\varphi(R) \tag{2.11}$$

where $\psi_R(r)$ implies that the electronic wave function depends functionally on r and parametrically on R. For simplicity we shall write ψ_e for $\psi_R(r)$ and ψ_n for $\varphi(R)$. Let us define ψ_e as a function which satisfies the electronic Schrodinger equation,

$$\widehat{H_e}\psi_e = (\,\widehat{T_e} + V_{en} + V_{e\,e}\,) = E_e\psi_e \tag{2.12}$$

Substituting $\psi(r,R) = \psi_e\psi_n$ in equation 2.10 and writing the expressions for $\hat{T}_e$ and $\hat{T}_n$ explicitly we get

$$(-\textstyle\sum_\mu \frac{\nabla_\mu{}^2}{2} - \sum_\mu \frac{\nabla_A{}^2}{2m_A} + V_{en} + V_{en} + V_{nn})\,\psi_e\psi_n = E\psi_e\psi_n \tag{2.13}$$

Now

$$-\sum_{\mu}\frac{\nabla_{\mu}^{2}}{2}(\psi_e\psi_n) = -\psi_n\sum_{\mu}\frac{\nabla_{\mu}^{2}}{2}\psi_e \tag{2.14}$$

$$-\sum_A\frac{\nabla_A^{2}}{2m_A}(\psi_e\psi_n) = -\sum_A\frac{1}{2m_A}(\psi_e\,\nabla_A^{2}\,\psi_n + \psi_n\,\nabla_A^{2}\,\psi_e + +2\nabla_A\psi_e.\nabla_A\,\psi_n) \tag{2.15}$$

Using equations 2.14 and 2.15 in 2.13 gives

$$-\psi_n\sum_{\mu}\frac{\nabla_{\mu}^{2}}{2}\psi_e - \left[\sum_A\frac{1}{2m_A}(\psi_n\,\nabla_A^{2}\,\psi_e + 2\nabla_A\psi_e.\nabla_A\,\psi_n)\right] - \psi_e\sum_A\frac{\nabla_A^{2}}{2m_A}\psi_n +$$

$$(V_{en} + V_{e\,e} + \mathrm{V_{nn}})\,\psi_e\psi_n = E\,\psi_e\psi_n \tag{2.16}$$

The square-bracketted terms of the above equation (2.16) describe the coupling of electronic and nuclear motion. These terms are neglected in the BO approximation. Dividing the remaining terms in this equation by ψ_n we gets

$$-\frac{\psi_e}{\psi_n}\sum_A\frac{\nabla_A^{2}}{2m_A}\psi_n + \left[-\sum_{\mu}\frac{\nabla_{\mu}^{2}}{2} + \mathrm{V_{ee}} + \mathrm{V_{en}}\right]\psi_e - \mathrm{E}\psi_e + \mathrm{V_{nn}}\,\psi_e = 0 \tag{2.17}$$

The second term in this equation is $\widehat{H_e}\psi_e$ (see equation 2.12). Writing $E_e\psi_e$ for this term and multiplying by $\frac{\psi_n}{\psi_e}$ one gets

$$\left(-\sum_A\frac{\nabla_A^{2}}{2m_A} + E_e + V_{nn}\right)\psi_n = E\,\psi_n \tag{2.18}$$

$$\text{or}\quad \left(-\sum_A\frac{\nabla_A^{2}}{2m_A} + E(R)\right)\psi_n = E\psi_n \tag{2.19}$$

where $E(R) = E_e + V_{nn}$.

In the frame work of the BO approximation the solution of equation 2.10 consists of two steps. First, equation 2.12 is solved for various nuclear conformations to obtain E_e. Adding V_{nn}

to it we get *E(R)* as a function of R. Then a suitable analytical expression for *E(R)* is substituted in equation 2.19. Solution of this equation gives the total enegy of the molecule. For a diatomic molecule, *R* is the internuclear distance and for a polyatomic molecule, *R* includes all possible internal coordinates (bond lengths, bond angles and dihedral angles). A plot of *E(R)* vs *R* is usually called a potential energy curve (for a diatomic molecule) or a multi-dimentional potential energy surface (for a poly atomic molecule).

Since for polyatomic molecule, the potential energy E is a function of n number of internal coordinates [where n is equal to $(3N-5)$ or $(3N-6)$] so we can write

$$E = f(q_1, q_2, \ldots\ldots, q_n). \tag{2.20}$$

The most interesting points on PES's are the stationary points (minima and saddle points) which occur when first partial derivative of the energy with respect to each geometric parameter is equal to zero

$$\text{i.e. } \frac{\partial E}{\partial q_1} = \frac{\partial E}{\partial q_2} = \cdots = \frac{\partial E}{\partial q_n} = 0 \tag{2.21}$$

Minima and maxima can be distinguished simply by second derivatives. Local energy minima (reactants and products) correspond to

$$\frac{\partial^2 E}{\partial q^2} > 0 \tag{2.22}$$

for all q.

Transition state corresponds to

$$\frac{\partial^2 E}{\partial q^2} > 0 \tag{2.23}$$

for all q except along the reaction coordinate and

$$\frac{\partial^2 E}{\partial q^2} < 0 \tag{2.24}$$

along the reaction coordinate.

2.6 Conceptual Density Functional Theory

Conceptual DFT does not imply the other branches of DFT. It concentrates on the extraction of chemically relevant concepts and principles from DFT. Conceptual DFT provides a very convenient framework for the discussion of chemical reactivity. A series of global and local quantities, the so called reactivity descriptors or indices, have been introduced to describe the extent of the response of a molecular system toward perturbations in either its number of electrons, N, its external potential, $v(r)$, or both.[4] An important example of these reactivity indices is the Fukui function, introduced by Parr and Yang,[5] defined as the response of the system's electron density $\rho(r)$ due to a perturbation in its total number of electrons N at a constant external potential $v(r)$. Due to the discontinuities in slope for the $\rho(r)$ versus N curve,[6] three different types of Fukui functions can be introduced, representing the case of a nucleophilic $f^+(r)$, electrophilic $f^-(r)$, and a neutral (radical) attack $f^0(r)$:

$$f^+(\vec{r}) = \left(\frac{\delta\rho(r)}{\delta N}\right)^+_{v(r)} \approx \rho_{N+1}(\vec{r}) - \rho_N(\vec{r}) \approx \rho_{LUMO}(\vec{r}) \tag{2.25}$$

$$f^-(\vec{r}) = \left(\frac{\delta\rho(r)}{\delta N}\right)^-_{v(r)} \approx \rho_N(\vec{r}) - \rho_{N-1}(\vec{r}) \approx \rho_{HOMO}(\vec{r}) \tag{2.26}$$

$$f^0(\vec{r}) = \frac{1}{2}(f^+ + f^-) \approx \frac{1}{2}(\rho_{N+1}(\vec{r}) - \rho_{N-1}(\vec{r})) \tag{2.27}$$

where $\rho_{N+1}(r)$, $\rho_N(r)$, $\rho_{N-1}(r)$ are the electron densities of the $N+1$, N, $N-1$ electron system respectively, all obtained at the geometry of the N electron system, due to the fact that the derivative is taken at a constant external potential. However in chemistry it is customary to work with properties associated with atoms and functional groups in the molecule. In this context, a useful approximation to describe the site reactivity is given by the condensed to atom Fukui indices by using an atomic charge partitioning scheme.[7]

$$f_k^+ \approx N_k(N+1) - N_k(\mathrm{N}) \tag{2.28}$$

$$f_k^- \approx N_k(N) - N_k(N-1) \tag{2.29}$$

$$f_k^\circ \approx \frac{1}{2}\left(N_k(N+1) - N_k(N-1)\right) \tag{2.30}$$

where $N_k(N+1)$, $N_k(N)$ and $N_k(N-1)$ represent the electron populations on atom k in the $N+1$, N and $N-1$ electron system.

For an N-electron system with external potential $v(r)$ and total energy E, Parr et al. showed that the electronegativity[8] could be identified as the negative of the electronic chemical potential μ:

$$\chi = -\mu = -\left(\frac{\delta E}{\delta N}\right)_{v(r)} \approx -\frac{I+A}{2} \tag{2.31}$$

Where I and A are the vertical ionization energy and electron affinity, respectively.

Chemical hardness and softness were introduced by Pearson[9] in 1963 when he was studying and classifying Lewis acid and base interactions. He formulated the hard – soft acids bases (HSAB) principle "hard acids prefer to bond to hard bases and soft acids prefer to interact with soft bases".[9] In 1983, Parr and Pearson proposed a quantitative definition of this hardness:[10]

$$\eta = \frac{1}{2}\left(\frac{\partial^2 E}{\partial N^2}\right)_{v(r)} = \frac{1}{2}\left(\frac{\partial \mu}{\partial N}\right)_{v(r)} \approx \frac{I-A}{2} \tag{2.32}$$

measuring the system's resistance toward charge transfer.

The softness S is defined as the inverse of the hardness:[11]

$$S = \frac{1}{2\eta} \tag{2.33}$$

The local counterpart of the softness, the local softness, was introduced by Parr and Yang as[11,12]

$$s(r) = \left(\frac{\delta \rho(r)}{\delta \mu}\right)_{v(r)} = \left(\frac{\delta \rho(r)}{\delta N}\right)_{v(r)} \left(\frac{\delta N}{\delta \mu}\right)_{v(r)} = S f(r) \tag{2.34}$$

One can interpret the reaction ability toward soft reagents of the the different parts of the molecules with the condensed form of the local softness, written as

$$s_k{}^i = S f_k{}^i \tag{2.35}$$

Where i equals to either +, −, or *0* depending on whether the system undergoes a nucleophilic, electrophilic, or radical attack.

2.7 References and notes

1. Orio, M.; Pantazis, D. A.; Neese, F. *Photosynth. Res.* **2009**, *102*, 443.
2. Hohenberg, P.; Kohn, W. *Phys. Rev.* **1964**, *136*, B864.
3. Kohn, W.; Sham, L. *J. Phys. Rev.* **1965**, *140*, A1133.
4. (a) Parr, R. G.; Yang, W. Density Functional Theory of Atoms and Molecules; Oxford University Press: New York, 1989. (b) Parr, R. G.; Yang, W. *Ann. Rev. Phys. Chem.* **1995**, 46, 701. (c) Kohn, W.; Becke, A. D.; Parr, R. G. *J. Phys. Chem.* **1996**, 100, 12974. (d) Chermette, H. *J. Comp. Chem.* **1999**, 20, 129. (e) Geerlings. P.; De Proft, F.; Langenaeker, W. *Adv. Quant. Chem.* **1999**, 33, 303. (f) Geerlings, P.; De Proft, F.; Langenaeker, W. *Adv. Quant. Chem.* **2003**, 103, 1793.
5. Parr, R. G.; Yang, W. *J. Am. Chem. Soc.* **1984**, 106, 4049.
6. Perdew, J. P.; Parr, R. G. Levy, M.; Balduz, J. L.; Jr. *Phys. Rev. Lett.* **1982**, 49, 1691.
7. Yang, W.; Mortier, W. J. *J. Am. Chem. Soc.* **1986**, 106, 5708.
8. Parr, R. G.; Donnelly, R. A.; Levy, M.; Palke, W. E. *J. Chem. Phys.* **1978**, 68, 3801.
9. (a) Pearson, R. G. *J. Am. Chem. Soc.* **1963**, 85, 3533. (b) Pearson, R. G. Chemical Hardness; Wiley: New York, 1997.
10. Parr, R. G.; Pearson, R. G. *J. Am. Chem. Soc.* **1983**, 105, 7512.
11. Yang, W.; Parr, R. G. Proc. Natl. Acad. Sci. **1985**, 82, 6723.
12. Lee, C.; Yang, W.; Parr, R. G. J. Mol. Struct. (THEOCHEM) **1988**, 163, 305.

Chapter 3

On protonation and methylation of benzene: A B3LYP DFT based study

In this chapter we have investigated mechanistic pathways for four different electrophilic addition processes with benzene (monoprotonation, diprotonation, monomethylation and dimethylation) in DFT framework. In all the cases, transition states have been isolated and characterized through intrinsic reaction coordinate calculations. Fukui functions, local softness values, local charge densities, different electrophile affinities, thermochemical parameters have been calculated and correlated. Fukui functions and local softness values have been found to be reliable descriptors for kinetically controlled products; whereas, prediction of thermodynamically controlled products can be made through local charge density values. Electrophile affinities are found to be additive and correlate well with thermochemical parameters.

3.1 Introduction

Most of the substitutions at aliphatic carbon are nucleophilic in nature, but the situation is reversed in case of an aromatic one. High π-electron density at the aromatic ring creates appropriate condition for electrophilic addition. Attachment of a positively charged species to benzene (Bz) ring occurs through a carbocation, which is a resonance hybrid known as sigma complex or arenium ion. This Wheland intermediate[1] has been isolated and characterized by many researchers. [2–5] Theoretical investigation on arenium ions is instrumental in the mechanistic study of reaction pathways involving such species. Olah and Khun[2] initiated such study, albeit from a classical point of view. Their work on isolation and characterization of different arenium ions serves as major land mark in the understanding of the mechanism of electrophilic attack on aromatic systems. Multistep character of electrophilic aromatic substitution has been ascertained by several such studies.[6] However, most of these studies were made in the gas phase to avoid the effect of complicating environment.

Protonation of benzene is the simplest example of electrophilic substitution to an aromatic ring. First experimental evidence of the existence of monoprotonated benzene (mpb) has been reported by Gold and Tye[4] and subsequently by Reid[5] through spectroscopic studies. Hehre and Pople carried out a thorough theoretical analysis on protonation of benzene and found the lowest energy structure for mpb where the proton is attached directly to one of the ring carbon atoms.[7] The possibility of diprotonated benzene (dpb) has first been predicted by Sumathy and Kryachko.[8] Diprotonated species can also be isolated due to their greater stability in comparison with the monoprotonated one. Through quantum chemical calculations, Sumathy and Kryachko extended their investigation to multi-protonation of benzene and have shown conclusively that mono, di even tri protonation of benzene can be possible, whereas tetra protonation leads to the opening of the aromatic ring. They concluded that meta diprotonated species with sigma complex type structure to be the global minima for BzH_2^{2+} potential energy surface. In a recent work, Roithova et al.[9] have studied the formation of doubly protonated species and

characterized it through mass spectrometry. They have also analyzed potential energy surface of different isomers of dpb through density functional formalism.

Beside proton, carbocation also acts as an electrophile to form arenium ion complexes. Because of the participation of carbocations in enzymatic reactions, much interest has been grown in the study of reaction dynamics of these reactions. Raos et al.[10] applied spin-coupled valence bond calculation on the reaction pathway for insertion of a methyl cation onto Bz, leading to the Wheland intermediate $BzCH_3^+$. This reaction has also been taken into account extensively by Miklis and coworkers where they predicted that CH_3^+ prefers a $\eta 1$ bonding with Bz rather than $\eta 6$ bonding.[11] Different forms of the arenium ions of this reaction were investigated through an ab initio direct molecular dynamics study by Ishikawa et al.[12] These results were compared with the results obtained through Car-Parrinello molecular dynamics by Zheng et al.[13]

Crux of our present work lies at the determination of the most plausible mechanistic pathways for different electrophilic additions to Bz in DFT framework. DFT-functionals which consider electron correlation appears effective in producing an accurate picture of electronic structures of reactants, products and transition states involved in the reaction mechanism. Reactivity at the sites of electrophilic attack has been quantified in terms of Fukui function, local softness, proton affinity etc., which are found supplementary to the mechanistic scheme of the reactions, intuited through electronic structure analysis. In this work we investigate mechanistic pathways for four different electrophilic addition reactions, (1) protonation of benzene, (2) protonation of monoprotonated benzene, (3) methylation of benzene and (4) methylation of monomethylated benzene (Scheme 3.1).

3.2 Methodology

A quantitative description of many electron systems can be obtained through rigorous post Hartree–Fock treatments; however, a reliable estimate of electronic properties can also be obtained in computationally economic density functional

framework. In this work, we explore mechanistic pathways for chosen electrophilic addition reactions through DFT studies. The geometries of all the reactants, products and transition states have been optimized using generalized gradient approach and split valence triple zeta diffused and polarized basis function. For all optimized structures, frequency analysis has been carried out at the same level of theory. This allows one to assign the reactants and products as genuine minima and shows at least one imaginary frequency for the transition states. To explicitly connect a particular transition state with relevant reactant(s) and product(s), the intrinsic reaction coordinate (IRC) has also been calculated for each transition state. The exchange correlation functional, which is used in this work, contains spurious electron self interaction, related to long range non-dynamic correlation of electron.[14] The self interaction error (SIE) influences the shape of the potential energy surface near the transition state by lowering the barrier height.[15] Being aware of this fact, our B3LYP results are further refined by carrying out single point calculations at MP2 level on the transition states.[16] Reactivity of any molecule can usually be described through global parameters such as electronegativity, hardness, softness etc. However, reactivity of a specific site can not directly be determined through these global reactivity parameters. Nevertheless, local reactivity parameters are found to be suitable to serve this purpose. In this study, we calculate local quantities such as Fukui function, local softness and charge density at different sites in a molecule. Regioselectivity for subsequent electrophilic attack at site k can be ascertained through evaluation of Fukui function (f_k^i),[17-19] an index which describes the reactivity towards an electrophilic attack and can be estimated using populations condensed to individual atoms (p_k) obtained through Mulliken population analysis as $f_k^- = [\rho_k(N) - \rho_k(N-1)]$, where N is the total number of electrons in the system.[20, 21] Local softness (s_k^i),[17-19] is another parameter for estimating the suitability of a specific site towards electrophilic attack, which is related to Fukui function as $s_k^i = f_k^i.S$ with $i = +$ or $-$, where S is the global softness.[22]

Proton affinity, which is the energy difference between protonated and deprotonated species is also suitable to explore mechanistic pathways.[8, 9, 23] This work includes the calculation of different electrophile affinities. These electrophile affinities

may in turn be related with the enthalpy of formation of different arenium ions. To draw this comparison, we also calculate the thermodynamic properties such as change in free energy and enthalpy.

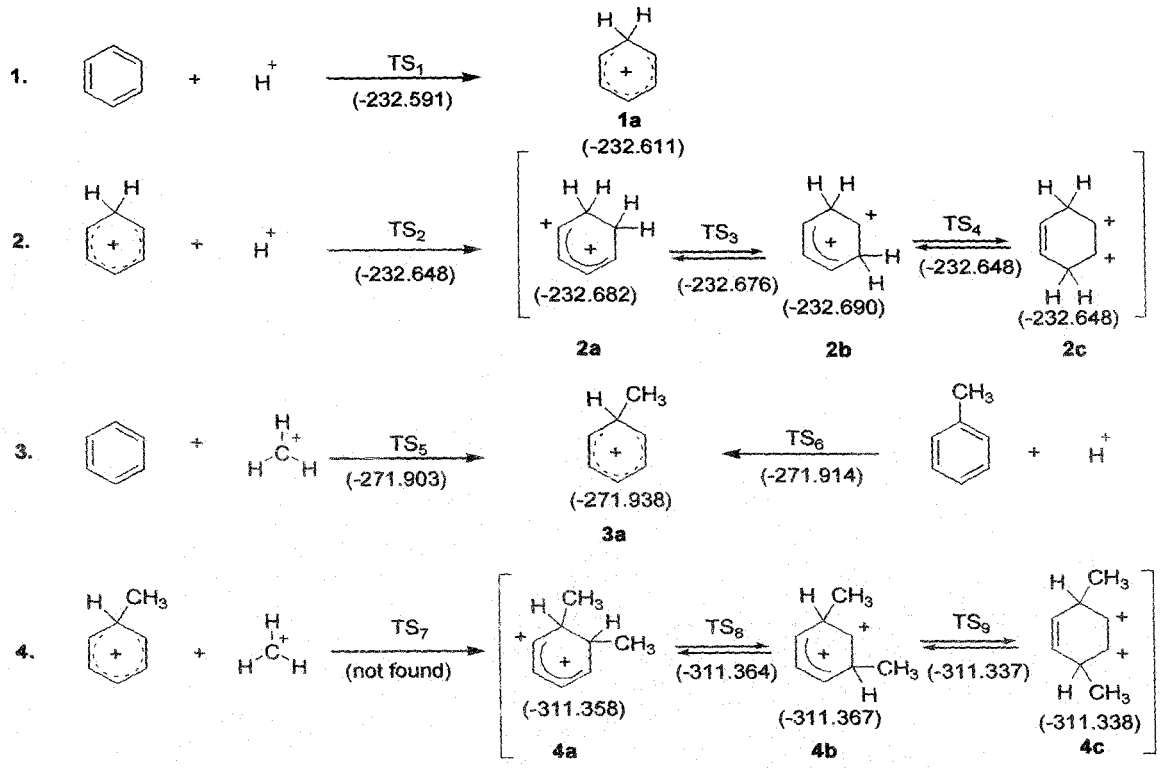

Scheme 3.1. Mechanistic pathways for the reactions under investigation. The engery values (a.u.) of the corresponding species are given in parenthesis.

3.3 Results and discussion

In this work, numerical calculations have been performed using UB3LYP exchange-correlational functional. Diffused basis functions have often been found to be effective in describing weak interaction among atoms.[24] Hence we use 6-311++G(d, p) basis function for a correct description of weak interactions which may prevail in the transition structures. The harmonic frequencies and zero point vibrational energies have been retained unscaled. These calculations are implemented through Gaussian 03W quantum chemical package.[25]

As evident from Scheme 3.1, six equivalent carbons in Bz are equally susceptible for electrophilic attack and protonation can take place arbitrarily at any one of them to produce mpb (1a), which has been found to have a methylene type of conformation where the proton resides on the C_{2v} symmetry axis; this observation is in good agreement with previous studies.[8] This is also well supported by the transition state TS_1. Methylenic protons in the transition state structure execute oscillation with a frequency of -1284 cm^{-1}, being equidistant from Bz ring. The proton affinity of the neutral benzene takes the value of 188 kcal/mol. The energy profile of this protonation process is given in Figure 3.1.

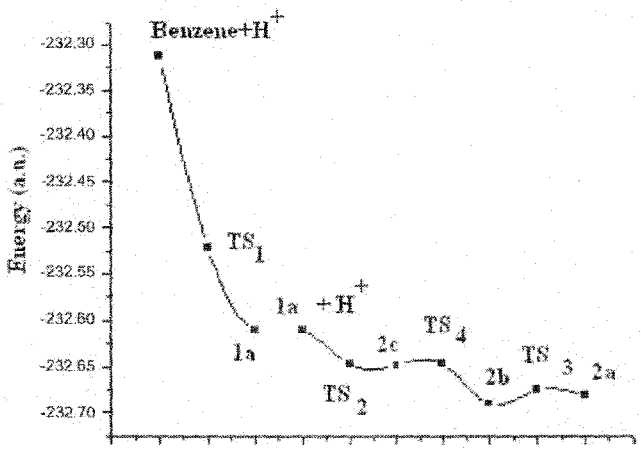

Figure 3.1 Energy ordering of reactants, products and transition states of protonation and diprotonation reactions

A monoprotonated species gives rise to the probability of three diprotonated isomers ortho (2a), meta (2b), and para (2c). From the energy values, displayed in Scheme 3.1, it is clear that among these three isomers, meta isomer is the most stable followed by ortho and para. The low energy barriers among the ortho, para and meta isomers facilitate proton walk among the sites and hence an equilibrium among the isomers of dpb is established. The energy ordering of the isomers can be viewed in Figure 3.1. Nucleophilicity of carbon centers in monoprotonated species is quantified in terms of Fukui functions (Table 3.1). Higher the value of Fukui function (f_k^-), greater is the probability of electrophilic attack at site k. In mpb, calculated Fukui functions predict highest nucleophilicity for the para position followed by meta and ortho. Apart from Fukui functions, we have also calculated local softness values for each carbon centers in

mpb (Table 3.1), which show the same trend. Further protonation of mpb proceeds through TS_2 which shows an imaginary frequency of -286 cm^{-1} originating from the oscillation of proton in between meta and para positions. Intrinsic reaction coordinate (IRC) study of the second reaction shows that the incoming proton prefers para position, and hence para disubstituted isomer seems to be kinetically controlled product. This is exactly suggested by Fukui functions and local softness values. This observation may initially appear contradictory to the energy values shown in Scheme 3.1. Nevertheless, meta isomer of dpb is the thermodynamically controlled product. Highest value of charge density at the meta position of mpb (Table 3.1) also supports this observation. Owing to the largest local reactivity parameters, para position becomes most susceptible to proton attack. Once H^+ attacks the para position, an interstitial proton transfer may follow, through a bridged intermediate. Ultimately thermodynamically stable meta di-substituted

Table 3.1

Fukui functions at different positions of protonated (1a) and methylated benzenium ion (3a)

Protonated benzene				Methylated benzene			
position	Softness	Fukui Function	Charge density	position	Softness	Fukui Function	Charge density
Ortho	0.937	0.151	0.586	Ortho	10.524	1.678	0.487
Meta	1.707	0.275	−0.515	Meta	6.592	1.051	−0.590
Para	1.993	0.321	0.300	Para	5.827	0.929	0.181

benzene is formed via transition state TS_4. Frequency calculation of TS_4 shows one negative frequency of -287 cm^{-1} which originates from the proton oscillation in between meta and para positions. One of the hydrogens in meta position of 2b can also migrate to ortho position through TS_3, which has one imaginary frequency of -540 cm^{-1}. Relative stabilities of different species involved in this diprotonation reaction are displayed in Figure 3.1. Proton affinity values of mpb as displayed in Table 3.2, also show highest and lowest degree of proton affinity in meta and para positions, respectively, supplementing the above fact. From the proton affinity values, second protonation to mpb appears less favorable than the first protonation. We also calculate the diproton affinity of Bz (Table

3.2). From Table 3.2, it is clear that the proton affinities follow the additivity rule. Free energy changes (ΔG) of reactions discussed above are tabulated in Table 3.3. The ΔG value in the formation of diprotonated benzene from monoprotonated species is maximum negative in case of meta di protonation, which stands for the spontaneity of that reaction. In dpb, negative ΔG values in the interconversion of isomers indicate a tendency of the reaction towards the meta isomer. Negative values of ΔH (Table 3.3) are found to have the same trend for conversions 1a→2a, 1a→2b and 1a→2c as that of their proton affinity values (Table 3.2). Positive values of proton affinities reflect higher stabilities of protonated species and hence exothermic nature of the reactions is well explicable.

Table 3.2

Proton affinity values of Bz, mpb (1a) and diproton affinity of bz. In the parentheses previously reported values and corresponding references are given.

Species		Proton affinity (kcal/mol)	Species		Diproton affinity (kcal/mole)
Benzene		188.269 (187.9)[7]	Benzene	Ortho	232.367
mpb	Ortho	44.098 (39.20)[9]		Meta	237.696
	Meta	49.427 (50.73)[9]		Para	211.506
	Para	23.237 (25.376)[9]			

Monomethylated benzene (mmb) (3a) can be obtained by reacting CH_3^+ to benzene through Friedel–Crafts type of reaction. An alternative route of getting 3a is obviously through addition of H^+ with toluene. Almost same energy of transition states TS_5 and TS_6 (Figure 3.2) predict equal probability of both routes. Nonetheless, in the second route, reaction coordinate is much steeper than that in the first one, and hence the rate through the second route should be higher. TS_5 has two imaginary frequencies, one of -261 cm^{-1} with relative intensity very small 0.01 and other -93 cm^{-1} with relative intensity 0.23. As a consequence, the higher intensity vibration would lead to the product. The methyl cation affinity (MCA) of benzene has been found to be 85 kcal/mol, which is in well agreement with the earlier results.[23]

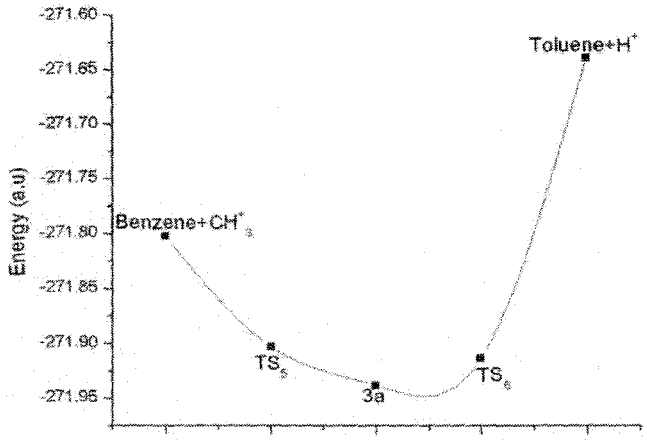

Figure 3.2 Energy ordering of reactants, products and transition states of monomethylation reaction.

This methylated benzene when subjected to further methylation, three isomers ortho (4a), meta (4b) and para (4c) may result. Energy values of optimized geometries of these three isomers reveal the meta to be the most stable (Scheme 3.1). However, softness and Fukui function calculations indicate a facilitating ortho attack (Table 3.1). To seek the transition state (TS_7) of this reaction, a methyl cation is suspended over monomethylated benzenium ion and output of the computation shows that the cation is attached to the ortho position; however, planarity of the benzene ring is lost (Figure 3.4). This puckeredness arises due to steric interaction between two methyl fragments in ortho position. To ensure this argument, we expose the monomethylated benzenium ion to a proton and the obtained transition state in this process shows that the proton is nearer to the ortho position as expected. The frequency of this transition state (-551 cm^{-1}) shows an oscillation of the proton between ortho and meta position keeping the planarity of the benzene ring intact. Leaving ortho position for obvious reason as described above, and through closer inspection of Table 3.1, one can surmise that the meta position will be the next preferred site for electrophilic attack and thus the meta isomer predominates (Scheme 3.1). The highest charge density value (Table 3.1) at meta position of methylated benzeneum ion also predicts the meta isomer to be the thermodynamically controlled product. Nevertheless, ortho and para isomers will be in equilibrium with meta dimethylated dication as can be seen from Figure 3.3. Inter conversion between ortho and

meta dimethylated benzene takes place through TS_8. It has one imaginary frequency of $-147\ cm^{-1}$. In this transition state, methyl group is placed in equitable distance from ortho and meta position and the negative frequency arises due to an unusual rotation of methyl group therein. Meta to para interconversion takes place through the transition state, TS_9 which is characterized by $-153\ cm^{-1}$ and the corresponding oscillation is executed between para and meta positions. The analysis of methyl cation affinity (MCA) strongly indicates it should exhibit the same additivity feature as that of the proton affinity, this is also apparent from Table 3.4 Thermochemical analysis of dimethylation reaction shows a positive change in free energy (Table 3.3). This observation suggests the requirement of activation energy for occurrence of the reactions as also shown by the energy profile of these reactions (Figure 3.3). However, free energy change for the interconversion between the different isomers of dimethylated species is negative, which indicates that ortho and para isomers can easily switch over to the energy-minimized meta isomer. Unlike diprotonation, dimethylation produces positive ΔH values (Table 3.3) and justifiably correspond to negative values of methyl cation affinities (Table 3.4).

Table 3.3
Free energy and enthalpy change of the reactions depicted in scheme 3.1

Conversion	ΔG (kcal/mol)	ΔH (kcal/mol)
Benzene→1a	−157.508	−155.939
1a→2a	−93.500	−92.434
1a→2b	−98.521	−97.712
1a→2c	−75.302	−73.865
2a→2b	−5.020	−5.279
2c→2b	−23.846	−23.847
Benzene + CH_3^+→3a	−99.776	−109.255
Toluene + H^+→3a	−180.098	−180.706
3a→4a	56.477	47.381
3a→4b	50.829	41.607
3a→4c	69.027	59.614
4a→4b	−5.648	−5.774
4c→4b	−17.571	−18.007

Table 3.4

Methyl cation affinity values of Bz, mmb (3a) and dimethyl cation affinity values of Bz. In the parenthesis previously reported value and corresponding reference is given.

Species		Methyl cation affinity (kcal/mol)	Species		Dimethyl cation affinity (kcal/mol)
Benzene		85.051 (81.4)[23]	Benzene	Ortho	40.267
mmb	Ortho	−44.784		Meta	45.871
	Meta	−39.180		Para	27.420
	Para	−57.631			

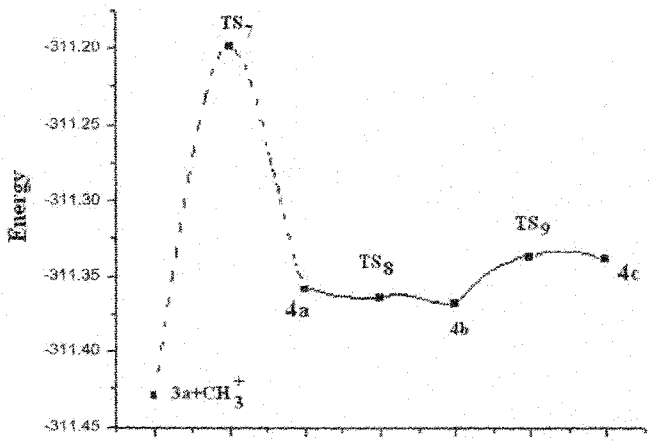

Figure 3.3 Energy ordering of reactants, products and transition states of dimethylation reaction.

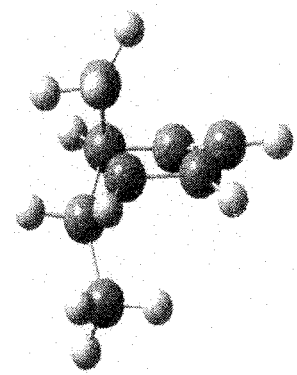

Figure 3.4 Puckered structure of TS_7.

As, the applied functional is reported to be inadequate in producing an accurate picture of potential energy surface,[14-16] the results have been compared with single point MP2 calculations on UB3LYP optimized geometries. Plotting of MP2 energies of the reactant, transition state and products reproduce the energy ordering of DFT functional, but with an overall scaled down representation. Comparison of DFT and post Hartree–Fock results are given in Tables 3.5 and 3.6.

Table 3.5

Energy of the transition states at UB3LYP and MP2 level. In the parentheses previously reported values and corresponding references are given.

Species	UB3LYP(a.u.)	MP2(a.u.)	Energy difference (a.u)
TS_1	−232.591	−231.860	0.731
TS_2	−232.648	−232.911	0.737
TS_3	−232.676 (−232.676)[9]	−232.930	0.746
TS_4	−232.648 (−232.652)[9]	−231.911	0.737
TS_5	−271.903	−271.043	0.86
TS_6	−271.914	−271.055	0.859
TS_8	−311.364	−310.364	1.000
TS_9	−311.337	−310.344	0.993

Table 3.6

Energy of different reactants and products at UB3LYP and MP2 level. In the parentheses previously reported values and corresponding references are given.

Species	UB3LYP (a.u)	MP2 (a.u.)	Energy difference (a.u.)
1a	−232.611	−231.871	0.740
2a	−232.682 (−232.681)[9]	−231.929	0.753
2b	−232.690 (−232.689)[9]	−231.938	0.752
2c	−232.648 (−232.651)[9]	−231.909	0.739
3a	−271.938 (−291.925)[11]	−271.072	0.866
4a	−311.358	−310.361	0.997
4b	−311.367	−310.363	1.004
4c	−311.338	−310.347	0.991

3.4 Summary

In this work we have studied electrophilic addition to benzene within DFT framework using UB3LYP hybrid functional and 6-311++G(d, p) basis function. The results reflect the same trend of mechanistic pathways in cases of diprotonation and dimethylation of benzene. In both the reactions the most stable product is a meta disubstituted one, followed by ortho and para. This is also well supported by simple valence bond based qualitative approach. In this approach, one can readily find only one possible structure for para disubstituted product in which two positive charges are geminal. In ortho and meta disubstituted products two resonating structures could be found; however, in case of ortho in one of these structures again charges are on neighboring sites, whereas, in case of meta isomer in none of them charges are adjacent. This clearly points out the meta disubstituted product to be most favorable energetically followed by ortho and para. This is also supported by local charge density values. Nevertheless, in case of diprotonation reaction the para isomer has been found to be kinetically controlled product, whereas the ortho one is the same for dimethylation reaction, which is also supported by the highest value of Fukui functions and local softness values in ortho and para isomers for diprotonation and dimethylation, respectively. Proton affinities and methyl cation affinities have been found to be additive in nature and these values also justify calculated thermochemical parameters. A correlation is observed between proton and methyl cation affinity with the change in enthalpy. Positive values of proton and methyl cation affinities proportionate to $-\Delta H$ values of the conversions and vice versa.

3.5 References and notes

1. Wheland, G. W. *J. Am. Chem. Soc.* **1942**, *64*, 900.
2. Olah, G. A.; Khun, S. J. *J. Am. Chem. Soc.* **1958**, *80*, 6535.
3. Olah, S.; Porter, M.; Kelley, M. *J. Am. Chem. Soc.* **1972**, *94*, 2034.
4. Gold, V.; Tye, F. L. *J. Chem. Soc.* **1952**, 2172.

5. Reid, C. *J. Am. Chem. Soc.* **1954**, *76*, 3264.

6. (a) Crestoni, M. E.; Fornarini, S. *J. Am. Chem. Soc.* **1994**, *116*, 5873. (b) Glukhovtsev, M. N.; Bach, R. D.; Bach, S.; Laiter, S. *J. Org. Chem.* **1997**, *62*, 4036. (c) Stock, L. M. *Aromatic Substitution Reaction*, Prentice-Hall, Englewood Cliffs, NJ, **1968**. (d) Terrier, F. *Nucleophilic Aromatic Displacement – The influence of the Nitro-group,* Feuer H. (Ed.), VCH publishers, New York, **1991**. (f) Chuparkhin, O. N.; Charushin, V. N.; Van Der Plas, H. C. *Nucleophilic Aromatic Substitution of H*, Academic Press, San Diego, **1994**. (g) Kryazev, V. N., Drozd, V. N. *Russ. J. Org. Chem.* **1995**, *31*, 1.

7. Hehre, W. J.; Pople, J. A. *J. Am. Chem. Soc.* **1972**, *94*, 6901.

8. Sumathy, R.; Kryachko, E. S. *J. Phys. Chem. A* **2002**, *106*, 510.

9. Roithova, J.; Schroder, D.; Berger, R.; Schwarz, H. *J. Phys. Chem. A* **2006**, *110*, 1650.

10. Raos, G.; Astorri, L.; Raimondi, M.; Cooper, D. L.; Gerrattand, J.; Karadakov, P. B. *J. Phys. Chem. A* **1997**, *101*, 2886.

11. Miklis, P. C.; Ditchfield, R.; Spencer, T. A. *J. Am. Chem. Soc.* **1998**, *120*, 10482.

12. Ishikawa, Y.; Yilmaz, H.; Yanai, T.; Nakajima, T.; Hirao, K. *Chem. Phys. Lett.* **2004**, *396*, 16.

13. Zheng, F.; Sa, R.; Cheng, Jiang, H.; Shen, J. *Chem. Phys. Lett.* **2007**, *435*, 24.

14. Polo, V.; Gräfenstein, J.; Kraka, E.; Cremer, D. *Theor. Chem. Acc.* **2003**, *109*, 22.

15. Johnson, B. G.; Gonzales, C. A.; Gill, P. M. W.; Pople, J. A.; *Chem. Phys. Lett.* **1994**, *221*, 100.

16. Eriksson, L. A.; Kryachko, E. S.; Nguyen, M. T.; *Int. J. Quantum Chem.* **2004**, *99*, 841.

17. Yang, W.; Morteir, W. J.; *J. Am. Chem. Soc.* **1986**, *108*, 5708.

18. Vos, A. M.; Schoonheydt, R. A.; De Proft, F.; Geerlings, P. *J. Catal.* **2003**, *220*, 333.

19. Chattaraj, P. K.; Maiti, B.; Sarkar, U. *J. Phys. Chem. A* **2003**, *107*, 4973.

20. Fukui, K.; Yonezawa, T.; Shingu, H. *J. Chem. Phys.* **1952**, *20*, 722.

21. Parr, R. G.; Yang, W. *J. Am. Chem. Soc.* **1984**, *106*, 404.

22. Yang, W.; Parr, R. G.; *Proc. Natl. Acad.* Sci. USA 826723. 1985.

23. Maksic, Z. B.; Maksic, M. E.; Knezevic, A. *J. Phys. Chem. A* **1998**, *102*, 2981.

24. Otto, A. H. *Phys. Chem. Commun.* **1999**, 12.

25. M.J. Frisch et al., GAUSSIAN 03 (Revision D.01) Gaussian, Inc., Wallingford, CT, **2004**.

Chapter 4

DFT based study on the mechanism of an unexpected reaction of aldehydes with 1, 3-dicarbonyl compounds

In this chapter we have investigated the mechanism of an unexpected reaction between two molecules of 1, 3-dicarbonyl compound and one molecule of the aldehyde in presence of molecular iodine by density functional theory based approach. The geometries and the frequencies of reactants, intermediates and transition states are calculated using Becke three parameter exchange and Lee-Yang-Parr correlation functional. The vibrational analysis, intrinsic reaction coordinate (IRC) calculation and ESP analysis verify the authenticity of the transition states. Depending on substitution pattern of 1, 3-dicarbonyl compound, there may be two pathways, one leads to furan derivative and the other to cyclopropane derivative. The nucleus independent chemical shift (NICS) values have been calculated for the intermediates, products and the corresponding transition states to ensure the aromaticity contribution to the reaction pathway. The results are in good agreement with the experimental findings.

4.1 Introduction

Cyclopropane ring is found both in natural products and in biologically active mole-cules.[1-5] The unusual bonding and ring strain make it an interesting moiety to organic and bioorganic chemists. It can easily undergo selective ring opening and [1, 2] cycloaddition reactions. A variety of cyclopropanation reactions are well documented.[6] The substituted dihydrofurans, an important class of heterocycles are widely present in numerous natural products and show antibacterial as well as antifungal activities.[7-13] Due to diverse roles in organic synthesis, the synthetic methodologies for dihydrofurans have also been studied in detail.[6a, 14]

Oxidative addition reaction of various aldehydes with 5,5-dimethylcyclohexane-1,3-dione and 1,3-indandione can selectively endow with spiro dihydrofuran and cyclopropane derivatives in presence of iodine and dimethylaminopyridine (DMAP).[6a] It is a solvent free reaction and reported to be an unexpected reaction. Generally 1, 3-dicarbonyl compound reacts with an aldehyde and gives aldol condensation product. However, in this case as iodine and DMAP are introduced, this reaction proceeds to further cyclization following an unusual pathway.

The mechanism of aldol condensation reactions has already been studied extensively.[15-20] Bouillon et.al have studied diastereoselective intramolecular aldol condensations of 1,6-diketones in ab initio method.[16] Arno and Domingo have studied proline catalyzed aldol reaction between acetone and isobutyraldehyde.[17] However, no such mechanistic study has been reported for the title reaction. So our present work aims to investigate the most plausible mechanistic pathway in DFT framework which will be beneficial to further theoretical and experimental studies. To understand the mechanism of this highly selective cyclization, we have theoretically investigated the common steps of the reaction with acetyl acetone as 1, 3-dicarbonyl compound and acetaldehyde. To study the step of cyclization, we have taken (1) dimedone and 3- nitro benzaldehyde in one plausible path and (2) 1,3-indanedione and 3-nitro benzaldehyde in another (Scheme 4.1).

4.2 Methodology

In this work, we explore mechanistic pathways for this unexpected reaction through DFT studies using Becke three parameter exchange and Lee-Yang-Parr correlation functional. Since the systems investigated in this work are quite large, the geometries of all the reactants, intermediates, transition states and products have been optimized using the simplest split-valence basis function for computational economy. As iodine is undefined in this standard basis set, LANL2DZ is used as an extrabasis function for iodine. For all optimized structures, frequency analysis has been carried out. This allows one to assign the reactants and products as genuine minima and shows one imaginary frequency for the transition states. Intrinsic reaction coordinate (IRC) calculations have been done to verify whether the transition states connect the reactants to the products. The exchange correlation functional, which is used in this work, contains spurious electron self interaction, related to long range nondynamic correlation of electron.[21] The self interaction error (SIE) influences the shape of the potential energy surface near the transition state by lowering the barrier height.[22] Being aware of this fact, we have further refined our B3LYP results by carrying out single point calculation at MP2 level on the transition states.[23] Reactivity of any molecule at a specific site can be determined by local reactivity parameters such as Fukui function and so on. In this study, we have calculated Fukui function at different sites of a molecule. Regioselectivity for nucleophilic or electrophilic attack at site k can be ascertained through evaluation of Fukui function (f_k^i), [24-26] and can be estimated using population analysis as

$$f_k^+ = [\rho_k(N+1) - \rho_k(N)] \quad \text{for nucleophilic attack} \tag{4.1}$$

$$f_k^- = [\rho_k(N) - \rho_k(N-1)] \quad \text{for eletrophilic attack} \tag{4.2}$$

where $\rho(N+1)$, $\rho(N)$ and $\rho(N-1)$ are the electron densities of the (N+1), N and (N−1) electron systems respectively.[27, 28] Condensed form of these functions was presented by Yang and Mortier[29] yielding

$$f_k^+ = [q_k(N+1) - q_k(N)]\,, \tag{4.3}$$

$$f_k^- = [q_k(N) - q_k(N-1)\,], \tag{4.4}$$

where $q_k(N+1)$, $q_k(N)$, $q_k(N-1)$ are the charges at atom *k* on the anion, neutral, and cation species obtained by different population analysis. Since here we do not use any diffused function, Mulliken population analysis (MPA) has been used to estimate the condensed Fukui function. In this work Fukui functions are calculated following Eqs. (4.3) and (4.4). The thermodynamic functions (ΔG and ΔH) are calculated within ideal gas, rigid-rotor and harmonic oscillator approximations at 298.15K temperature and 1 atm pressure. The nucleus independent chemical shift (NICS) is a useful tool to analyze the contribution of aromaticity to the reaction path.[30-34] We have calculated the NICS values for the intermediates, products and also for the transition states to ensure the σ [NICS(0)] and π [NICS(1)] aromaticity contribution to the reaction path.

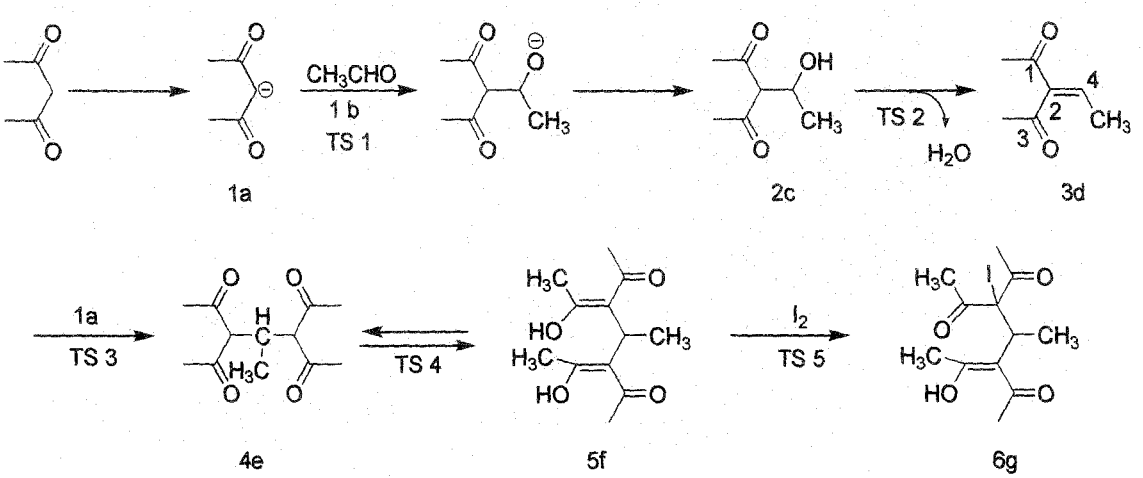

(A)

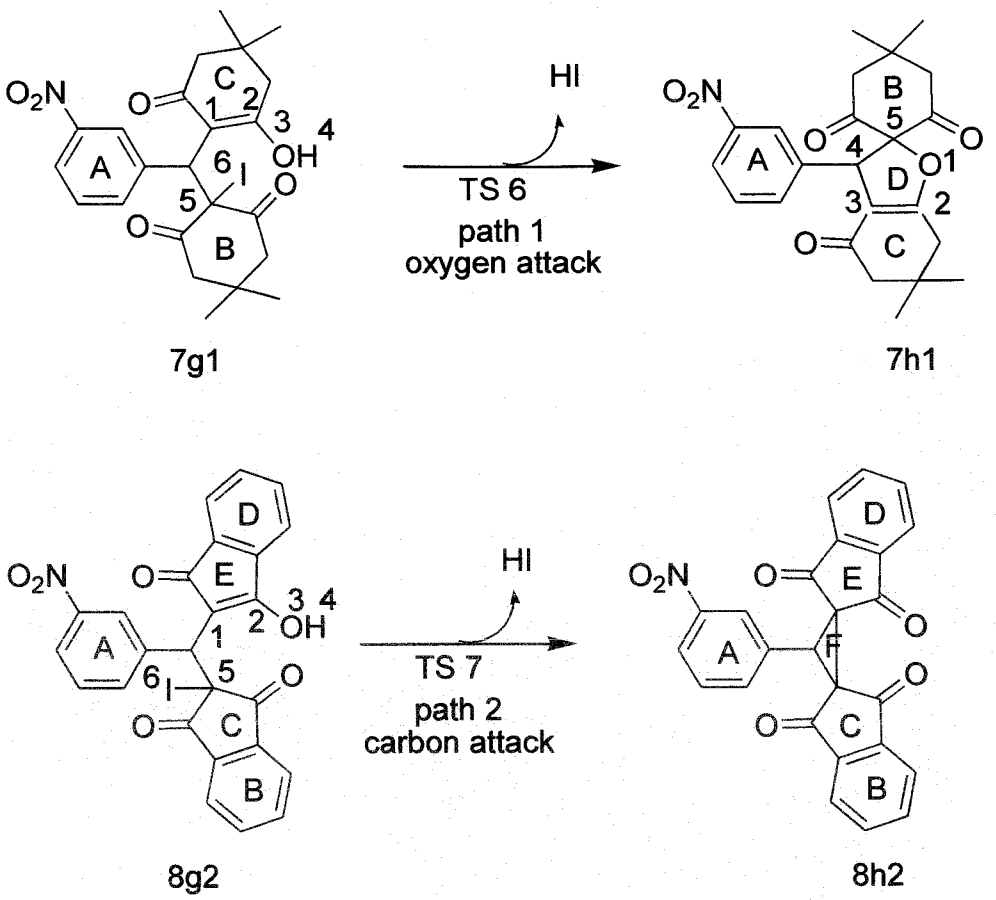

(B)

Scheme 4.1: (A) Schematic mechanism for the general steps of the reaction. (B) Two possible paths of cyclization; $7g_1$ is formed in the reaction between dimedone and 3-nitro benzaldehyde and $8g_2$ is formed in the reaction between 1,3-indanedione and 3-nitro benzaldehyde which on subsequent cyclization form $7h_1$ and $8h_2$ respectively.

4.3 Results and discussion

In this work, we have investigated the reaction mechanism using exchange-correlation functional B3LYP in the unrestricted DFT formalism. All structures are optimized using 3-21G basis function. LANL2DZ is used as an extrabasis function for iodine. All calculations are implemented through Gaussian 03W quantum chemical

package.[35] The potential energy map for the pathways related to the reaction between two molecules of the 1,3-dicarbonyl compound and one molecule of the aldehyde in presence of molecular iodine in basic medium is illustrated in Figure 4.1 where the relative energies in the parenthesis are taken from Table 4.1.

Our investigation shows that 1,3 dicarbonyl compound produces a carbanion (1a) in alkaline medium (Scheme 4.1). Now the carbanion (1a) undergoes nucleophilic attack to an aldehyde (1b) and gives the aldol condensation product (2c) via the transition state (TS1). The unique imaginary frequency of TS1 is -62.44 cm^{-1} and therefore it can be affirmed as the real one. This reaction is a barrier less exothermic reaction having $\Delta H=-1534.695$ kJ mol^{-1}. The spontaneity of this step is also apparent from the negative ΔG value (Table 4.2). Subsequent elimination of water from (2c) gives the product (3d) through TS2 which shows an imaginary frequency -1249.34 cm^{-1} originating from oscillation of the acidic proton from carbon to –OH group. This step of the reaction is slightly endothermic in nature ($\Delta H=117.661$ kJ mol^{-1}) and requires an activation energy of 195.300 kJ mol^{-1}. Electrophilicity of carbon centers in (3d) is quantified in terms of condensed Fukui functions (Table 4.3). Higher the value of Fukui function (f_k^+), greater is the probability of nucleophilic attack at site *k*. Now the carbanion (1a) produced from the second molecule of 1, 3 dicarbonyl compound reacts with double bonded C attached with –Me group of (3d) as predicted from Fukui functions via the transition state TS3 and 1,4 Michael addition takes place. Before the transition state can be achieved an intermediate (IM_2) is formed by the weak vanderwaals interaction. Frequency calculation of TS3 shows an imaginary frequency -255.26 cm^{-1} leading towards the product (4e). This step of reaction requires small activation barrier of 46.988 kJ mol^{-1}. Therefore it is expected to be fast. This is also supported by negative ΔG value (-1526.653 kJ mol^{-1}). Thermochemical analysis shows that this step is highly exothermic (Table 4.2) in nature. The compound (4e) undergoes enolization with an activation barrier of 294.981 kJ mol^{-1}. Here we have observed that the keto form (4e) is energetically lower than the corresponding enol form (5f). The tautomerism takes place through a four membered transition state (TS4) (Figure 4.2) which shows an imaginary frequency -1732.10 cm^{-1} originating from the oscillation of proton from carbon to carbonyl oxygen. In this context one can note that the tautomeric process is endothermic in nature. The enol form (5f)

which seems to be an intermediate, undergoes iodination at the most activated site to give the key intermediate (6g) via TS5 which is a six membered transition state (Figure 4.2) having an imaginary frequency −176.90 cm^{-1}. This step requires activation energy of 1302.609 kJ mol^{-1}. Nonetheless according to thermochemical analysis, this step is slightly exothermic in nature.

Table 4.1

Theoretical prediction of total energy (Hartree) at MP2, ZPVE (Hartree/particle) and relative energies ΔE (a.u) for reactants, products, intermediates and transition states.

Species	Total energy		ZPVE	ΔE (a.u)
	UB3LYP	MP2		
1a+1b	-496.284	-494.099	0.166	0.0
IM1	-496.322	-494.300	0.169	-0.032
TS1	-496.270	-494.252	0.169	0.016
2c	-496.889	-494.883	0.184	-0.6
TS2	-496.814	-494.795	0.179	-0.517
3d+H_2O	-496.839	-494.660	0.177	-0.561
3d+1a	-764.170	-760.765	0.267	-266.666
IM2	-764.217	-761.076	0.270	-266.707
TS3	-764.199	-761.068	0.270	-266.699
4e	-764.795	-761.681	0.285	-267.297
TS4	-764.682	-761.552	0.279	-267.174
5f	-764.797	-761.613	0.285	-267.229
5f+ I_2	-14546.340	-14537.359	0.285	-14043.141
TS5	-14545.841	-14535.624	0.283	-14041.408
6g+HI	-14546.279	-14537.774	0.278	-14043.563
7g1	-8281.182	-8272.880	0.464	--
TS6	-8280.921	-8272.779	0.454	--
7h1+HI	-8281.172	-8272.860	0.452	--
8g2	-8349.764	-8341.350	0.342	--
TS7	-8349.485	-8341.260	0.330	--
8h2+HI	-8349.710	-8341.295	0.326	--

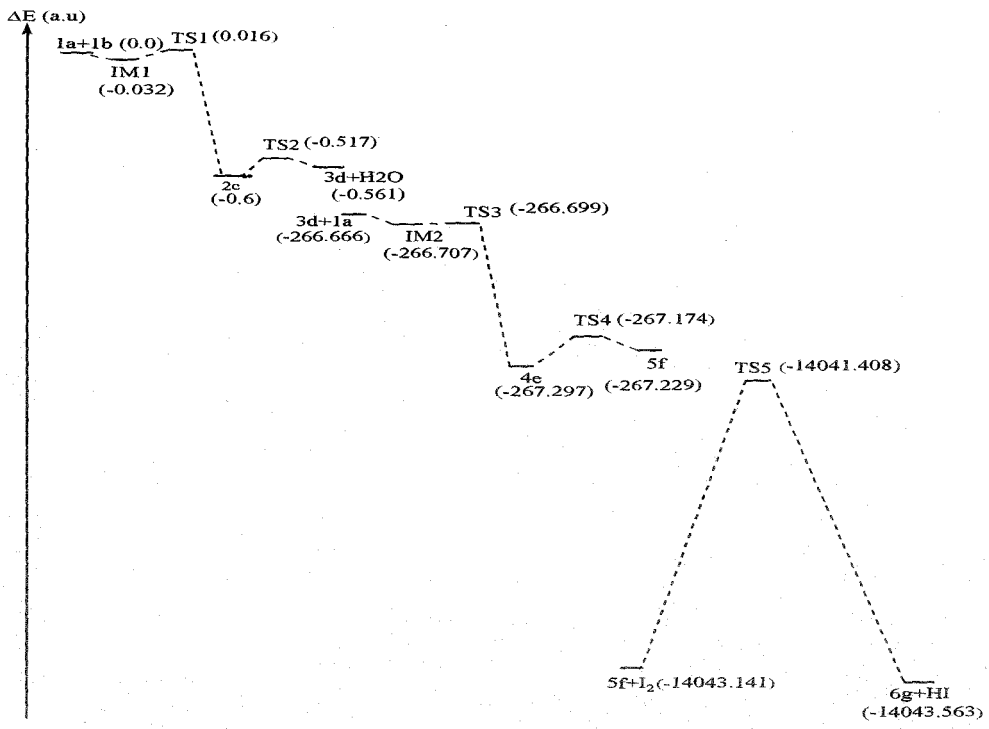
ΔE (a.u)
1a+1b (0.0)
TS1 (0.016)
IM1
(-0.032)
TS2 (-0.517)
2c
(-0.6)
3d+H2O
(-0.561)
3d+1a
(-266.666)
TS3 (-266.699)
IM2
(-266.707)
TS4 (-267.174)
4e
(-267.297)
5f
(-267.229)
TS5 (-14041.408)
5f+I2(-14043.141)
6g+HI
(-14043.563)

(A)

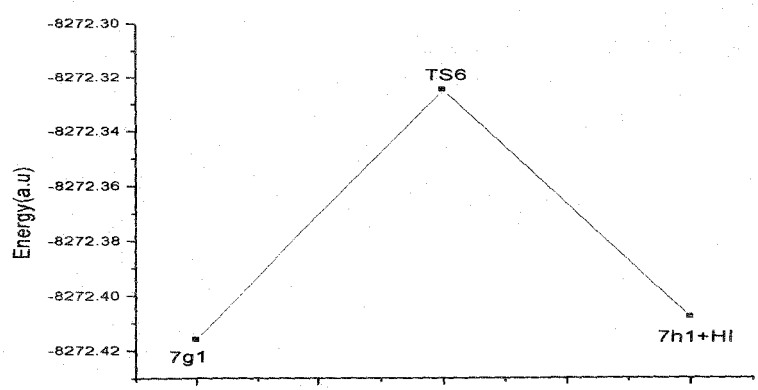
-8272.30
-8272.32
-8272.34
-8272.36
-8272.38
-8272.40
-8272.42
Energy(a.u)
TS6
7g1
7h1+HI

(B)

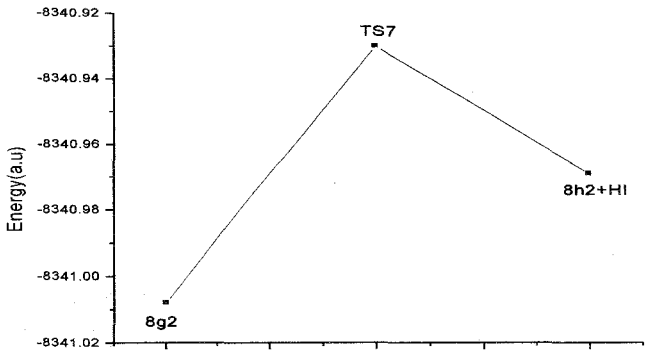

(C)

Figure 4.1 (A) shows the schematic representation of the energy profile (reactants, intermediates, transition states and products) for the general steps of the reaction [Scheme 4.1:(A)]. Whereas (B) and (C) show that of two cyclization pathways [Scheme 4.1: (B)].

Table 4.2

Free energy and enthalpy change of the reactions.

Conversion	$\Delta G(kJ\ mol^{-1})$	$\Delta H(kJ\ mol^{-1})$
1a + 1b → 2c	−1478.460	−1534.695
2c →3d	70.304	117.661
1a + 3d → 4e	−1526.653	−1584.673
4e → 5f	148.337	146.037
5f → 6g	−2.513	−9.585
$7g_1 \rightarrow 7h_1$	−34.765	8.149
$8g_2 \rightarrow 8h_2$	72.788	121.509

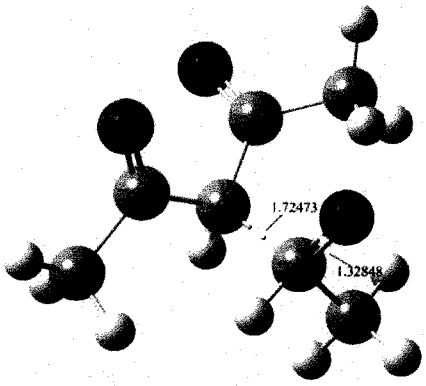

TS1

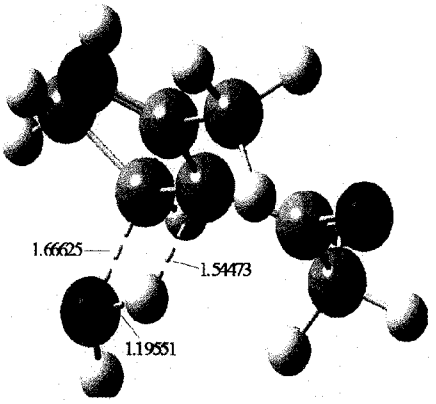

TS2

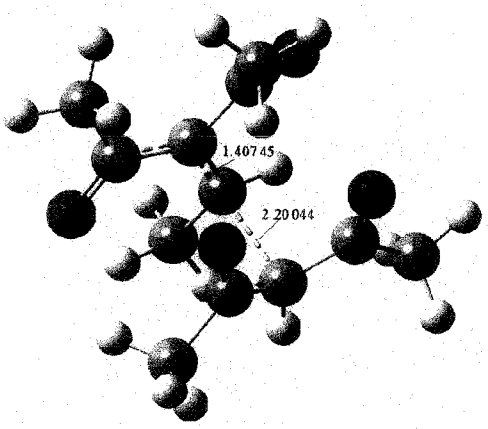

TS 3

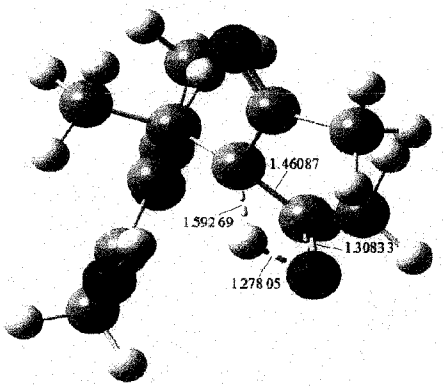

TS4

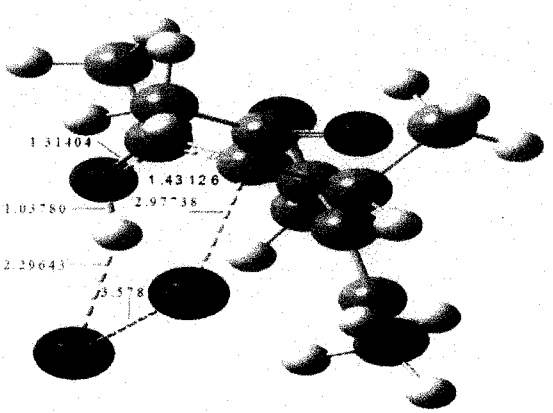

TS5

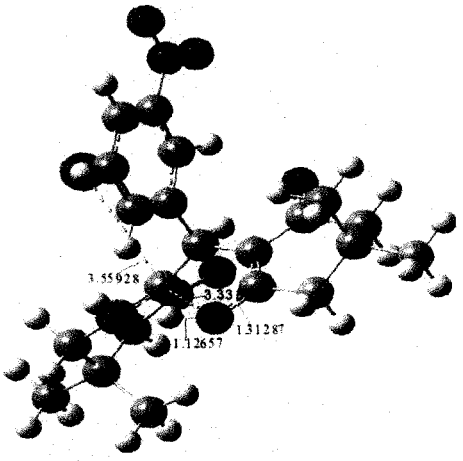

TS6

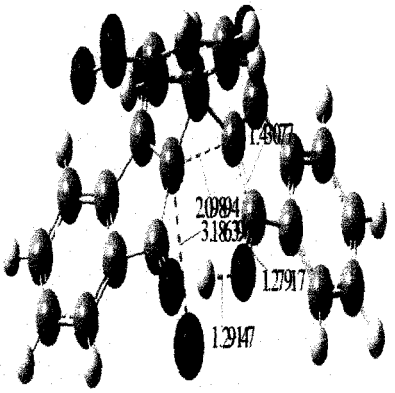

TS7

Figure 4.2 The optimized structures of the transition states corresponding to scheme 1. Distances are given in angstrom.

Table 4.3

Condensed Fukui functions at different probable positions of 3d for nucleophilic attack.

position	Condensed Fukui function
1-C	0.062
2-C	0.014
3-C	0.062
4-C	0.095

The discussion about the complication of the reaction mechanism is due here. The intermediate (6g) can undergo cyclization in two different ways (path 1 and path 2) which depends on the substitution pattern. In path 1, an intramolecular nucleophilic O-attack with an elimination of HI yields dihydrofuran. On the other hand, in path 2 a nucleophilic C-attack produces cyclopropane with an elimination of HI. To study two alternative pathways we have selected two different sets of reactants as shown in scheme 4.1(B). Reaction between dimedone and 3-nitro benzaldehyde goes via the first path i.e., the nucleophilic attack of oxygen which results dihydrofuran derivative and the corresponding transition state (TS6) is characterized by its negative frequency −237.73 cm^{-1}. Condensed Fukui function (f_k^-) calculation of intermediate $7g_1$ (Table 4.4) suggests

Table 4.4

Condensed Fukui functions at two different active sites of $7g_1$ and $8g_2$ for electrophilic attack.

Species	position	Condensed Fukui function
$7g_1$	1-C	0.013
	3-O	0.028
$8g_2$	1-C	0.082
	3-O	0.068

the higher electrophilicity of oxygen atom rather than carbon atom. Hence it can be predicted that the intermediate (7g1) must follow path 1. This prediction can be further supported by the analysis of electrostatic potential (ESP). The calculated electrostatic potential partial charges of the reacting sites of the intermediate ($7g_1$) and the transition state (TS6) are given in Table 4.5. There is some positive ESP charge on I atom in the intermediate whereas in the transition state it gains negative ESP charge. As the reaction proceeds from the intermediate to the transition state the negative ESP charge on C-5 atom shrinks and it is strewn on the I atom so that the I atom can be eliminated as I^- leaving C-5 as a site for nucleophilic attack. Increase of ESP charge (from 0.436 to 0.447) on hydrogen atom of –OH in the transition state (TS6) indicates the liberation of proton. The authenticity of the transition state (TS6) is thus justified by ESP analysis and the mechanism of this step is well understood. This step of the reaction requires an activation barrier of 680.747 kJ mol^{-1} and it is impulsive in nature (ΔG =–34.765 kJ mol^{-1}).

Table 4.5

ESP partial atomic charges of 7g1 and TS6 computed at the UB3LYP level.

Atom[a]	Partial atomic charges	
	7g1	TS6
C1	−0.460	−0.546
O3	−0.546	−0.534
H4	0.436	0.447
C5	−1.255	−0.816
I6	0.165	−0.014

[a] The atomic numbering system is shown in scheme 4.1.

However, in case of the reaction between 1, 3-indanedione and 3-nitro benzaldehyde the alternative path is followed; i.e., reaction takes place through C-attack. In this case the reaction proceeds through the transition state, TS7 (imaginary frequency $-230.84\ cm^{-1}$). Condensed Fukui function (f_k^-) has been calculated for the intermediate $8g_2$ (Table 4.4) which indicates higher susceptibility of electrophilic attack at carbon atom rather than oxygen atom. So the involvement of path 2 for the second case is well supported and predicted. This prophecy is further justified by ESP analysis. There is negative ESP charge on C-5 in the intermediate ($8g_2$) but it gains positive ESP charge (+0.051) in the transition state (Table 4.6). Positive ESP charge on hydrogen atom of OH increases from +0.442 to +0.505 in the transition state and iodine gains negative ESP charge (−0.321) in the transition state. This indicates liberation of proton and iodide ion in the form of HI. So the reaction proceeds in the right direction through this transition state (TS7) i.e., the authenticity of the transition state as well as the mechanism of this step are established by ESP analysis. This step of cyclization requires an activation energy of 728.312 kJ mol^{-1} and it is slightly endothermic (ΔH=121.509 kJ mol^{-1}) in nature.

Table 4.6

ESP partial atomic charges of 8g2 and TS7 computed at the UB3LYP level.

Atom[b]	Partial atomic charges	
	8g2	TS7
C1	−1.245	−0.236
C2	0.550	0.632
O3	−0.576	−0.558
H4	0.442	0.505
C5	−0.821	0.051
I6	0.130	−0.321

[b] The atomic numbering system is shown in scheme 4.1.

For the last two alternating steps we have calculated the nucleus independent chemical shift (NICS) of the intermediates, transition states and products (Table 4.7 and

Table 4.8) to establish the feasibility of the reaction. If we consider the first path (path 1), in the intermediate (7g1) all the rings are seen to be aromatic in nature [negative NICS(0) and NICS(1)]. Now when the intermediate (7g1) undergoes cyclization via TS6 an additional ring (D) is formed. In the transition state NICS(0) and NICS(1) values of the new ring (D) are found to be negative. For ring D, NICS(1) value is smaller than NICS(0) and both values increase in the product (7h1). Now for the second path of cyclization (path 2), the intermediate (8g2) possesses four aromatic rings. In the transition state (TS7) an additional ring (F) is being formed which is extremely aromatic in nature [NICS(0) value −35.56]. Both values [NICS(0) & NICS(1)] of ring (F) increase in the product (8h2). So the driving force of these two pathways is obviously the huge gain in aromaticity. Indeed this argument lends a strong support for this so-called unusual reaction.

Table 4.7

NICS(0) and NICS(1) values of 7g1, TS6 and 7h1 computed at the UB3LYP level.

	7g1		TS6		7h1	
Ring	NICS(0)	NICS(1)	NICS(0)	NICS(1)	NICS(0)	NICS(1)
A	−8.51	−10.72	−6.56	−8.40	−9.00	−10.96
B	−0.42	−1.29	0.26	0.07	−1.09	−3.10
C	−1.32	−1.53	0.86	−2.69	−1.32	−1.54
D	--	--	−2.88	−0.32	−5.10	−1.49
$NICS_{Total}$	−10.25	−13.54	−8.32	−11.34	−16.51	−17.09

Table 4.8

NICS(0) and NICS(1) values of 8g2, TS7 and 8h2 computed at the UB3LYP level.

	8g2		TS7		8h2	
Ring	NICS(0)	NICS(I)	NICS(0)	NICS(I)	NICS(0)	NICS(I)
A	−9.34	−10.94	−8.80	−10.87	−8.61	−10.55
B	−7.45	−10.83	−6.31	−9.33	−7.6	−10.49
C	3.90	−3.28	5.78	−0.78	5.78	−1.21
D	−6.24	−9.15	−6.65	−8.97	−7.54	−10.61
E	6.60	0.87	4.58	−0.85	5.66	−0.96
F	--	--	−36.25	−4.77	−35.56	−6.11
$NICS_{Total}$	−12.53	−33.33	−47.65	−35.57	−47.87	−39.93

As the applied functional is reported to be inadequate in producing an accurate picture of potential energy surface, [21-23] the results have been compared with single point MP2 calculations on B3LYP optimized geometries. MP2 energies of the reactants, transition states and products reproduce the energy ordering of DFT functional but with an overall scaled down representation. Comparison of DFT and post Hartee-Fock results are given in Table 4.1.

4.4 Summary

In this work we have studied the addition mechanism of two molecules of 1, 3-dicarbonyl compound and one molecule of aldehyde in presence of molecular iodine within unrestricted DFT framework using B3LYP hybrid functional. General steps of the reaction are studied using acetyl acetone as 1, 3-dicarbonyl compound and acetaldehyde. There may be two pathways depending on the substitution pattern of 1, 3-dicarbonyl compound. One leads to spiro dihydrofuran and other cyclopropane derivatives. Paths being followed in either situation can be predicted by condensed Fukui function calculation and by ESP analysis. In each steps transition states are calculated. Vibrational analysis, IRC calculations and ESP analysis confirm these transition states. The nucleus independent chemical shift (NICS) calculation suggests that the gain in aromaticity plays an important role in the last step of the reaction. Thermochemical analysis is in good agreement with each step of the proposed mechanism. As a whole, the present DFT study explains well the experimental finding and also provides the details of the reaction mechanism.

4.5.1 References and notes

1. Salaun, J.; Baird, M. S. *Curr. Med. Chem.*, **1995**, *2*, 511.
2. Lin, H. W.; Walsh, C. T. *The Chemistry of the Cyclopropyl Group*; (Ed. Rappoport, Z.) John Willey and Sons Ltd., New York, **1987**.
3. Salaun, J. *Top. Curr. Chem.* **2000**, *207*, 1.

4. Faust, R. *Angew. Chem. Int. Ed,* **2001**, *40*, 2251.
5. Wessjohann, L. A.; Brandt, W. *Chem. Rev.* **2003**, *103*, 1625.
6. (a) Wang, G. W.; Gao, J. *Org. lett.*, **2009**, *11*, 2385. (b) Lebel, H.; Marcoux, J. F.; Molinaro, C.; Charette, A. B. *Chem. Rev.*, **2003**, *103*, 977. (c) Long, J.; Yuan, Y.; Shi, Y. *J. Am. Chem. Soc.*, **2003**, *125*, 13632. (d) Yang, D.; Gao, Q.; Lee, C. S.; Cheung, K. K. *Org. Lett.* **2002**, *4*, 3271. (e) Ni, A.; France, J. E.; Davies, H. M. L. *J. Org. Chem.*, **2006**, *71*, 5594. (f) Xu, Z. H.; Zhu, S. N.; Sun, X. L.; Tang, Y.; Dai, L. X. *Chem. Commun.* **2007**, 1960. (g) Hashimoto, T.; Naganawa, Y.; Kano, T.; Maruoka, K. *Chem. Commun.* **2007**, 5143. (h) Thompson, J. L.; Davies, H. M. L. *J. Am. Chem.* Soc. **2007**, *129*, 6090.
7. Nakanishi, K. *Natural Products Chemistry*, Kodansha Ltd., Academic, New York, **1974**.
8. Meyers, A. I. *Heterocycles in Organic Synthesis*, John Wiley & Sons, New York, **1974**, pp. 128-129.
9. Dean, F. M. *In Advances in Heterocyclic Chemistry*; (Ed. Katritzky, A. R.), Academic, New York, **1982**, *30*, 167.
10. Vernin, G. *The Chemistry of Heterocyclic FlaVoring and Aroma Compounds*; Ellis Horwood, Chichester, **1982**.
11. Danheiser, R. L.; Stoner, E. J.; Koyama, H.; Yamashita, D. S.; Klade, C. A. *J. Am. Chem. Soc.*, **1989**, *111*, 4407.
12. Fraga, B. M. *Nat. Prod. Rep.*, **1992**, *9*, 217.
13. Merrit, A. T.; Ley, S. V. *Nat. Pro. Rep.*, **1992**, *9*, 243.
14. (a) Mcdonald, F. E.; Connolly, C. B.; Gleason, M. M.; Towne, T. B.; Treiber, K. D. *J. Org. Chem.*, **1993**, *58*, 6952. (b) Pirrung, M. C.; Blume, F. *J. Org. Chem.* **1999**, *64*, 3642. (c) Lee, Y. R.; Suk, J. Y. *Tetrahedron.*, **2002**, *58*, 2359. (d) Lee, Y. R.; Hwang, J. C. *Eur J. Org. Chem.*, **2005**, 1568. (e) Hwu, J. R.; Chen, C. N.; Shiao, S. S. *J. Org. Chem.* **1995**, *60*, 856. (f) Nishino, H.; Nguyen, V. H.; Yoshinaga, S.; Kurosawa, K. *J. Org. Chem.*, **1996**, *61*, 8264. (g) Garzino, F.; Meou, A.; Brun, P. *Tetrahedron Lett.*, **2000**, 41, 9803. (h) Burgaz, E. V.; Yilmaz, M.; Pekel, A. T.; Oktemer, A *Tetrahedron* **2007**, *63*, 7229. (i) Wang, G. W.; Dong, Y. W.; Wu, P.; Yuan, T. T.; Shen, Y. B. *J. Org. Chem.*, **2008**, *73*, 7088.

15. Gennari, C.; Todeschini, R.; Beretta, M. G.; Favini, G.; Scolastico, C. *J. Org. Chem.* **1986**, *51*, 612.
16. Bouillon, J.-P. ; Portella, C.; Bouquant, J.; Humbel, S. *J. Org. Chem.* **2000**, *65*, 5823.
17. Arno, M.; Domingo, L. R. *Theor. Chem. Acc.*, **2002**, *108*, 232.
18. Zardoost, M. R. *Russ. J. Phys. Chem. B.*, **2013**, *7*, 540.
19. Liu, J.; Yang, Z.; Wang, Z.; Wang, F.; Chen, X.; Liu, X.; Feng, X.; Su, Z.; Hu, C. *J. Am. Chem. Soc.*, **2008**, *130*, 5654.
20. Fu, A.; Zhao, C.; Li, H.; Tian, F.; Yuan, S.; Duan, Y.; Wang, Z.; *J. Phys. Chem.* A., **2013**, *117*, 2862.
21. Polo, V.; Grafenstein, J.; Kraka, E.; Cremer, D. *Theor. Chem. Acc.*, **2003**, *109*, 22.
22. Johnson, B. G.; Gonzales, C. A.; Gill, P. M. W.; Pople, J. A. *Chem. Phys. Lett.*, **1994**, *221*, 100.
23. Eriksson, L. A.; Kryachko, E. S.; Nguyen, M. T. *Int. J. Quantum. Chem.* **2004**, *99*, 841.
24. Yang, W.; Morteir, W. J. *J. Am. Chem. Soc.*, **1986**, *108*, 5708.
25. Vos, A. M.; Schoonheydt, R. A.; Proft, F. D.; Geerling, P. *J. Catal.*, **2003**, *220*, 333.
26. Chattaraj, P. K.; Maiti, B. ; Sarkar, U. *J. Phys. Chem.* A., **2003**, *107*, 4973.
27. Fukui, K.; Yonezawa, T.; Shingu, H. *J. Chem. Phys.*, **1952**, *20*, 722.
28. Parr, R. G.; Yang, W. *J. Am. Chem.* Soc., **1984**, *106*, 4049.
29. Yang, W.; Mortier, W. J. *J. Am. Chem.* Soc., **1986**, *108*, 5708 .
30. Morao, I.; Cossio, F. *J. Org. Chem.*, **1999**, *64*, 1868.
31. Jiao, H.; Schleyer, P. V. R. *J. Phys. Org. Chem.*, **1998**, *11*, 655.
32. Gonzalez-Navarrete, P.; Coto, P. B.; Polo, V. Andres, J. *Phys. Chem. Chem. Phys.*, **2009**, *11*, 7189.
33. Pena-Gallego, A.; Rodriguez-Otero, J.; Cabaleiro-Lago, E. M. *Tetrahedron.*, **2007**, *63*, 11617.
34. Poater, A.; Ribas, X.; Liobet, A.; Cavallo, L.; Sola. M. *J. Am. Chem. Soc.*, **2008**, *130*, 17710.
35. Frisch, M. J.; Trucks, G. W.; Schlegel, H. B.; Scuseria, G. E.; Robb, M. A.;

Cheeseman, J. R.; Montgomery, J.; Vreven, Jr. T.; Kudin, K. N.; Burant, J. C.; Millam, J. M.; Iyengar, S. S.; Tomasi, J.; Barone, V.; Mennucci, B.; Cossi, M.; Scalmani, G.; Rega, N.; Petersson, G. A.; Nakatsuji, H.; Hada, M.; Ehara, M.; Toyota, K.; Fukuda, R.; Hasegawa, J.; Ishida, M.; Nakajima, T.; Honda, Y.; Kitao, O.; Nakai, H.; Klene, M.; Li, X.; Knox, J. E.; Hratchian, H. P.; Cross, J. B.; Adamo, C.; Jaramillo, J.; Gomperts, R.; Stratmann, R. E.; Yazyev, O.; Austin, A. J.; Cammi, R.; Pomelli, C.; Ochterski, J. W.; Ayala, P. Y.; Morokuma, K.; Voth, G. A.; Salvador, P.; Dannenberg, J. J.; Zakrzewski, V. G.; Dapprich, S.; Daniels, A. D.; Strain, M. C.; Farkas, O.; Malick, D. K.; Rabuck, A. D.; Raghavachari, K.; Foresman, J. B.; Ortiz, J. V.; Cui, Q.; Baboul, A. G.; Clifford, S.; Cioslowski, J.; Stefanov, B. B.; Liu, G.; Liashenko, A.; Piskorz, P.; Komaromi, I.; Martin, R. L.; Fox, D. J.; Keith, T.; Al-Laham, M. A.; Peng, C. Y.; Nanayakkara, A.; Challacombe, M.; Gill, P. M. W.; Johnson, B.; Chen, W.; Wong, M. W.; Gonzalez, C. and Pople, J. A. Gaussian 03, Revision D.01, Gaussian, Inc., Wallingford, CT, **2004**.

Chapter 5

Performance of the Widely Used Minnesota Density Functionals for the Prediction of Heat of Formations, Ionization Potentials of Some Benchmarked First Row Transition Metal Complexes

We have computed and investigated the performance of Minnesota density functionals especially the M05, M06 and M08 suite of complementary density functionals for the prediction of the heat of formations (HOFs) and the ionisation potentials (IPs) of various benchmark complexes containing nine different first row transition metals. The eight functionals of M0X family, viz. the M05, M05-2X, M06-L, M06, M06-2X, M06-HF, M08-SO and M08-HX are taken for the computation of the above mentioned physical properties of such metal complexes along with popular Los Alamos National Laboratory 2 double-ζ (LANL2DZ) basis set. Total 54 benchmark systems are taken for HOF calculation, whereas the 47 systems among these benchmark complexes are chosen for the calculation of IPs due to lack of experimental results on rest of the 7 systems. The computed values of HOFs and IPs are compared with the experimental results obtained from the literature. The deviation of these computed values from the actual experimental results is calculated for each eight different M0X functionals to judge their performances in evaluating these properties. Finally, a clear relationship between the exchange correlation energy of eight M0X functionals and their efficiency are made to predict the different physical properties.

5.1 Introduction

The performance to cost ratio advantage makes Kohn-Sham density functional theory (KS-DFT), one of the most accepted tools to the researchers of theoretical and computational chemistry. Lots have been said and published about DFT in the last two decades.[1] A simple Google search about DFT fetches 16,600,000 wave pages just in 0.15 second where much of the content is about theory, methodical developments, applications and so on. The DFT is a powerful methodology for chemical simulation where the energy of the systems can be defined in terms of its electron probability density (ρ), that is, in DFT formalism the electronic energy E is treated as the functional of the electron density $E(\rho)$. Further, the simplicity of the DFT based methods over *ab initio* methods can be best understood by considering a system having n electrons. In such systems the wavefunctions have 3 coordinates for each electron and there must be one extra coordinate if spin is taken into consideration. However, the electron density actually depends on the 3 coordinates and is independent of the number of total electrons of the system. As a matter of fact, if complexity in the wavefunction is increased for the large systems the electron density keeps up the same number of variables, irrespective of the size of the system.[2]

Today, one can find different functionals which are developed by manipulating the different values of exchange and correlation contributions. However, Perdew and Schmidt[3] have successfully represented their vision on the progress of DFT functionals in the form of Jacob's ladder, the famous allusion from the book of *Genesis* (*28, 10-12*), in a DFT symposium in Menton, France. The ladder has five different rungs depicting the five different generations of DFT functionals (Scheme 5.1). One gets local density approximation (LDA) in the first rung, generalized gradient approximation (GGA) stands in the second rung, meta generalized gradient approximation (M-GGA) remains in the third rung, whereas the hybrid generalized gradient approximation (H-GGA) and hybrid meta generalized gradient approximation (HM-GGA) stand in the fourth rung and the fully nonlocal approximation remains in the last rung when moving from the lower to the higher steps in the Jacob's ladder. One should note that, the HM-GGA functional is the

combination of GGA, M-GGA and H-GGA functionals. If one climbs up with the ladder one needs to assume more and more sophisticated and complicated approximation and eventually reach the heaven of chemical accuracy. A point to be mentioned here is that, each rung has its own drawbacks and advantages. Although the better rung gives better results than its lower one, however, the choice of functionals somehow depends on the nature of the problems. All the above mentioned discussions are nicely portrayed in an elaborate review of Ramos et al.[4] Another point to be mentioned here is that a new class of rung on the Jacob's ladder called "rung 3.5" which is an intermediate between the local and hybrid functionals is implemented by Janesko.[5] The rung 3.5 has the potential to produce more accurate results than the local and semilocal functionals.

Scheme 5.1 The vision of Perdew for Jacob's ladder of five generation DFT functionals from the world of Hartree to the heaven of chemical accuracy, with the indication of most popular eight different M0X density functionals.

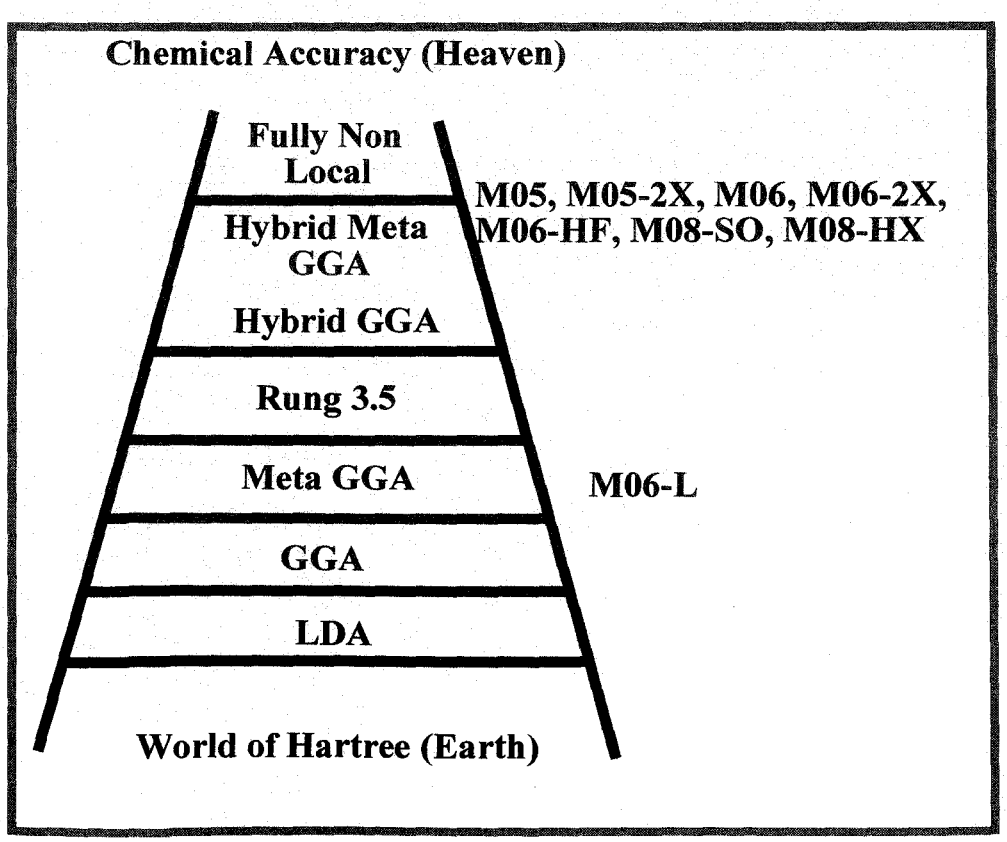

After, early 1990s with the appearance of Becke 3 parameter exchange and Lee, Yang, Parr correlation functional (B3LYP),[6] the computational treatment has multiplied the wide possibilities of this field of research. The most admired and robust exchange correlation functional B3LYP having 20% exact exchange assorted with exact GGA functional gives excellent results in myriad studies. However, in predicting the energy barriers, weak intramolecular interactions, and bonding in transition metals (TMs), B3LYP has faced some serious drawbacks. The hybrid B3LYP functional has failed to predict properties of different extended systems than other hybrid functionals. Even in the prediction of atomization energies the semiemperical B3PW98 functional has shown improved performance compared to the hybrid B3LYP functional.[7] As a result, past decade has witnessed the development and validation of different exchange correlation functionals by various research groups in order to surmount these pitfalls. A notable point is that, the choice of functionals depends on the problem in hand, that is, on the nature of the systems, property of the systems, and obviously on the computational cost and accessibility of these functionals. Zhao and Truhlar[8] have presented and parameterized new suite of functionals with flourishing performances. To carry out both for TMs and main group chemistries they have proposed Minnesota 2005 hybrid meta GGA exchange correlation functional, the M05 functional,[9] with 28% exact exchange (χ) which reduces the self interaction error (SIE) and the self correlation error (SCE) from the calculations. In the next year, M05-2X[10] functional has been developed in which they have doubled the exact exchange (χ =56%) contribution while trimming down the SIE. In 2006, with the next attempt they have developed two other functionals, the non-hybrid meta GGA, the M06-L[11] functional with χ=0% and the hybrid meta GGA M06-HF functional[12] having χ=100%. Being a local functional M06-L can be applied for large systems with low costs. The M06-L functional is also very suitable for TM systems. The M06-HF functional is constructed as a variant of M06-L having full Hartee Fock exchange which completely takes out SIE from the functional, although due to the multireference character it is generally recommended for main group elements. After designing M06-L and M06-HF they have redesigned and reoptimized M05 to get M06[13] with χ=27% instead of χ=28% in M05. After that, they have developed the M06-2X functional[11] in doubling the amount of exact exchange correlation (χ=54%), as in M06. In

2008 they have further developed two improved versions of M06-2X namely Minnesota 2008 high X represented as M08-HX and Minnesota 2008 second order designated as M08-SO, both having fractional HF exchange viz. χ=52.23% and 56.79% respectively. In M08-HX functional the 'X' is the usual HF exchange, and in M08-SO the 'SO' denotes second order gradient expansion. These two functionals are mainly parameterized for the main group thermo chemistry, kinetics and non-covalent interactions. Nonetheless, the execution of M08-HX functional in the calculation of main group thermochemistry, non-covalent interactions and kinetics is slightly better than the other two functionals viz. M08-SO and M06-2X functionals and considerably better than M05-2X functional as advocated by the developers.[14] One can consider that, the M05 and the M05-2X functionals are the earlier version of M06 and M06-2X functionals, whereas, the M08-HX and M08-SO are regarded as two improved future versions of the M06-2X functionals. The readership may note that, in paper after paper, the poor performances of the M05-2X,[8,10] M06-2X,[8,10] M06-HF,[8,12] M08-SO[14] and M08-HX[14] functionals in predicting the thermochemical parameters in TM systems are advocated by Zhao and Truhlar. The eight different M0X functionals, their year of invention, their type according to Perdew ladder and the percentage of HF exchange are depicted in Table 5.1. It is to be noted here that, except non hybrid meta GGA functional M06-L which resides in the third rung of Jacob's ladder, all other above mentioned functionals are HM-GGA functionals and correspond to the fourth rung of Jacob's ladder (Scheme 5.1) as proposed by Perdew et al.[3]

In different literatures Merz and co-workers[15] have studied lots of TM- complexes with different DFT functionals from GGA to HMGGA (excluding LSDA) as DFT is not a single method rather a family of methods.[3] The accuracy in predicting exchange coupling constants through M0X suite of functionals has been studied by Ruiz.[16] The application and validation of Minnesota density functionals highlighting nanochemistry, organic, inorganic, biological and medicinal chemistry, catalysis etc. have been illustratively reviewed by Zhao and Truhlar.[8]

Table 5.1 The eight M0X suite of functionals, their year of invention, type and percentage of Hartree-Fock (HF) exchange which are used in this work are depicted below.

Functionals	Year of invention	Type	Percent of HF exchange (χ)
M05	2005	HMGGA	28
M05-2X	2006	HMGGA	56
M06-L	2006	MGGA	0
M06	2008	HMGGA	27
M06-2X	2008	HMGGA	54
M06-HF	2006	HMGGA	100
M08-SO	2008	HMGGA	56.79
M08-HX	2008	HMGGA	52.23

Ionisation potential (IP) is a significant property of a molecule or atom from which one can assess the firmness by which an electron is bound with the system and therefore it is a descriptor of stability and reactivity of that substance. On the other hand, the heat of formation (HOF) is the enthalpy change due to the formation of one mole of a substance in its most stable state from its constituent elements. This property is used to evaluate the stability as well as other different thermodynamic parameters. However, these two physical parameters have momentous impact on photoelectron spectroscopy, thermo chemistry and so on.

Recent past has witnessed the performance of DFT methodology to describe the several properties for systems containing TMs.[17] Merz and co-workers have carried out two different works on first row TM complexes applying four different rungs of DFT functionals with varying basis sets to analyze their different physical properties.[15] Quadruple ζ-quality basis set has been used to evaluate bond energies, molecular structures, dipole moments etc. of TM complexes by Furche and coworkers.[18] The B3LYP exchange correlation functional along with LANL2DZ and CEP-31G* basis set have been used by Cundari et al. to evaluate the accuracy in predicting HOF for metal based systems.[19] Several iron containing systems have been studied by Glukhovtsev et

al.[20] to assess their bond dissociation energies, ionization potentials, enthalpies of formations etc. with B3LYP functional and pseudo-potential based basis set. Truhlar and coworkers have theoretically studied different coordination compounds of zinc to focus on the metal-ligand bond distance, dipole moments and so on with two different basis sets along with 39 DFT methodologies.[21] Logically, as a matter of fact, the diverse work with TM complexes have inspired our urge to analyse thoroughly the different physical properties of first row TM complexes by applying eight different M0X functionals with most popular LANL2DZ basis set and to compare these results with the recent experimental data which are found in literature. The main goal of this work is to analyze the accuracy and consistency of eight different M0X suite of functionals on different first row TM complexes in predicting the ionization potentials (IPs) and the heat of formations (HOFs). Further one may note that, all these M0X functionals are being tested in predicting different physical parameters outside our recommended usage domain in the recent past.[8,14]

5.2 Methodology

We are in an era of change. Although B3LYP is the most widely used functional in the quantum chemistry panacea; however, the different M0X group of functionals have the ability to compete with the B3LYP results in defining several chemical properties.[4] Here, on one hand, we have taken one non-hybrid meta GGA functional and on the otherhand seven hybrid meta GGA functionals to form the M0X family of functionals for our study. The calculations in this study have been done using Gaussian 09W quantum chemical software.[22] As Gaussian 09W does not consider M08 set of functionals; hence, we have chosen Gamess[23] code to evaluate the HOF and IP values in M08-SO[14] and M08-HX[14] functionals. Gauss view 5.0[24] is used for the structural analysis, frequencies, and forces of these different transition metal complexes. Riley et al. have advocated over the fact that in calculating the IP values, the hybrid meta GGA functionals give best results, whereas the meta GGA functionals along with the earlier hybrid meta GGA functionals is found suitable to evaluate the HOF results.[25] Along with this M0X suite of functionals we have used pseudo-potential based Los Alamos National Laboratory 2

double-ζ (LANL2DZ) basis set. In this economic and widely applied basis set, the core electrons correspond to the effective core potential and the outer electrons are represented by double-ζ atomic orbitals. In general, the metals are well described by this LANL2DZ basis set.[26] We have calculated the IPs in the adiabatic framework. The HOFs values are calculated form the method described in the white paper "*Thermochemistry in Gaussian*" as always available in web. The experimental results are taken from *NIST Chemistry WebBook* for both IPs and HOFs as suggested by Merz and co-workers.[15] We have optimized the molecular geometries of these TM complexes at first and then with the optimized structures having lowest electronic energy we have computed HOFs and IPs at the same level of theory. The gas phase optimizations have been carried out with four different spin multiplicities of each system in accordance with the total number of electrons in such system as advocated by Merz et al,[15] and then the single point calculations for the evaluation of zero point energy and enthalpy correction have also been carried out with the geometry of the particular multiplicity where the energy is lowest. The readers may note that, we have used the multiplicities from 1 to 7 for the systems where the multiplicity is odd, whereas for the even multiplicity systems we have considered the multiplicities from 2 to 8 as different DFT methods predict different ground spin states. The tight key word is used for calculating single point calculations of atoms. The spin state with lowest Hartree-Fock energy is taken as ground state of that particular TM complex. The ground state spin multiplicity of the each complex is given categorically in the tabular form in the appendix. This ground state of each complex is further used for the frequency calculations required for IP and HOF estimations. One point to be noted here is that, error means the difference between experimental and theoretical values of the respective parameters. The experimental HOF and IP results in tabular form (Table 1 and Table 2, Appendix) and the required corresponding references from where these experimental values are taken are given in the appendix.

5.3 Results and discussion

The accuracy which is expected from the keen readership of M0X functionals in predicting the HOF and IP values is the main goal of this work as already mentioned. We

have chosen first row TM based benchmark molecules to evaluate their HOF, IP values. All the computed results have been compared with recent experimental (the references 1-12, available in appendix) and the theoretical[15] results. Here, we have taken 54 different TM complexes (six complexes from each nine metals) for calculating HOFs and among them only 47 systems have been taken for the calculation of IP values due to lack of experimental results on the rest 7 systems. IP is a significant character of a molecule or atom by which one can estimate the firmness of an electron to bind with the particular species. As a matter of fact, the IP is a descriptor of stability and reactivity of a substance. On the other hand, HOF basically is the enthalpy change due to the formation of one mole of a substance from its constituent elements. This is another physical parameter which is used to measure the stability as well as to estimate different thermodynamic parameters. These two physical parameters have momentous impact on the photoelectron spectroscopy, thermochemistry and so on.

5.3.1 Heat of Formation (HOF)

In this study, the HOF values of each of the 54 benchmark transition metal based complexes are calculated with eight Minnesota density functionals in combination with LANL2DZ basis set as already mentioned in the methodology section. These computed and experimental HOF values along with the respective deviations are shown in the group of tables represented as Table 4 in Appendix. Figure 5.1 depicts the average unsigned HOF errors for the complete set of TM complexes highlighting the performances of the different M0X suite of functionals. At a first glance of Figure 5.1, one can see that the local functional M06-L is the best performer among all eight M0X functionals which are used in this study. The HOF results obtained from the M05 and M06 functionals show little bit more deviation than the M06-L results. On the other hand, much more deviated results are obtained from M05-2X, M06-2X, M08-SO and M08-HX functionals compared to the other three brethren functionals as mentioned previously. Nonetheless, the M06-HF functional gives the highest deviation in unsigned HOF results. From the above discussion it seems that the

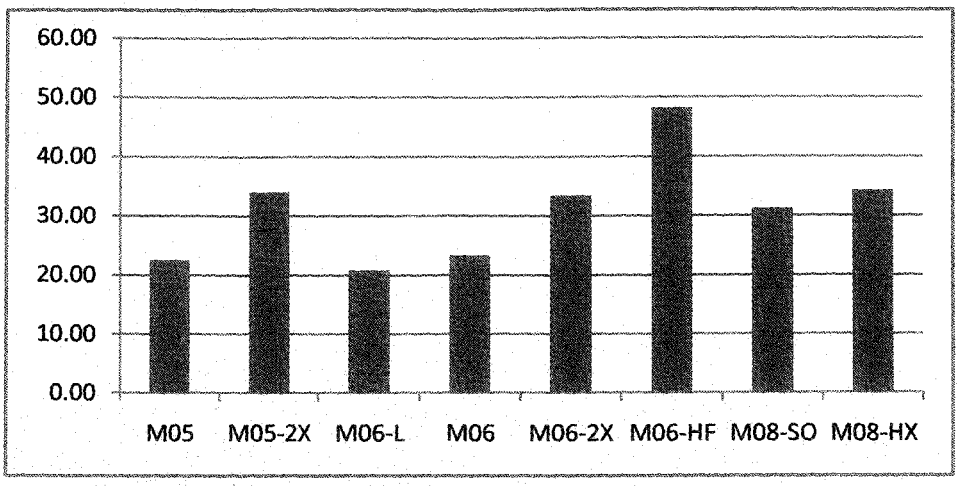

Figure 5.1 The average unsigned heat of formation errors (Kcal/mole) for the complete set of complexes, highlighting the performance of different M0X suite of functionals with LANL2DZ basis set, containing transition metals taken in this study.

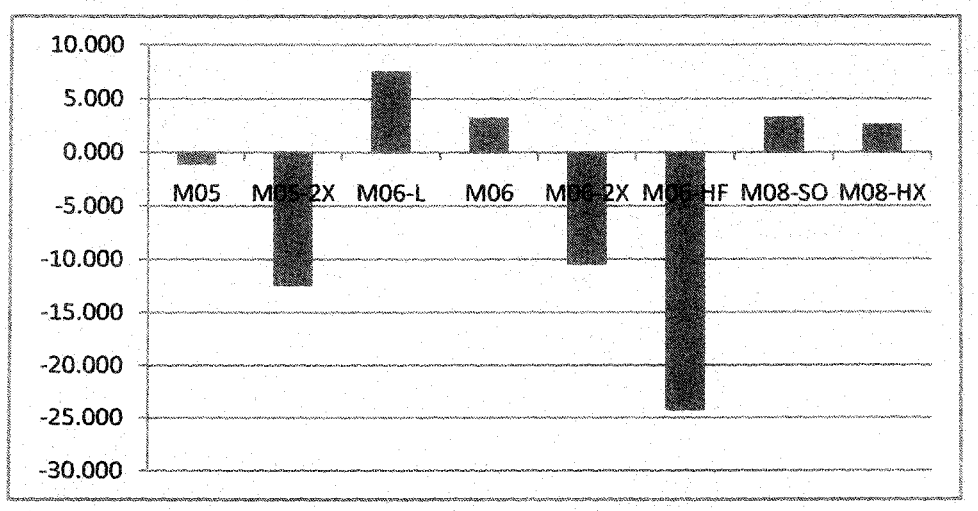

Figure 5.2 The average signed heat of formation errors (Kcal/mole) for the complete set of complexes, highlighting the performance of different M0X suite of functionals with LANL2DZ basis set, containing transition metals taken in this study.

quality of the computed averaged unsigned HOF errors for different TM complexes is increased with the decreased HF exchange. Figure 5.2 describes the average signed HOF errors for the entire 54 TM complexes, where the performances of eight different M0X functionals are decorated. Here, we find that the M06-L, M06, M08-SO and M08-HX

functionals have underestimated the signed HOF errors, whereas another four functionals which are considered in this study have overestimated the same. It is to be noted here is that, among the four best performer functionals mentioned above the performance of the M05 functional is markedly the best. Although the efficiencies of the functionals M06-2X, M08-SO and M08-HX are almost remain in the same range in calculating different thermochemical parameters are claimed by the developers,[14] however, the better performances from the last two functionals (M08-SO and M08-HX) compared to the first one (M06-2X) in predicting HOF errors are found from our study. Nonetheless, the M08-HX functional is found to be the second best performer among the M0X functionals series in predicting the signed HOF errors. The M05-2X and M06-2X have performed almost in a similar fashion whereas the M06-HF is the worst performer among all functionals in predicting the signed HOF errors for these complexes. Here, the M06-L functional gives the average performance in predicting the signed HOF errors, although for the determination of unsigned HOF error its performance is excellent compared to other functionals.

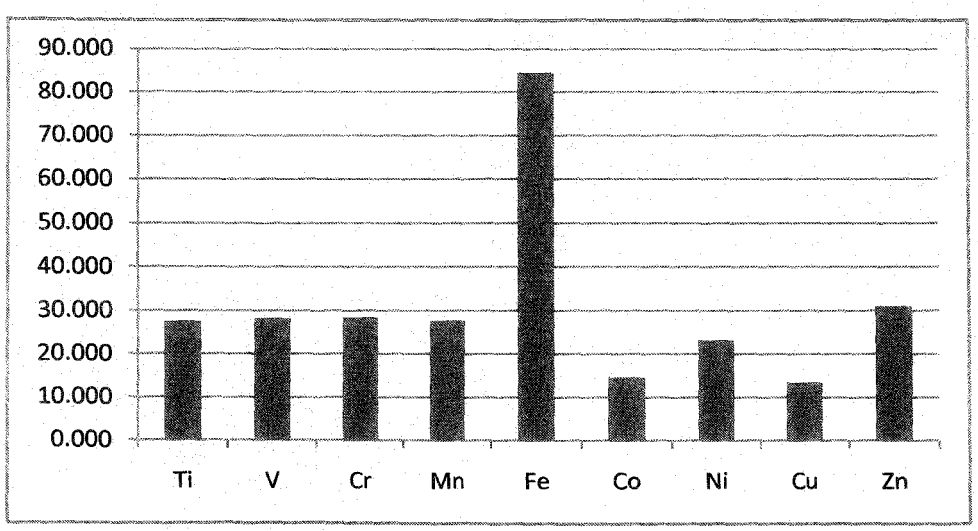

Figure 5.3 The average unsigned heat of formation errors (Kcal/mole) for nine different transition metal complexes considered in this study.

The average unsigned HOF errors for the different TM complex systems are shown in Figure 5.3. If we focus on the Figure 5.3, it is clear that the Co and Cu containing

complexes give the best performances, compared to the complexes containing Ti, V, Cr, Mn, Ni and Zn. These TMs (stated afterwards) containing complexes show average performances inpredicting signed HOF errors. However, the Fe containing complexes give very poor results among the whole TMs series. Riley and Merz have found that the Cr, Ni and Cu are the most problematic transition elements with 6-31G(d,p) basis set; however, this problem is overcome by using mixed basis set approach.[15a] On the other hand, Yang et al.[15b] have found that the Cu complexes give the best average performance

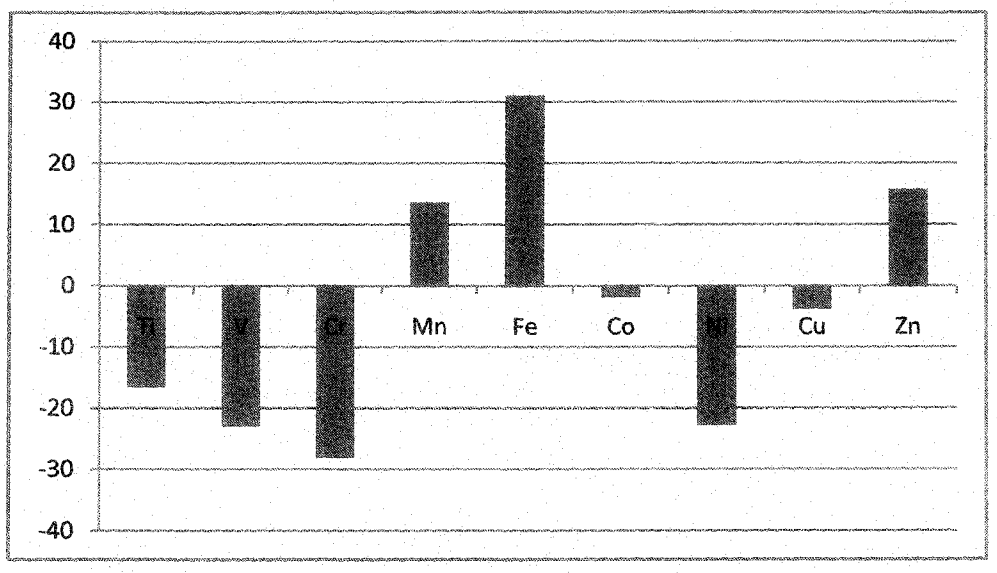

Figure 5.4 The average signed heat of formation errors (Kcal/mole) for nine different transition metal complexes considered in this study.

and Zn complexes give impressive result for its closed shell structure. The Figure 5.4 depicts the average signed HOF errors for the different TM complex systems which are considered in this work. From this Figure, we find that the average signed HOF errors for the Mn, Fe and Zn containing complexes are positive, whereas for other TM complexes these values are negative. Here, in predicting the average signed HOF errors, we also have found that the Co and Cu containing complexes are the best performers, although the Co complexes are the best in accordance with their performances. The Mn and Zn complexes show the almost the same average value of signed HOF errors. This fact is attributed due to the half filled and full filled *d*-orbitals of such metals. Other TMs like Ti, V, Cr, Fe, Ni produce almost similar errors in predicting the average signed HOF

results. One may note that, like unsigned HOF errors the Fe complexes also produce larger deviation of results in predicting the signed HOF.

The Figure 5.5 exhibits the average unsigned HOF errors for various TM-coordinating groups which are considered in this study. It is clear form Figure 5.5 that the carbonyl and methyl ligands containing complexes show most poor results, while the hydride and hydroxide ligands appear to be the most worthy in nature. From Figure 5.6, which gives the average signed HOF errors for various TM ligands used in this study, it

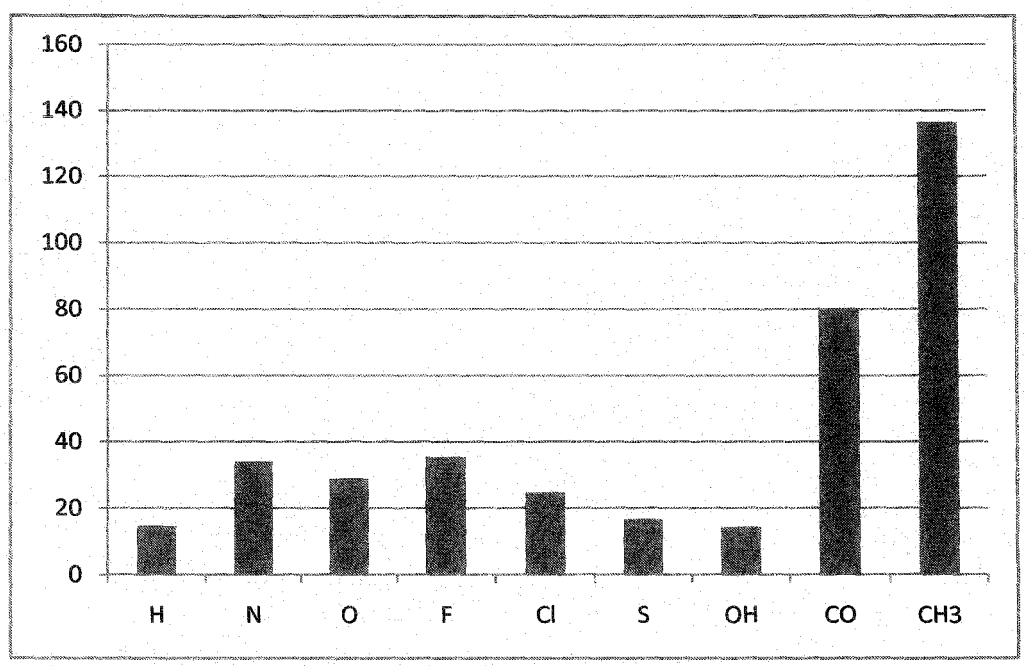

Figure 5.5 The average unsigned heat of formation errors (Kcal/mole) for different transition metal bonding partners treated in this study.

is observed that the hydride, chloride and methyl ligands (3 ligands out of 9) containing TM complexes have overestimated the results, while the other coordinating groups have underestimated the same. Like Figure 5.5, from Figure 5.6 we also have found that the methyl and carbonyl groups containing TM complexes show poor results. However, these latter stated two ligands show errors in opposite direction (Figure 5.6). The admirable signed HOF results are observed from the –H and –F ligands containing complexes.

Nonetheless, it is also observed both from the Figure 5.5 and Figure 5.6 that the $-CH_3$ ligands containing TM complexes show the most disappointment in HOF results.

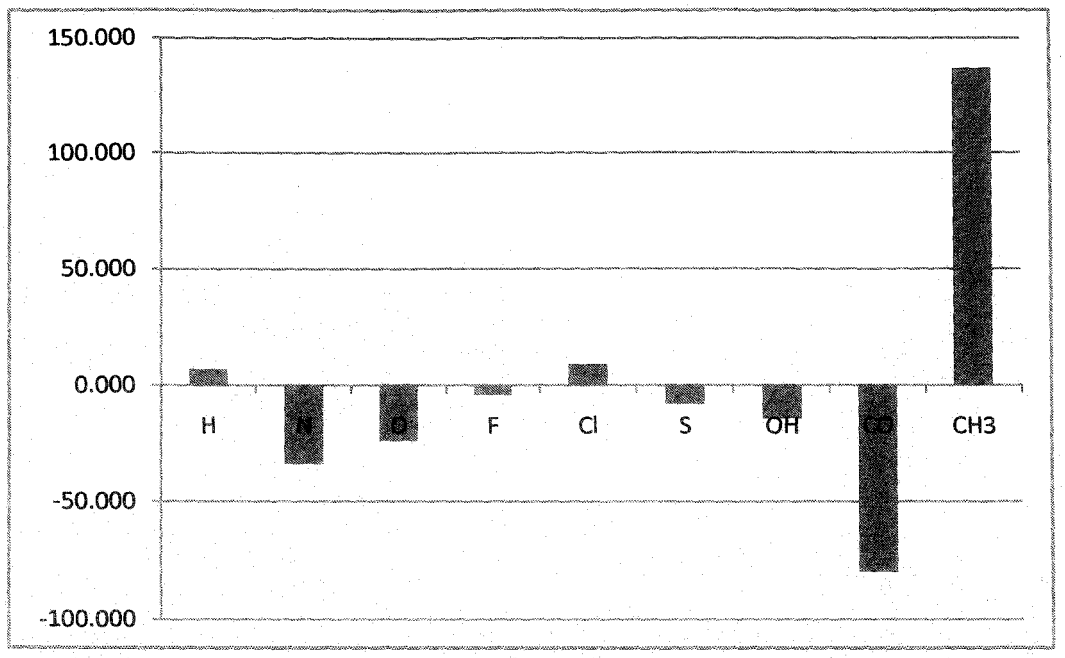

Figure 5.6 The average signed heat of formation errors (Kcal/mole) for different transition metal bonding partners treated in this study.

The Table 5.2 shows the average unsigned HOF errors for the entire set of systems containing various first row TMs against eight different DFT functionals taken in this study. At a first glance on Table 5.2, one can see from the average value that the M06-L functional gives the best performance among all the eight functionals. We also find that the complexes of the Mn, Fe and Zn are the most problematic in predicting their unsigned HOF values with the M06-L functional. The M05 functional shows the best performance for Co complexes only, whereas for Fe and Zn complexes the same functional show the worst results. If we consider the performances of the M05-2X and M06-2X functionals, the Ti, V, Cr, Mn, Fe, Ni and Zn complexes furnish poor results (7 out of 9 cases), whereas the Cu complexes bring better results compared to the other TM complexes. The Fe complexes are shown most erroneous when calculating with the M05-2X, M06-2X, M08-SO, M08-HX and M06-HF functionals. Please be noted that, from the average values (Table 5.2), one can easily surmise that these four M0X functionals,

Table 5.2 The average unsigned heat of formation errors (Kcal/mol) for different TM complexes in different M0X family of functional with LANL2DZ basis set.

Functional	Ti	V	Cr	Mn	Fe	Co	Ni	Cu	Zn	Average
M05	15.805	10.903	18.515	16.377	68.105	8.923	19.362	13.348	31.322	22.518
M05-2X	34.570	32.438	39.532	22.632	83.042	21.163	29.272	12.595	31.347	34.066
M06-L	18.763	10.242	8.653	30.670	66.847	8.330	9.563	5.955	27.773	20.755
M06	18.783	11.802	19.868	23.910	66.708	4.785	19.180	12.847	31.397	23.253
M06-2X	28.570	35.187	41.040	25.977	84.855	18.392	20.752	17.157	29.058	33.443
M06-HF	52.782	60.802	41.502	48.135	99.090	23.867	54.297	23.502	29.293	48.141
M08-SO	28.271	13.839	29.692	18.069	106.262	13.999	20.277	14.882	35.561	31.206
M08-HX	22.515	51.080	28.465	36.163	100.563	17.266	12.486	7.020	32.287	34.205

Table 5.3 The average signed heat of formation errors (Kcal/mol) for different TM complexes in different M0X family of functionals with LANL2DZ basis set.

Functional	Ti	V	Cr	Mn	Fe	Co	Ni	Cu	Zn	Average
M05	-7.775	-10.903	-18.515	16.377	29.005	4.123	-19.362	-13.348	10.108	-1.143
M05-2X	-34.570	-32.438	-39.532	22.632	16.738	-12.960	-29.272	-11.368	8.317	-12.495
M06-L	-6.233	3.872	-7.990	30.670	40.193	2.917	-7.670	0.382	12.120	7.585
M06	-9.577	-6.095	-19.868	23.910	37.185	2.722	-19.180	11.353	8.727	3.242
M06-2X	-27.107	-35.187	-41.040	25.977	19.998	-11.675	-20.752	-17.157	12.378	-10.507
M06-HF	-51.368	-60.803	-40.125	-47.562	5.643	-12.810	-54.297	21.555	20.903	-24.318
M08-SO	-3.951	8.535	-29.692	6.796	45.600	13.197	-20.277	-14.882	24.138	3.274
M08-HX	8.016	-51.080	-28.184	30.047	54.322	-0.502	-11.535	-6.734	29.286	2.626

namely, M05-2X, M06-2X, M08-SO and M08-HX having higher but almost closer HF exchange perform almost in a similar fashion in predicting the unsigned HOF errors. The M06-HF functional is the worst performer among all the M0X series of functionals in predicting the unsigned HOF values for all the TM complexes as evident from the average value. The Table 5.3 lists the average signed HOF errors of the entire set of TM

complexes against different M0X group of functionals considered in this work. From the Table 5.3 it is clear that among the 5 out of 8 functionals the Fe complexes are found to be most problematic. However, the Fe complexes show best result with M06-HF functional (5.643 Kcal/mol) and worst results are furnished by the M08-SO (45.600 Kcal/mol) and M08-HX (54.322 Kcal/mol) functionals. Here, we find from Table 5.3 that the M06-L functional shows the least amount of signed HOF errors for the five out of total nine cases. Nonetheless, these results are found to be lower or nearly equal to the B3LYP results.[15]

Table 5.4 The average unsigned heat of formation errors (Kcal/mol) for the various transition metal bonding partners against different M0X set of functional with LANL2DZ basis set.

Atoms	M05	M05-2X	M06-L	M06	M06-2X	M06-HF	M08-SO	M08-HX	Average
H	7.950	11.808	14.188	10.464	10.830	15.564	19.551	26.264	14.577
N	18.080	50.990	0.250	20.720	46.450	77.030	0.041	58.192	33.969
O	14.886	33.417	9.252	15.116	34.129	58.817	28.850	36.409	28.859
F	29.837	37.906	27.722	33.265	40.286	54.958	32.024	27.377	35.422
Cl	21.376	30.059	20.631	21.502	28.397	28.299	25.517	22.694	24.810
S	10.813	19.467	10.430	7.750	17.117	30.243	13.346	24.730	16.737
OH	16.710	20.290	13.530	18.500	22.390	18.210	4.541	0.314	14.311
CO	49.787	86.320	33.997	41.780	85.770	111.113	99.748	129.118	79.704
CH3	124.290	118.990	119.680	120.370	124.310	137.410	172.548	174.224	136.478

Table 5.5 The average signed heat of formation errors (Kcal/mol) for the various transition metal bonding partners against different M0X set of functionals with LANL2DZ basis set.

Atoms	M05	M05-2X	M06-L	M06	M06-2X	M06-HF	M08-SO	M08-HX	Average
H	3.006	1.768	8.688	3.756	3.322	-7.344	17.566	24.015	6.847
N	-18.080	-50.990	0.250	-20.720	-46.450	-77.030	0.041	-58.192	-33.896
O	-10.504	-32.833	1.448	-10.812	-33.151	-55.355	-16.962	-33.657	-23.978
F	0.395	-5.219	7.375	-1.110	-8.043	-30.837	-5.025	9.808	-4.082
Cl	6.359	0.175	12.254	10.574	6.433	5.505	14.978	15.512	8.974
S	-1.400	-19.467	10.430	2.057	-17.117	-22.863	-6.671	-9.542	-8.072
OH	-16.710	-20.290	-13.530	-18.500	-22.390	-18.210	-4.541	0.314	-14.232
CO	-49.787	-86.320	-33.997	-41.780	-85.770	-111.113	-99.748	-129.118	-79.704
CH3	124.290	118.990	119.680	120.370	124.310	137.410	172.548	174.224	136.478

We also find that when one moves from left to right of the first row TM series, then with the increase of *d* electrons the performance of the functionals having higher exchange correlation energies are increased. From Table 5.4, which shows average unsigned HOF errors for various TMs bonding partners against different M0X set of functionals, it is clear that for the TM-hydrides the M06-L, M06-HF, M08-SO and M08-HX functionals give the pitiable results. For –N and –O containing TM complexes the M06 -L and M08-SO functionals are the best players. For –S– containing TM complexes the use of the M06 functional is suggested. Functional group –OH containing TM complexes give average performance among all the functionals, however, the use of M08-HX is recommended. Carbonyl group containing TM complexes are the poor performers with all the functionals. TMs having $-CH_3$ group as ligands find as the worst player among the entire coordination groups with all the functionals studied here. The performance of the M06-L functional is found to be the best at least in four out of nine cases. Nonetheless, its performances are much better than the performance of the B3LYP functional for the same complexes as obtained in earlier work.[15] The signed HOF errors for various TMs bonding partners against the different M0X set of functionals are shown in the Table 5.5. A close look on the average value furnished in the Table 5.5 shows that the hydride and

fluoride ligands containing TM complexes show better performances than all other ligands, nonetheless the methyl group containing metal complexes show worst performance in predicting the same.

5.3.2 Ionisation Potential (IP)

We have taken 47 TM complexes to evaluate theoretically their IP values using eight different M0X suite of functionals in combination with LANL2DZ basis set as mentioned earlier. The detailed results of IPs for these 47 complexes are depicted in the bunch of tables named as Table 5 in appendix. We have excluded seven TM complexes from the total 54 benchmarked complex systems, *viz*, TiCl, VCl, VF, CoF_2, $CoCl_3$, CuO and CuS due to lack of experimental findings, as without experimental findings it is impossible to calculate the amount of IP errors. We compare these computed IP values with their respective experimental results obtained from the literature. Average unsigned and average signed IP errors for the entire set of TM complexes with respect to the eight M0X suite of functionals are represented with a graphical format in Figure 5.7 and Figure 5.8 respectively. Now, if we take a quick look on Figure 5.7, we can find that maximum erroneous results are shown by M06-HF functional, whereas, M06 functional shows the

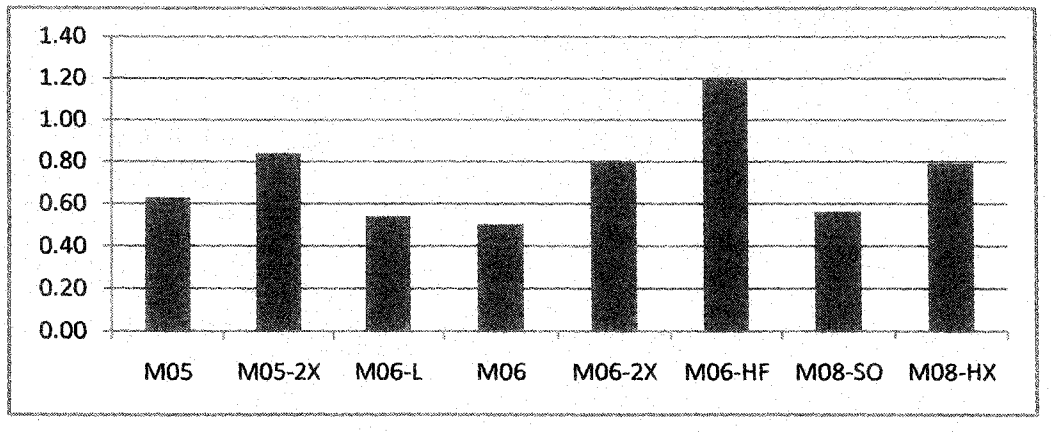

Figure 5.7 The average unsigned ionisation potential errors (*eV*) for the whole set of complexes with these transition metals against different M0X set of functionals with LANL2DZ basis set considered in this study.

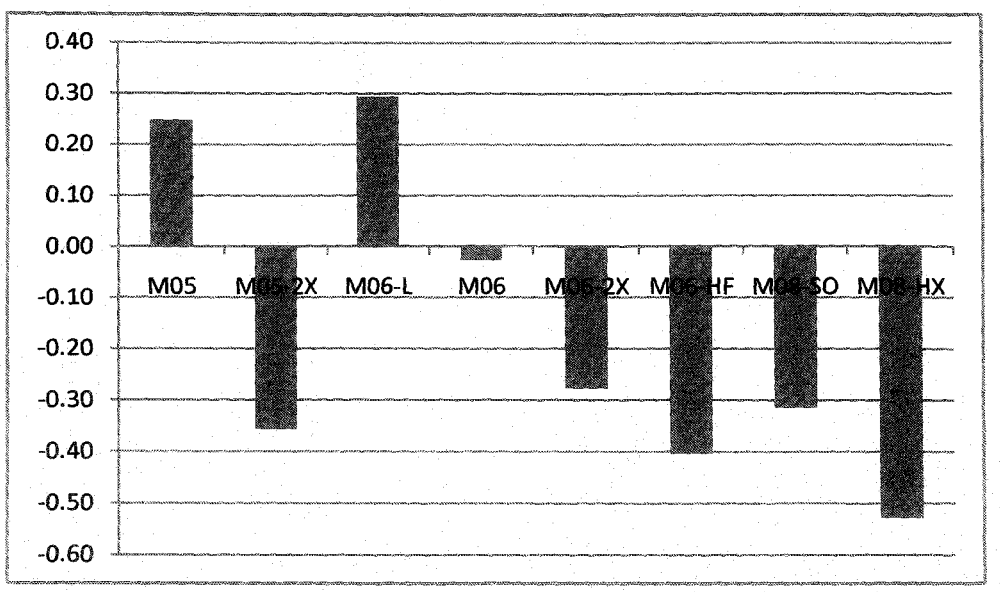

Figure 5.8 The average signed ionisation potential errors (*eV*) for the whole set of complexes with these transition metals against different M0X set of functionals with LANL2DZ basis set in this study.

most correct results among the eight such functionals. The second best functional is M06-L having no HF exchange correlation energy. Please be noted that, the third best is M08-SO functional, which is even better than the M05-2X, M06-2X and M08-HX functionals having almost equal HF exchange. Nonetheless, the accuracy of finding unsigned IP errors by the M06-2X and M08-HX for these TM complexes are found to be almost close to each other. From the Figure 5.8, it is clear that the functionals M05 and M06-L show the errors in positive direction which means that our theoretical calculations for these two functionals give lower values than the corresponding actual experimental results. However, the other six functionals in this family show errors in the negative direction. Although there is a huge difference in χ between the functionals M06-L with the M06-2X and M08-SO; however, their performances are almost same in predicting the signed IP errors although the errors producing by the last two functionals have opposite in sign with that of the first one. If one takes a bird's eye view to both of the Figure 5.7 and Figure 5.8, one can find that the performance of M06 functional is excellent compared to the other functionals in M0X family for the predicting the IP values for the first row TM complexes. Nonetheless, it is needless to say that the performance of M06-HF for the

calculation of unsigned IP errors and the performance of M08-HX for the prediction of signed IP errors is worst among this family of eight functionals.

The average values of the unsigned and signed IP errors of different TM systems against different M0X suite of functionals are given in Table 5.6 and Table 5.7 respectively. In first sight one should get the values of unsigned and signed errors of every individual TMs irrespective of their complexes against all eight M0X functionals from these two tables. From Table 5.6 it is clear that, The computationally low cost local functional M06-L shows overall less erroneous results compared with other meta-hybrid functionals of this family, and some cases these computed values are found to be even lower than the B3LYP errors.[15] We also find a competition between the results among M06-L, M06 and M08-SO functionals, although their HF exchanges are increases sequentially. A quick look on the unsigned IP values reveals that the Ti, Ni, and Zn complexes give less correct results irrespective of all the functionals. However, Ti complexes show more deviation in unsigned IP results as χ increases with an exception for the M08 set of functionals. The highest deviation of results (2.775 eV) is obtained for Cu complexes with the M08-HX functional. The lowest deviation of results (0.11 eV) is observed for M06 functional in case of Cu complexes and also for the M08-SO functional in case of Ti complexes. If one takes all the cases then it is obvious that the worst performer is none other than M06-HF (gives huge errors in 5 out of 9 cases) with cent percent exchange correlation energy. Now, we want to discuss over the values of signed IP errors which are depicted in Table 5.7. Here, one finds that the Zn complexes are most problematic among different molecules taken for this study. The results of Zn and Ni containing complexes deviate more than 0.5 eV with 6 out of 8 functional cases. However, the Ti complexes also have shown same range of deviations in 3 cases. For Ti complexes at higher χ the results are problematic with an exception of M08 set of functionals. Highest deviation (–2.775 eV) is found for M08-HX functional in case of Cu complexes and the lowest deviation i.e. more accurate results (0.035 eV) are observed for Co in case of M06-L functional. From Table 5.7 it is also clear that the M06 functional is the best performer throughout the M0X series for calculating the signed IP errors of these TM complexes, although, the performances of the M06-L, M05 and M06-2X functionals

are also not yet to be neglected. Point to be mentioned here is that, the B3LYP results[15] are found to be outperformed in many cases after calculating these physical quantities with the above mentioned Minnesota density functionals.

Table 5.6 The average unsigned ionisation potential errors (eV) for all the systems containing various transition metals against different M0X set of functionals with LANL2DZ basis set.

Functional	Ti	V	Cr	Mn	Fe	Co	Ni	Cu	Zn	Average
M05	0.680	0.405	0.573	0.748	0.458	0.405	0.705	0.483	1.173	0.626
M05-2X	1.112	0.983	0.985	0.947	0.593	0.72	1.085	0.48	0.643	0.839
M06-L	0.454	0.673	0.503	0.337	0.267	0.575	0.552	0.553	0.932	0.538
M06	0.488	0.275	0.527	0.640	0.402	0.393	0.880	0.11	0.798	0.501
M06-2X	1.300	0.795	0.738	0.657	0.607	0.708	1.198	0.458	0.695	0.795
M06-HF	1.568	0.965	1.063	0.948	1.482	1.275	1.312	1.280	0.877	1.197
M08-SO	0.107	0.079	0.488	0.231	1.684	0.847	0.923	0.422	0.277	0.562
M08-HX	0.263	0.266	0.263	0.242	0.923	0.863	1.109	2.775	0.418	0.791

Table 5.7 The average signed ionisation potential errors (eV) for all the systems containing various transition metals against different M0X set of functionals with LANL2DZ basis set considered for this study.

Functional	Ti	V	Cr	Mn	Fe	Co	Ni	Cu	Zn	Average
M05	-0.348	0.380	0.193	0.525	0.055	-0.120	-0.115	0.483	1.173	0.247
M05-2X	-0.848	-0.318	-0.815	-0.297	-0.287	-0.525	-0.965	0.203	0.643	-0.357
M06-L	0.322	0.673	0.207	0.313	-0.133	0.035	-0.065	0.553	0.742	0.294
M06	-0.156	0.100	-0.127	0.243	-0.115	-0.298	-0.733	0.045	0.798	-0.027
M06-2X	-1.032	-0.050	-0.685	-0.093	-0.18	-0.548	-0.795	0.205	0.690	-0.276
M06-HF	-1.500	-0.510	-1.128	-0.712	-0.375	0.655	-1.125	0.400	0.668	-0.403
M08-SO	0.107	0.079	-0.488	0.231	-1.684	-0.847	-0.923	0.422	0.277	-0.314
M08-HX	0.263	0.266	-0.263	0.242	-0.923	-0.863	-1.109	-2.775	0.418	-0.527

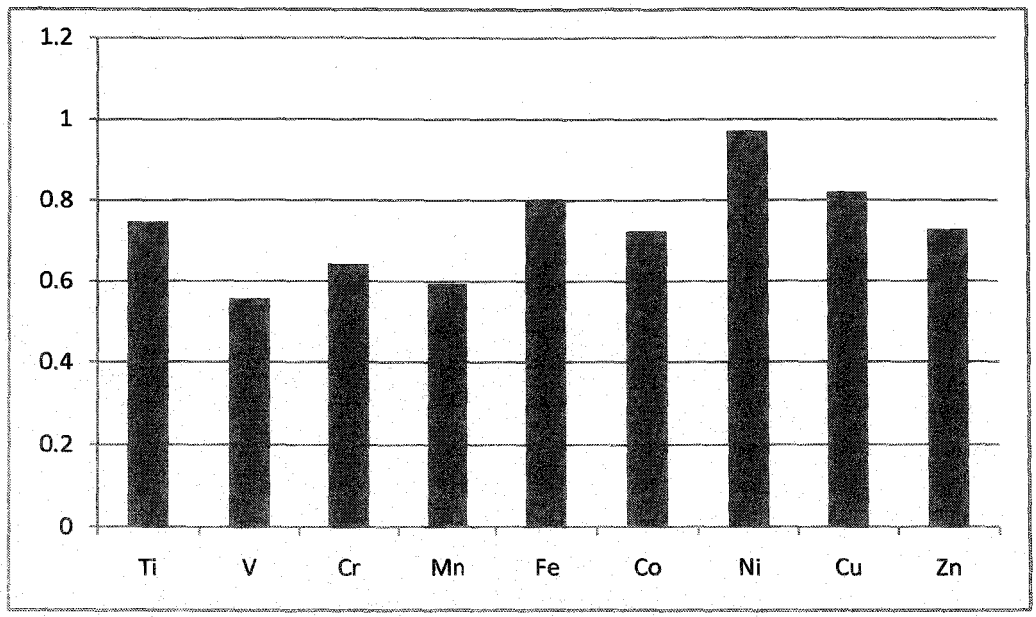

Figure 5.9 The average unsigned ionisation potential errors (eV) for the nine different transition metal systems considered in this study.

The Figure 5.9 and Figure 5.10 depict the average unsigned and signed IP errors respectively for different TM complexes which are chosen for this work. From Figure 5.9 it is clear that V containing complexes show best results among all the TM systems studied here. On the other hand, we find that the results of unsigned IP errors for Fe, Ni and Cu complexes are very large and among them the deviation made by Ni complexes is highest. Nonetheless, the unsigned IP error limits for the other TM complexes are almost in the same range. If one look at Figure 5.10, one can find that the V, Mn and Zn containing complexes show errors in the positive direction, that is the theoretically computed IP values of these complexes are below the respective experimental results and for the other six TM complexes the sign of errors are negative. The lowest signed IP errors are shown by the Mn and Cu complexes but the direction is opposite, whereas like unsigned IP errors the signed IP errors shown by Ni complexes are highest among the series.

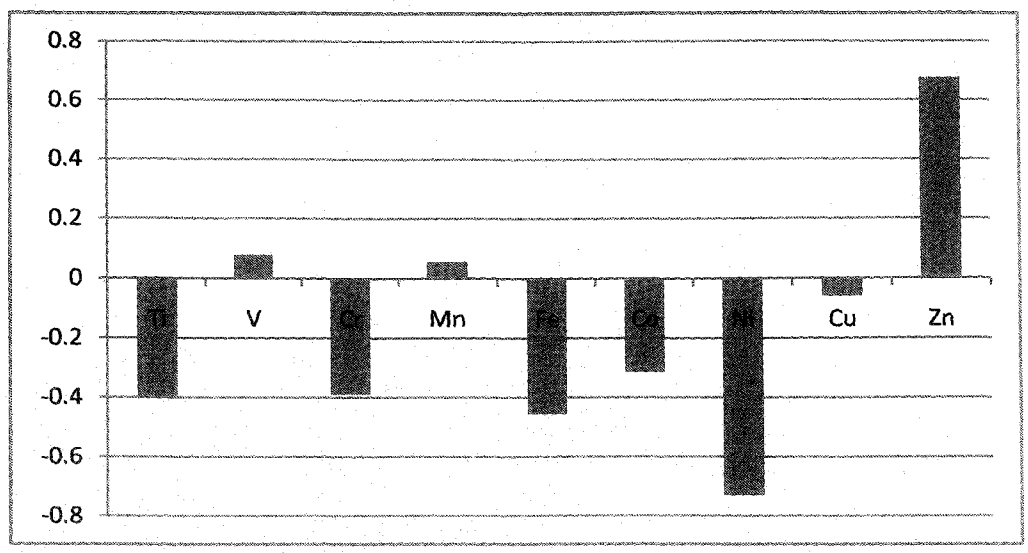

Figure 5.10 The average signed ionisation potential errors (*eV*) for the nine different transition metal systems considered in this study.

The Table 5.8 and Table 5.9 represent the values of unsigned and signed IP errors respectively in different M0X functionals against the different ligands which are used to form different TM complexes. One can easily understand from these two tables that how the different ligands can act in determining IP values irrespective of the different TMs. It is obvious from Table 5.8 that the functionals M05, M06 and M06-L perform well in predicting the average unsigned IP values for systems containing a particular bonding partner. It is also found from the literature that when a particular bonding ligand has more than one atom then the performance of B3LYP[15] functional is increased. From the Table 5.8 it is clear that the M08-HX functional shows the lowest error (0.018 eV) with the –OH functional group among the series and the next less deviated result (0.050 eV) is shown by the M05 functional when –N acts as a ligand. On the other hand, the maximum error (2.135 eV) is observed for the carbonyl group than any other bonding partners with the M08-HX functional. Hence, one can conclude that, the highest and the lowest unsigned IP errors are furnished by the M08-HX functional with the –CO and –OH ligands respectively. On the other hand, in a quick look on the Table 5.9, we find that the M05 functional shows the lowest error (0.005 eV) with the –Cl ligand among the series and the next less deviated results (–0.007 eV) are also shown by the same functional when –CO acts as a ligand. Here, one point to be mentioned is that, for the $-CH_3$ ligand both of the M06-2X and M06-HF functionals give same magnitude of deviation in IP

results (0.08 eV), but they are opposite in sign. If we take an overall view on the results of Table 5.9, we find that the M05 functional performs well (out of 9 cases it gives lowest error in 3 cases). After the M05 functional the credit of accuracy goes to M06-2X functional as it shows less erroneous results in 2 cases each.

Table 5.8 The average unsigned ionisation potential errors (*eV*) for all the systems containing various transition metals coordinating groups against different M0X set of functionals with LANL2DZ basis set considered for this study.

Atoms	M05	M05-2X	M06-L	M06	M06-2X	M06-HF	M08-SO	M08-HX	Average
H	0.966	0.738	0.712	0.988	0.972	0.768	0.929	0.719	0.849
N	0.050	1.160	1.330	0.270	0.920	0.650	0.539	0.075	0.624
O	0.528	0.986	0.496	0.288	0.867	1.140	0.852	0.948	0.763
F	0.695	0.996	0.493	0.534	0.856	1.650	1.738	1.834	1.099
Cl	0.567	0.893	0.327	0.538	0.840	1.284	1.125	1.807	0.923
S	0.425	1.155	0.605	0.355	0.670	0.980	1.127	0.422	0.717
OH	0.130	0.080	0.260	0.140	0.330	0.170	0.061	0.018	0.149
CO	0.740	0.413	0.620	0.830	0.407	0.890	1.437	2.153	0.936
CH3	0.530	0.170	0.320	0.150	0.080	0.080	0.161	0.264	0.219

Table 5.9 The average signed ionisation potential errors (*eV*) for all the systems containing various transition metals coordinating groups against different M0X set of functionals with LANL2DZ basis set considered for this study.

Atoms	M05	M05-2X	M06-L	M06	M06-2X	M06-HF	M08-SO	M08-HX	Average
H	0.474	0.274	0.216	0.164	-0.040	0.112	0.344	0.362	0.238
N	-0.050	1.160	1.330	-0.270	0.920	-0.650	-0.539	0.075	0.247
O	0.488	-0.783	0.298	0.172	-0.416	-0.613	-0.311	-0.237	-0.175
F	0.303	-0.088	0.317	0.148	-0.504	-1.510	-0.721	-0.779	-0.354
Cl	0.005	-0.720	0.242	-0.266	-0.692	-1.149	-0.943	-1.692	-0.652
S	-0.185	-1.155	0.605	-0.355	-0.640	-0.980	-0.134	-0.067	-0.364
OH	0.130	-0.080	0.260	-0.140	-0.330	-0.170	-0.061	0.018	-0.047
CO	-0.007	0.413	-0.620	-0.830	0.407	0.890	1.437	2.153	0.480
CH3	0.530	0.170	0.320	0.150	0.080	-0.080	0.161	0.264	0.199

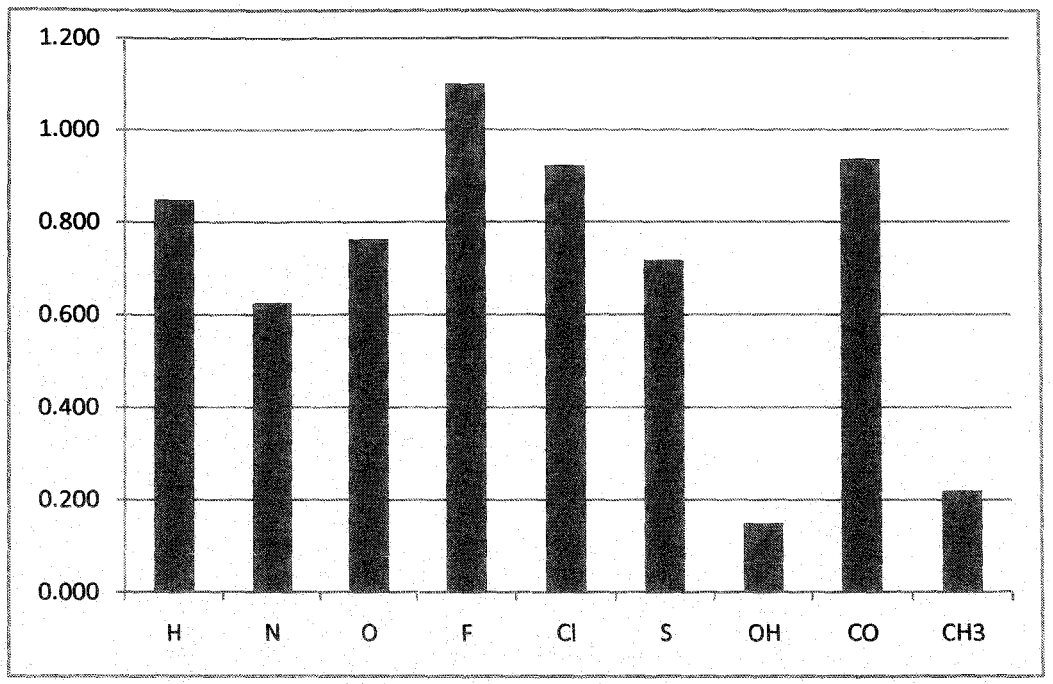

Figure 5.11 The average unsigned ionisation potential errors (eV) for different transition metal coordinating groups considered in this study.

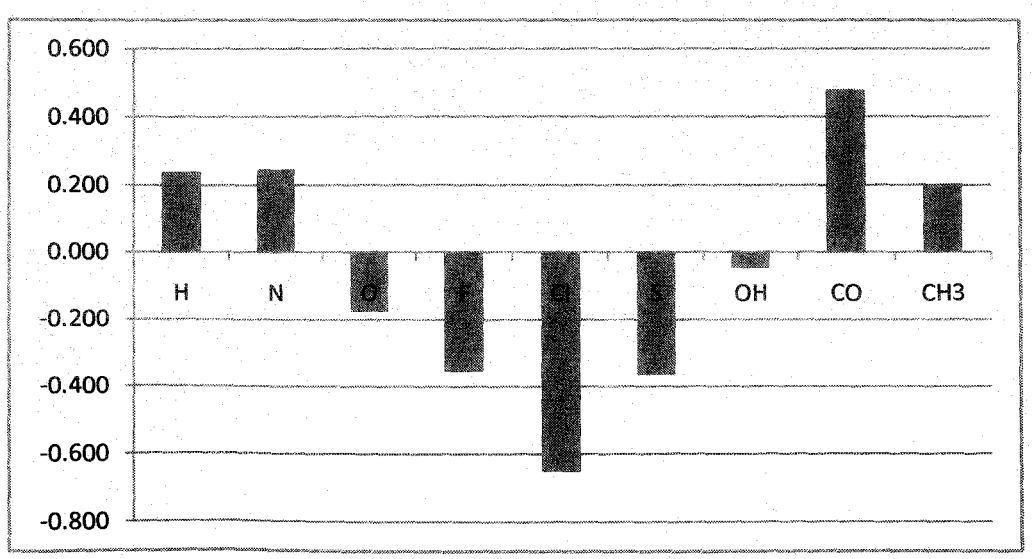

Figure 5.12 The average signed ionisation potential errors (eV) for different transition metal coordinating groups considered in this study.

The Figure 5.11 and Figure 5.12 graphically show the average unsigned and signed IP errors respectively for different coordinating groups which are used to form these benchmarked TM complexes. At a first look on Figure 5.11, one can easily find that the −OH and the $-CH_3$ groups show smallest amount of errors among these series of prototype ligands, whereas the ligand −F shows the highest unsigned IP error. Now, if one consider the Figure 5.12, one can readily infer that the ligands −H, −N, −CO and $-CH_3$ show the signed IP errors in positive direction, whereas the rest of the five ligands which are taken in this study show the signed IP errors in the negative direction. Here, we find that the coordinating group −OH shows the least error among these series of ligands but the error direction is negative. Nonetheless, the ligands −Cl and −CO are found to be most problematic in predicting these signed IP errors.

5.4 Summary

This work provides a benchmark study of the performance of different versions of the M05, M06 and M08 set of Minnesota density functionals with first row transition metal compounds. More preciously, in this study, we have evaluated the accuracy and reliability of eight M0X suite of functionals for the prediction of HOF and IP values of different first row transition metal complexes. We have taken 54 benchmark TM complexes for calculating the HOF values, whereas only 47 systems among these molecules are taken for evaluating IP values due to lack of experimental results. Following the procedure used by Riley and coworkers[15] we have computed these molecular properties for our selected TM systems. The M06-L functional is the best average performer among the M0X series of functionals in predicting these thermodynamic parameters of different first row TM complexes, whereas the robust functional M06-HF gives the worst performance in predicting such properties confirming the recommendation of the developers of these functionals that the Minnesota density functionals with high H-F exchange should not be used for the TM compounds. Nonetheless, almost similar performance of the M06-2X, M08-SO and M08-HX functionals having closely HF exchange in treating the thermochemical parameters of the TMs is also claimed by them.[8,11,12,14] The Fe complexes show most notorious HOF

results, whereas Ni complexes are found to be most problematic for the prediction of IP values. The discussion about the huge average HOF errors produced by the Fe complexes by our chosen eight Minnesota density functionals is due here. Notably, there are difficulties in dealing TM complexes by computational techniques due to the partial filling of *d* orbitals which is also responsible for degeneracy. Another point to be mentioned here is that, Merz and co-workers[15a] have found that the –CO group containing TM complexes are found to be problematic in predicting the HOF errors. Riley and co-workers[15] have chosen ten systems of iron, whereas we have taken only six complexes among those systems with one mono- and one bi-carbonyl complex. Secondly, they have found that the mono coordinated TM systems show best results and as the number of coordination increase the average unsigned HOF errors increases, that is the performance of the functionals decreases. It is also noteworthy that, we have taken three complexes for iron where the coordination higher than one. Nonetheless, they also have found that all the HGGA and HMGGA methods overestimate the HOF errors for TM complexes.[15a] Here, in this work out of eight functionals the seven functionals are HMGGA type. In another study, Reiher and co-workers[27] have analysed the spin density distribution in some Fe-nitrosyl complexes in DFT framework and they have found that the satisfactory description of spin densities in such complexes are not to be properly provided. In another effort Swart[28] have found that the reliable prediction of accurate spin ground state energies for the Fe complexes is tricky job both for theory and experiment. On the otherhand, in case of the prediction of IP values the deviation from the experimental results is much smaller than that of HOF results. Besides M06-L functional, the M05 and M06 functionals are also to be recommended for the theoretical prediction of these thermochemical parameters for the first row TM complexes. Point to be noted is that, the non-hybrid meta GGA functional M06-L takes 5-10% less effective CPU time consumption for calculating these physical parameters of these benchmarked TM complexes than the seven other hybrid meta GGA functionals. However, this argument is true for these small systems, but it underestimates the issue for larger systems, such that when one has a system with ~100 atoms, the cost for $\chi = 0$ is more than an order of magnitude smaller than for systems with nonzero χ, and for periodic calculations the speedup becomes 2-to-3 orders of magnitude greater. From the results obtained in this

work, one can categorically extract the following points- (i) The non-hybrid meta GGA M06-L functional with zero exchange correlation energy outdo all other functionals in predicting unsigned HOF values of the respective species. (ii) In predicting the IP results the performance of the M06 functional is found to be even better than the results obtained from M06-L functional. (iii) The hybrid meta GGA M05 and M06 functionals show quite accurate results after the local one compared to the other hybrid functionals taken for this study. (iv) With the increase of exchange correlation energy the performance of the M0X group of functionals to predict these physical properties for different first row TM complexes is noticeably found to be lowered. (v) The M06-HF functional having cent percent exact exchange contribution gives huge deviated results in all the field of calculations used in this study. (vi) We conclude that the M05 and M06 functionals found to be the good alternative to the popular B3LYP functional to study the HOFs and IPs. (vii) Considering the signed and unsigned HOF and IP errors (shown in Figure 5.1, Figure 5.2, Figure 5.7 and Figure 5.8 respectively), one can find with ease that 3 out of 4 cases the performance which has made by M08-SO is considerably more accurate than its other M08 counterpart as also advocated by the developers.[14] Nonetheless, this study has two quite different aspects: (a) Testing of the functionals *viz.* M06-L, M05 and M06 which are excellent candidates for the transition metal applications can forms a new transition metal database, and (b) Double checking the original recommendations that the functionals with $\chi > 30$ should not be used for transition metals.[8,14] At last an interesting note is that all existing M0X family of functionals have their own strength as well as weaknesses, hence there lies a difficulty in choosing the right functional to evaluate a particular physical property. We hope that, upcoming years will see a new M0X functional with all the merits which all would exist in the today's M0X functionals.

5.5 References and Notes

1. (a) Ziegler, T. *Chem. Rev.* **1991**, *91*, 651. (b) Gonze, X. *Phys. Rev. A* **1995**, *52*, 1096. (c) Kohn, W.; Becke, A. D.; Parr, R. G. *J. Phys. Chem.* **1996**, *100*, 12974. (d) Chermette, H. *Coord. Chem. Rev.* **1998**, *180*, 699.

2. Jensen, F. *Introduction to Computational Chemistry*, 1st ed.; John Willy & Sons: Chichester, England, **2004**.
3. Perdew, J. P.; Schmidt, K. *AIP Conference Proceedings*; AIP: Melville, NY, **2001**; *577*, 1-20.
4. Sousa, S. F.; Fernandes, A.; Ramos, M. J. *J. Phys. Chem. A* **2007**, *111*, 10439.
5. Janesko, B. G. *Int. J. Quantum Chem.* **2013**, *113*, 83–88.
6. (a) Becke, A. D. *J. Chem. Phys.* **1993**, *98*, 5648. (b) Lee, C.; Yang, W.; Parr, R. G. *Phys. Rev. B* **1988**, *37*, 785.
7. (a) Paier, J.; Marsman, M.; Kresse, G. *J. Chem. Phys.* **2007**, *127*, 024103 (b) Zhao, Y.; Truhlar, D. G. *Acc. Chem. Res.* **2008**, *41*, 157.
8. Zhao, Y.; Truhlar, D. G. *Chem. Phys. Lett.* **2011**, *502*, 1, and references therein.
9. Zhao, Y.; Schultz, N. E.; Truhlar, D. G. *J. Chem. Phys.* **2005**, *123*, 161103.
10. Zhao, Y.; Schultz, N. E.; Truhlar, D. G. *J. Chem. Theory Comput.* **2006**, *2*, 364.
11. Zhao, Y.; Truhlar, D. G. *J. Chem. Phys.* **2006**, *125*, 194101.
12. Zhao, Y.; Truhlar, *J. Phys. Chem. A* **2006**, *110*, 13126.
13. Zhao, Y.; Truhlar, D. G. *Theor. Chem. Acc.* **2008**, *120*, 215.
14. Zhao, Y.; Truhlar, D. G. *J. Chem. Theory Comput.* **2008**, *4*, 1849, and references therein.
15. (a) Riley, K. E.; Merz, K. M. Jr. *J. Phys. Chem. A.* **2007**, *111*, 6044. (b) Yang, Y.; Weaver, M. N.; Merz, K. M. Jr. *J. Phys. Chem. A.* **2009**, *113*, 9843.
16. Ruiz, E. *Chem. Phys. Lett.* **2008**, *460*, 336.
17. (a) Barone, V.; Adamo, C. *Int. J. Quantum Chem.* **1997**, *61*, 443. (b) Schultz, N. E.; Zhao, Y.; Truhlar, D. G. *J. Phys. Chem. A* **2005**, *109*, 11127. (c) Furche, F.; Perdew, J. P. *J. Chem. Phys.* **2006**, *124*, 044103. (d) Zhao, Y.; Truhlar, D. G. *J. Chem. Phys.* **2006**, *124*, 224105.
18. Weigned, F.; Furche, F.; Ahlrichs, R. *J. Chem. Phys.* **2003**, *119*, 12753.
19. Cundari, T. R.; Leza, H. A. R. Grimes, T.; Steyl, G.; Waters, A.; Wilson, A. K. *Chem. Phys. Lett.* **2005**, *401*, 58.
20. Glukhovtsev, M. N.; Bach, R. D.; Nagel, C. J. *J. Phys. Chem. A.* **1997**, *101*, 316.
21. Amin, E. A.; Truhlar, D. G. *J. Chem. Theory Comput.* **2008**, *4*, 75.

22. Frisch, M. J.; Trucks, G. W.; Schlegel, H. B.; Scuseria, G. E.; Robb, M. A.; Cheeseman, J. R.; Scalmani, G.; Barone, V.; Mennucci, B.; Petersson, G. A.; et al. Gaussian'09W, Revision A.02; Gaussian, Inc.: Wallingford CT, **2009**.

23. Schmidt, M. W.; Baldridge, K. K.; Boatz, J. A.; Elbert, S. T.; Gordon, M. S.; Jensen, J. J.; Koseki, S.; Matsunaga, N.; Nguyen, K. A.; Su, S.; Windus, T. L.; Dupuis, M.; Montgomery, J. A. *J. Comput. Chem.* **1993**, *14*, 1347.

24. GaussView, Version 5.0, Dennington, R.; Keith, T.; Millam, J. *Semichem Inc.*, Shawnee Mission KS, **2009**.

25. Riley, K. E.; Op't Holt, B. T.; Merz-Jr. K. M. *J. Chem. Theory Comput.* **2007**, 3, 407.

26. (a) Hay, P. J.; Wadt, W. R. *J. Chem. Phys.* **1985**, *82*, 270. (b) Hay, P. J.; Wadt, W. R. *J. Chem. Phys.* **1985**, *82*, 284. (c) Hay, P. J.; Wadt, W. R. *J. Chem. Phys.* **1985**, *82*, 299.

27. Boguslawski, K.; Jacob, C. R.; Reiher, M. *J. Chem. Theory Comput.* **2011**, *7*, 2740.

28. Swart, M. *J. Chem. Theory Comput.* **2008**, *4*, 2057.

Chapter 6

Regioselective nitration of 4-quinolones: Convergence of theoretical and experimental findings

Regioselective nitration of 4-quinolone, the highly privileged scaffold, has been investigated through density functional theory (DFT) based approach. Nitro group can selectively be introduced in the diverse position simply by tuning the reactivity of the moiety. Discrimination is being achieved through the selective protection of free N-H group. The selection of protecting group is screened theoretically with the help of Fukui function and local softness calculations. Theoretical predictions are synchronized well with the experimental findings. Thus, this selective nitration allows the access of the structurally diverse 4-quinolones.

6.1 Introduction

Nitration is one of the most extensively studied organic reactions since its discovery in 1834.[1] Nitro compounds are significantly beneficial synthetic intermediates and have potential application in various fields especially in chemical industry as well as pharmaceuticals.[2] Nitration with mixed acids always results in the mixture of products. Many regioselective nitration techniques viz. ipso-nitration/oxidation of amine[3] or azide,[4] functional group directed nitration[5] etc., have been developed till now to overcome those shortcomings.

Quinolone scaffold is charm of medicinal chemistry as it constitutes major structural and functional components of drugs with varied applicability. A bevy of popular drugs dominating the market for more than four decades are based upon the quinolone ring system as the basic pharmacophore. Slight variation in the substituent nature or position (Figure 6.1) brings inconsiderable to magnificent potency of the quinolone based drugs. It enables effective structure activity relationship studies and hence tuning of requisite therapeutic properties. This is one of the reasons that these moieties have emerged with great success in the arena of drug chemistry. Medicinal activities of many nitroheterocycles including nitrofuranylamides, nitroimidazoles, nitroimidazopyran and 5-nitro-2, 3-dihydroimidazo-oxazole have been reported.[6] Therefore nitration in quinolones is also anticipated to enhance drug efficiency. Very limited, mostly 6-nitro derivatives of 4-quinolones have been synthesized and their medicinal values are evaluated so far.[7,8] Many nitroquinolone derivatives have been reported to possess antifilarial, antiviral, antitumor and antibacterial capabilities.[7] 4-quinolone based drug chemistry has flourished with prolific developments. Nevertheless, synthesis and study of nitroquinolones is still limited. Majority of reported nitroquinolones bear nitro substituent at 6-position of the 4-quinolone skeleton and effects of nitration at 5 and 7 positions are not extensively explored. Many 4-quinolones with 3-carboxylic acid, carboxamide, or carboxylate substitution are reported to have vital pharmacokinetic applicabilities.[9] Hence we have chosen various ethyl-4-quinolone-3-carboxylate derivatives to study the orientation effects of different C-6 and C-8

substituents on nitration and we also report tuning of regioselectivity by varying the –N protecting groups in these systems.

Many theoretical investigations on various regioselective reactions are available in literature.[10] Scales et.al.,[10b] have studied the regioselective nucleophilic substitution of unsymmetrical 3,5-dichloloropyrazine. It has been observed that the electron withdrawing groups at 2-position in pyrazine direct substitution at 5-posititon, while for the presence of electron donating groups substitution occurs at 3-position. The experimental surveillance is well correlated with theoretical rationalization using Fukui indices. Zhang et.al., have investigated the metal controlled cycloaddition of 2-alkynyl-1, 4-benzoquinones and electron rich styrenyl systems.[10a] Their DFT study shows that the regioselectivity of the cycloaddition results from the divergent activation modes of catalysts $Bi(OTf)_3$ and AuCl. Kasende et.al,[10c] studied extensively the regioselectivity of the interaction of two pyrimidone isomers with two series of ligands namely boron lewis acids and alkali lewis acids. According to the molecular electrostatic potential (MEP) map and natural bond orbital analysis, a strong regioselectivity was observed for boron acids interaction preferring the N site in both pyrimidone isomers.

In the present contribution we have investigated the complete regioselective nitration of 4-quinolones. It has been found that the selectivity can easily be tuned by proctecting the free N-H group of 4-quinolone. Choice of protecting groups are screened with the help of DFT based reactivity descriptors Fukui function and local softness calculation. Moreover, our theoretical predictions are well synchronized with the experimental findings.

6.2 Computational methodology

All calculations were performed at the (U)B3LYP level using the Gaussian 03 W quantum chemical package[11] using the 6-31G(d,p) basis set. Reactivity of any molecule at a specific site can be determined by local reactivity indices such as Fukui function,

local softness and so on. The Fukui function (f_k^i), instigated in DFT by Parr and Yang,[12,13] is the most important local reactivity index. Regioselectivity for nucleophilic or electrophilic attack at site k can be ascertained through evaluation of Fukui function (f_k^i)[12,14] and can be estimated using population analysis as

$$f_k^+ = [\rho_k(N+1) - \rho_k(N)] \quad \text{for nucleophilic attack} \qquad (6.1)$$

$$f_k^- = [\rho_k(N) - \rho_k(N-1)] \quad \text{for eletrophilic attack} \qquad (6.2)$$

where $\rho(N)$ and $\rho(N-1)$ are the electron densities of the N+1, N and (N−1) electron systems respectively.[15,16] Local softness (s_k^i)[12,14] is another parameter in analyzing the regioselectivity, which is related to Fukui function as $s_k^i = f_k^i.S$ with $i = +$ or $-$, where S is the global softness given as $S=1/2\eta$ where η is the global hardness.[17] In this study we have calculated electrophilic Fukui function (f_k^-) and local softness (s_k^-) at different sites of a molecule.

6.3 Results and discussion

Density functional theory provides a very convenient framework for the discussion of chemical reactivity. Fukui function (f_k^i) and local softness ($s_k i$) are two reliable reactivity parameters to predict and interpret the regioselectivity of a reaction. In this work we have investigated the probable sites of nitronium ion addition of assorted ethyl-4-quinolone-3-carboxylate derivatives and their corresponding N substituted analogs. For this rationale we have calculated nucleophilic Fukui functions (f_k^-) and local softness (s_k^-) of all the compounds. The detail results of the nucleophilic Fukui function (f_k^-) and local softness (s_k^-) calculations are shown in Table 6.1and 6.2.

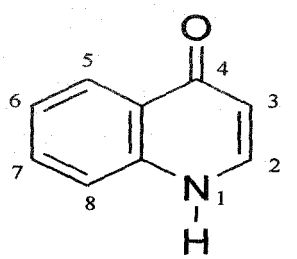

Figure 6.1 Structure of quinolone.

Our study begins with the prediction of the reactive sites for nitronium ion addition to 4-quinolone 3-carboxylate. The unsubstituted 4-quinolone 3-carboxylate **A** has been selected as a model compound for this study.

Scheme 6.1

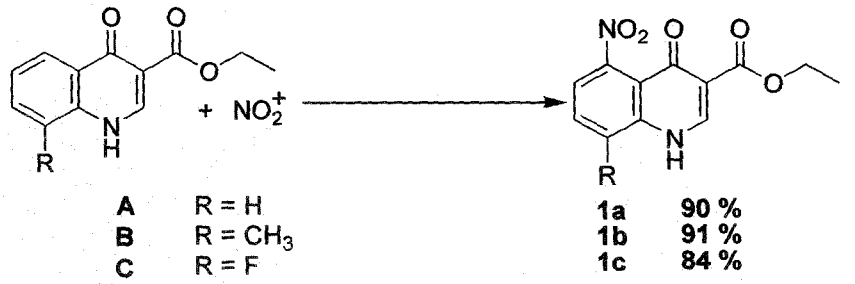

A R = H
B R = CH_3
C R = F

1a **90 %**
1b **91 %**
1c **84 %**

Table 6.1 Fukui function (f_k^-) and local softness (s_k^-) calculation at UB3LYP/6-31G(d,p).

Entry	Fukui functions				Local softness				Theoretically Preferred Carbon	Experimentally Preferred Carbon
	C-5	C-6	C-7	C-8	C-5	C-6	C-7	C-8		
A	0.043	0.030	0.015	-	0.244	0.170	0.085	-	C-5	C-5
B	0.038	0.027	0.019	-	0.218	0.155	0.109	-	C-5	C-5
C	0.042	0.026	0.020	-	0.240	0.149	0.114	-	C-5	C-5
D	0.037	0.025	0.027	-	0.214	0.145	0.156	-	C-5	C-5 & C-7
E	0.034	0.028	0.022	-	0.199	0.164	0.129	-	C-5	C-5
F	0.021	0.017	0.028	-	0.124	0.100	0.165	-	C-7	C-7
G	0.041	-	0.018	0.042	0.236	-	0.104	0.242	C-8	C-8
H	0.032	-	0.013	0.025	0.183	-	0.074	0.143	C-5	C-5
I	0.038	-	0.015	0.037	0.220	-	0.087	0.214	C-5	C-5

From Table 6.1, it is evident that for reactant **A** (Scheme 6.1), the preferable site for electrophilic attack is at C-5 as this carbon possesses higher reactivity indices (f_k^-=0.043, s_k^-=0.244) than the other probable sites C-6(0.030, 0.170) and C-7(0.015, 0.085). So, it has been predicted that compound **A** on nitration results 5-nitro quinolone derivative. Similar to **A**, different substituted 4-quinolones **B** and **C** possess higher values of reactivity indices at C-5 position (Table 6.1) than the other plausible sites.

Experimentally these results have also been verified. Consequently compound **A** on nitration with mixed acid at ambient condition results in 90 % yield of the corresponding 5-nitro derivative (1a) upon isolation. In the similar situation **B** and **C** smoothly undergo selective nitration to furnish the desired 5-nitro products with excellent yields (91% and 84% respectively). These results clearly show that the presence of electron donating group ($-CH_3$) and strong electron withdrawing group (-F) literally have no significant role in defining the position of incoming electrophile (nitronium ion).

Scheme 6.2

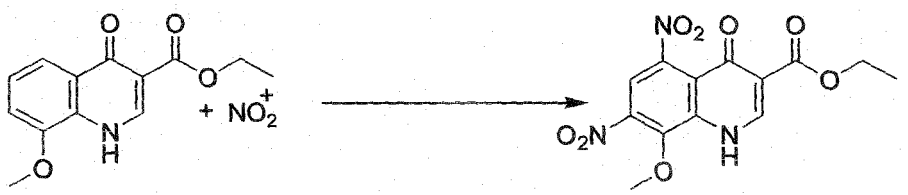

Then we have studied the selective nitration of another model compound **D** (Scheme 6.2). According to the DFT calculation (Table 6.1), for compound **D** the order of nucleophilicity of the possible reacting sites is C-5 (0.037, 0.214)>C-7 (0.027, 0.156)>C-6 (0.025, 0.145). It reveals that for electrophilic attack the most reactive site is C-5, then comes C-7 and C-6 is the least one. It has been observed experimentally that nitration of compound **D** always results in the corresponding 5, 7-dinitro quinolone derivative (2d). To bring a control over it, nitration was carried out at lower temperature ($0^{\circ}C$) but the second nitration could not be stopped. This is probably the methoxy group which facilitates the second nitration in its ortho position.

Scheme 6.3

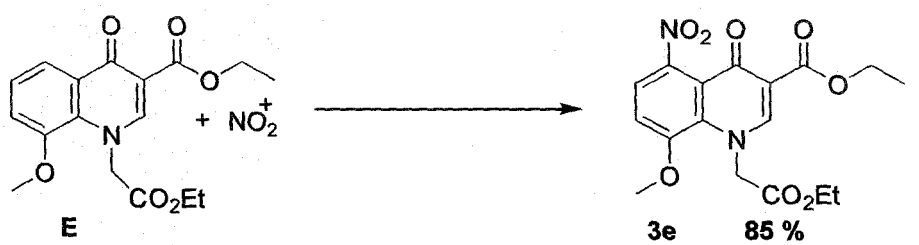

However this observation stipulates us to develop a regioselective nitration technique. Accordingly, an additional functional group has been introduced so that it

could reduce the reactivity of the parent compound **D** and thereby restrict the second nitration. Selection of the protecting group has been done with the help of conceptual density functional theory (DFT) calculation. It is clear from theoretical rationale (Table 6.1 and 6.2) that either an alkyester or $-CH_2Ph$ group can be chosen as protecting

Table 6.2 Fukui function (f_k^-) and local softness (s_k^-) calculation at UB3LYP/6-31G(d,p).

Entry	Sites	Fukui function(f_k^-)	Local softness (s_k^-)	Theoretically preferred carbon
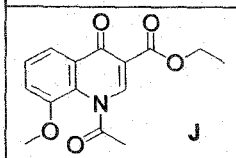 J	C-5	0.0215	0.1311	C-7
	C-6	0.0173	0.1055	
	C-7	0.0293	0.1786	
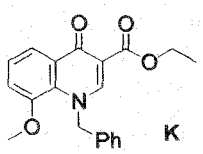 K	C-5	0.0330	0.1938	C-5
	C-6	0.0284	0.1668	
	C-7	0.0163	0.0957	
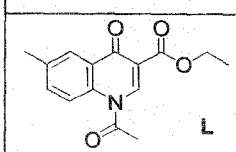 L	C-5	0.0298	0.1817	C-5
	C-7	0.0187	0.1140	
	C-8	0.0272	0.1655	
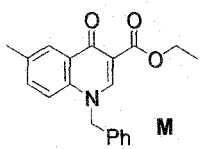 M	C-5	0.0383	0.2430	C-5
	C-7	0.0134	0.0848	
	C-8	0.0377	0.2391	

group of free N-H to restrict the second nitration. From Table 6.1, it is evident that for compound, **E** (Scheme 6.3) C-5 possesses higher Fukui function and local softness (f_k^-=0.034, s_k^-=0.199) than the other possible sites C-6 (0.028, 0.164) and C-7 (0.022, 0.129) i.e., C-5 is more prone to electrophilic attack than the other sites. For experimental verification we have selected the alkyester group for the protection of free N-H group as the resulting moiety **E** can serve as an amino acid precursor. Indeed nitration of

compound **E**, selectively results in the corresponding 5-nitroderivative (3e) in excellent yield (85%) upon isolation.

Scheme 6.4

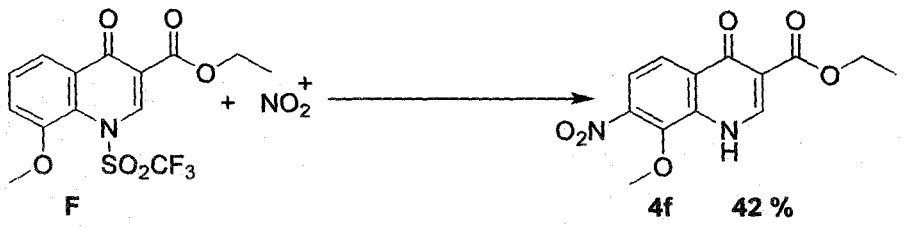

Now the remaining major challenge is the introduction of nitro group selectively at 7-position of the same moiety (compound **D**). Screening of several protecting groups with the help of conceptual DFT, we found $-SO_2CF_3$ may be chosen in this case (Table 6.1). As for $-SO_2CF_3$ N-protecting group C7 is susceptible for electrophilic attack having highest reactivity indices ($f_k^- = 0.028$, $s_k^- = 0.165$) than the other probable sites C5 (0.021, 0.124) and C6 (0.017, 0.100). Theoretical prediction is followed by experimental justification. Accordingly the parent compound **D** on treatment with triflic anhydride in the presences of tetrabutylammoniumhydrogensulfate results in desired *N*-protected 4-quinolone **F** in moderate yield. Compound **F** on nitration results in mono substituted, 7-nitro derivative selectively with excellent yield (Scheme 6.4). Thus our theoretical predictions are again is in good accordance with experimental rationalization.

The above study showed that *N*-protecting group plays a vital role for defining the position of nitration. Validity of it was further justified using another model compound **G**, where methyl group present at 6-postion (Scheme 6.5). DFT calculation suggests that the most preferred position for the nitration of compound **G** is C-8 as it possesses higher values of Fukui function and local softness ($f_k^- = 0.042$, $s_k^- = 0.242$) than the other feasible sites C-5(0.041, 0.236) and C-7(0.018, 0.104). But the position can be altered if the free N-H be protected with any of the four groups triflate, alkylester, amide and $-CH_2Ph$ (Table 6.1 and 6.2). The theoretical prediction is validated when nitration of compound **G** produces 8-nitro derivative (5g) in quantitative yield. Based on the theoretical analysis the free N-H group has been protected with triflate and alkylester and nitration has been

carried out on the protected forms (compound **H** and **I**). In fact, nitration results in the desired 5-nitro derivatives in almost quantitative yields. So based on our theoretical predictions, we have achieved selective nitration of different quinolone derivatives at 5 and 8 positions.

Scheme 6.5

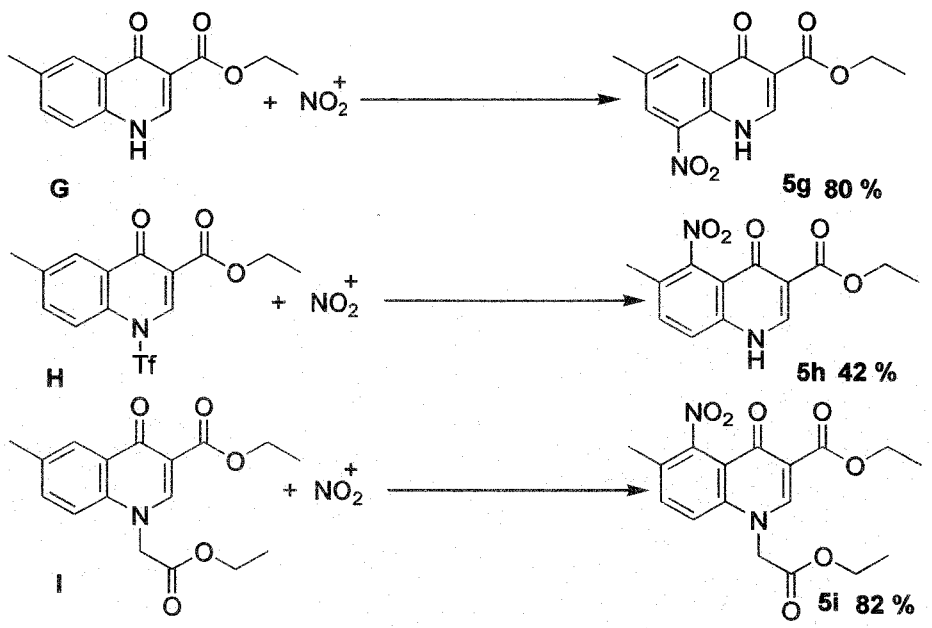

6.4 Summary

In this work, we have presented a study on the regioselectivity of nitronium ion addition to 4-quinolones using DFT based reactivity descriptors. Fukui function and local softness are calculated for different model compounds (**A-M**). From theoretical analysis we have found that regioselectivity can easily be tuned by selective protection of free – NH group. Moreover our theoretical predictions are justified by experimental rationalizations. Good agreement was found when comparing the predicted regioselectivities with experimental data. Finally this selective nitration allows introducing nitro group in the diverse position of the 4-quinolone ring and this study will

definitely be useful for the target synthesis of new bioactive molecules based on the 4-quinolone system.

6.5 References and notes

1. Mitscherlich, E. *Annln. Phys. Chem.* **1834**, *31*, 625; (b) Mitscherlich, E. *Annln. Pharm.* **1834**, *12*, 305.
2. Ono, N. *The nitro group in organic synthesis*, (Ed. H. Feuer), WILEY-VCH, USA, **2001**.
3. Reddy, K. R.; Maheswari, C. U.; Venkateshwar, M.; Kantam, L. *Adv. Synth. Catal.* **2009**, *351*, 93-96.
4. Rozen, S.; Carmeli, M. *J. Am. Chem. Soc.* **2003**, *125*, 8118.
5. (a) Saito, S.; Koizumi, Y. *Tetrahedron Lett.* **2005**, *46*, 4715. (b) Fors, B. P.; Buchwald, S. L. *J. Am. Chem. Soc.* **2009**, *131*, 12898. (c) Yang, H. J.; Li, Y.; Jiang, M.; Wang, J. M.; Fu, H. *Chem. Eur. J.* **2011**, *17*, 5652. (d) Yan, G.; Zhang, L.; Yu, J. *Lett. Org. Chem.* **2012**, *9*, 133.
6. (a) Mukherjee, T.; Boshoff, H. *Future Med. Chem.* ***2011***, *3*, 1427. (b) Tangallapally, R. P.; Yendapally, R.; Lee, R. E.; Hevener, K.; Jones, V. C.; Lenaerts, A. J. M.; McNeil, M. R.; Wang, Y.; Franzblau, S.; Lee, R. E. *J. Med. Chem.* **2004**, *47*, 5276. (c) Lenaerts, A. J.; Gruppo, V.; Marietta, K. S.; Johnson, C. M.; Driscoll, D. K.; Tompkins, N. M.; Rose, J. D.; Reynolds, R. C.; Orme, I. M. *Antimicrob Agents Chemther.* **2005**, *49*, 2294. (d) Ashtekar, D. R.; Costa-Perira, R.; Nagrajan, K.; Vishvanathan, N.; Bhatt, A. D.; Rittel, W. *Antimicrob Agents Chemther.**1993**, 37, 183.*
7. a) Srivastava, S. K.; Chauhan, P. M. S.; Bhaduri, A. P.; Fatima, N.; Chatterjee, R. K. *J. Med. Chem.* **2000**, *43*, 2275. (b) Gupta, R. A.; Kaskhedikar, S. G. *Med. Chem. Res.* **2012**, *21*, 3907. (c) Senthilkumar, P.; Dinakaran. M.; Yogeeswari, P.; Sriram, D.; China, A.; Nagaraja, V. *Eur. J. Med. Chem.* **2009**, *44*, 345. (d) Peet, N. P.; Baugh, L. E.; Sunder, S.; Lewis, J. E. *J. Med. Chem.* **1985**, *28*, 298, (e) Shul'gina, M. V.; Fadeeva, N. I.; Bol'shakova, T. N.; Levshin, I. B.; Glushkov, R. G. *Pharm. Chem. J.* **1999**, *33*, 343. (f) Artico, M.; Mai, A.; Sbardella, G.; Massa,

S.; Musiu, C.; Lostia, S.; Demontis, F.; La Colla, P. *Bioorg. Med. Chem. Lett.* **1999**, *9*, 1651.

8. Sbardella, G.; Mai, A.; Artico, M.; Setzu, M. G.; Poni, G.; Colla, P. L.; *Framaco*, **2004**, *59*, 463.
9. Pasquini, S.; De Rosa, M.; Ligresti, A.; Mugnaini, C.; Brizzi, A.; Caradonna, N. P.; Cascio, M. G.; Bolognini, D.; Pertwee, R. G.; Di Marzo, V.; Corelli, F.; Eur. J. Med. Chem. **2012**, 58, 30.
10. (a) Zhang, L.; Li, Z.; Fan, R. *Org. Lett.* **2013**, *15*, 2482. (b) Scales, S.; Johnson, S.; Hu, Q.; Do, Q. Q.; Richardson, P.; Wang, F, Braganza, J.; Ren, S.; Wan, Y.; Zheng, B.; Faizi, D.; McAlpine, I. *Org. Lett.* **2013**, *15*, 2156. (c) Kasende, O. E.; Muya, J. T.; Broeckaert, L.; Maes, G.; Geerlings, P. *J. Phys. Chem. A* **2012**, *116*, 8608. (d) Sengupta, D.; Chandra, A. K.; Nguyen, M. T. *J. Org. Chem.* **1997**, *62*, 6404. (e) Catak, S.; D'hooghe, M.; Verstraelen, T.; Hemelsoet, K.; Nieuwenhove, A. V.; Ha, H-J.; Waroquier, M.; Kimpe, N. D.; Speybroeck V. V. *J. Org. Chem.* **2010**, *75*, 4530.
11. Frisch M.J.; et al., GAUSSIAN 03 (Revision D.01) Gaussian, Inc., Wallingford, CT, **2004**.
12. Yang, W.; Mortier, W. J. *J. Am. Chem. Soc.* **1986**, *108*, 5708.
13. Parr, R. G.; Yang, W. *Density Functional Theory of Atoms and Molecules*; Oxford University Press: New York, **1999**.
14. (a) Vos, A.M.; Schoonheydt, R.A.; De Proft, F.; Geerlings, P. *J. Catal.* **2003**, *220*, 333. (b) Chattaraj, P.K.; Maiti, B.; Sarkar, U. *J. Phys. Chem. A*, **2003**, *107*, 4973. (c) Fukui, K.; Yonezawa, T.; Shingu, H.; *J. Chem. Phys.* **1952**, *20*, 722.
15. Fukui, K.; Yonezawa, T.; Shingu, H.; *J. Chem. Phys.* **1952**, *20*, 722.
16. Parr, R.G.; Yang, W.; *J. Am. Chem. Soc.* **1984**, *106*, 404.
17. Yang, W.; Parr, R.G. *Proc. Natl. Acad. Sci.* USA 826723, **1985**.

Chapter 7

Conclusions

Comprehensive conclusions of this dissertation are presented here.

Conclusions

This chapter portrays summary and concluding remarks of all the preceding chapters of this thesis. Here we have emphasized on the theoretical exploration of organic reactions. In this vast area of knowledge we have selected to cram the addition reactions. In chapter one there is a general introduction about the theoretical analysis of addition reactions. The background of the present thesis is elucidated here. At the very beginning, we have discussed the addition reaction-its definition, types and mechanism. Finally, we have discussed about the scope of applications and various mechanistic aspects of addition reactions. The objectives of this thesis are also categorically described.

Chapter two deals with the theoretical platform for the calculation of electronic energy, charge density and potential energy surface of different species involved in a reaction. We have discussed the theoretical setting for calculation of transition state with the help of Born-Oppenheimer approximation. The background for the prediction of reactivity of a molecule towards an attacking reagent is also conferred here.

In chapter three, we have investigated the electrophilic addition of benzene (monoprotonation, diprotonation, monomethylation & dimethylation) in DFT framework using UB3LYP hybridfunctional with the 6-311++G(d, p) basis function. The results reflect the same trend of mechanistic pathways for diprotonation and dimethylation reactions. For both the reactions, the most stable product is a meta disubstituted one followed by ortho and para isomers. It is also evident from simple valence bond based qualitative approach. In this approach, one can readily find only one possible structure for para disubstituted product in which two positive charges are geminal. In ortho and meta disubstituted products two resonating structures could be found; however, in case of ortho in one of these structures again charges are on neighboring sites, whereas, in case of meta isomer in none of them charges are adjacent. This clearly points out the meta disubstituted product to be most favorable energetically followed by ortho and para. This is also supported by local charge density values. Nevertheless, in case of diprotonation

reaction the para isomer has been found to be kinetically controlled product whereas the ortho one is the same for dimethylation reaction. Fukui function and local softness have been found to be good descriptors for kinetically controlled product. Proton affinities and methyl cation affinities have been found to be additive in nature and these values justify the calculated thermochemical parameters. A correlation is observed between proton and methyl cation affinity with the change in enthalpy.

In the forth chapter, we have studied the addition mechanism of two molecules of 1, 3-dicarbonyl compound and one molecule of aldehyde in presence of molecular iodine within unrestricted DFT framework using B3LYP hybrid functional. General steps of the reaction are studied using acetyl acetone as 1, 3-dicarbonyl compound and acetaldehyde. There may be two pathways depending on the substitution pattern of 1, 3-dicarbonyl compound. One leads to spiro dihydrofuran and other cyclopropane derivatives. Paths being followed in either situation can be predicted by condensed Fukui function calculation and by ESP analysis. In each steps transition states are calculated. Vibrational analysis, IRC calculations and ESP analysis authenticate these transition states. The nucleus independent chemical shift (NICS) calculation suggests that the gain in aromaticity plays an important role in the last step of the reaction. Thermochemical analysis is in good agreement with each step of the proposed mechanism. As a whole, the present DFT study explains well the experimental findings and also provides the details of the reaction mechanism.

Chapter five contains a benchmark study of the performance of different versions of the M05, M06 and M08 set of Minnesota density functionals with first row transition metal compounds. In this study, we have evaluated the accuracy and reliability of eight M0X suite of functionals for the prediction of HOF and IP values of different first row transition metal complexes. We have taken 54 benchmark TM complexes for calculating the HOF values, whereas only 47 systems among these molecules are taken for evaluating IP values due to lack of experimental results. It has been found that the M06-L functional is the best average performer among the M0X series of functionals in predicting thermodynamic parameters of different first row TM complexes, whereas the

robust functional M06-HF gives the worst performance in predicting such properties confirming the recommendation of the developers of these functionals that the Minnesota density functionals with high H-F exchange should not be used for the TM compounds. Nonetheless, almost similar performance is shown by the M06-2X, M08-SO and M08-HX functionals having closely HF exchange in treating the thermochemical parameters of the TMs. The Fe complexes show most notorious HOF results, whereas Ni complexes are found to be most problematic for the prediction of IP values. The discussion about the huge average HOF errors produced by the Fe complexes by our chosen eight Minnesota density functionals is due here. Notably, there are difficulties in dealing TM complexes by computational techniques due to the partial filling of *d* orbitals which is also responsible for degeneracy. In case of the prediction of IP values the deviation from the experimental results is much smaller than that of HOF results. Besides M06-L functional, the M05 and M06 functionals are also to be recommended for the theoretical prediction of these thermochemical parameters for the first row TM complexes. From the results obtained in this work, one can categorically extract the following points- (i) The non-hybrid meta GGA M06-L functional with zero exchange correlation energy outdo all other functionals in predicting unsigned HOF values of the respective species. (ii) In predicting the IP results the performance of the M06 functional is found to be even better than the results obtained from M06-L functional. (iii) The hybrid meta GGA M05 and M06 functionals show quite accurate results after the local one compared to the other hybrid functionals taken for this study. (iv) With the increase of exchange correlation energy the performance of the M0X group of functionals to predict these physical properties for different first row TM complexes is noticeably found to be lowered. (v) The M06-HF functional having cent percent exact exchange contribution gives huge deviated results in all the field of calculations used in this study. (vi) We conclude that the M05 and M06 functionals found to be the good alternative to the popular B3LYP functional to study the HOFs and IPs. (vii) Considering the signed and unsigned HOF and IP errors, one can find with ease that 3 out of 4 cases the performance which has made by M08-SO is considerably more accurate than its other M08 counterpart. Nonetheless, this study has two quite different aspects: (a) Testing of the functionals *viz.* M06-L, M05 and M06 which are excellent candidates for the transition metal

applications can forms a new transition metal database, and (b) Double checking the original recommendations that the functionals with $\chi > 30$ should not be used for transition metals. At last an interesting note is that all existing M0X family of functionals have their own strength as well as weaknesses, hence there lies a difficulty in choosing the right functional to evaluate a particular physical property. We hope that, upcoming years will see a new M0X functional with all the merits which all would exist in the today's M0X functionals.

In the sixth chapter, we have investigated the regioselective nitronium ion addition to 4-quinolones using DFT based reactivity descriptors. Fukui function and local softness are calculated for different model compounds. From theoretical analysis, we draw the conclusion that regioselectivity can easily be tuned by selective protection of free –NH group. Moreover our theoretical predictions are justified by experimental rationalizations. Good agreement was found when comparing the predicted regioselectivities with experimental data. Finally this selective nitration allows introduction of nitro group in the diverse position of the 4-quinolone ring and this study will definitely be useful for the target synthesis of new bioactive molecules based on the 4-quinolone system.

Appendix

Table 1. The experimental values of the heat of formation (HOF) for all 54 transition metal complexes which are taken in this work (Kcal/mol) are depicted below. These experimental HOF values are taken from the different relevant literatures.

TiS	76.2 ± 2.2[1]	$MnCl_2$	-63.0 ± 0.5[1,2]	NiO	75.0 ± 5.0[1]
TiF_2	-164.5 ± 10.0[2,3]	MnCl	11.3 ± 2.1[1]	NiH	85.6 ± 2.6[1]
TiO	13.7 ± 2.2[1]	MnF_2	-126.2 ± 1.0[1]	NiF_2	-77.8 ± 1.1[1]
TiH	116.4 ± 2.3[4]	MnH	64.2 ± 7.0[1]	NiCl	41.7 ± 1.6[11]
TiF_3	-284.1 ± 10.0[2,3]	MnO	29.6 ± 3.0[1]	$NiCl_2$	-17.4 ± 1.0[11]
TiCl	24.2[1]	MnF	-19.9 ± 3.0[1]	Ni(CO)	35.1 ± 5.8[9]
V2	187.4 ± 5.2[1]	FeF_2	-93.0 ± 3.4[5]	Cu2	113.8 ± 2.6[1]
VS	80.4 ± 3.2[1]	$Fe(CO)_2$	0.2 ± 4.9[9]	CuCl	19.3 ± 2.0[1]
VN	121.0 ± 3.0[1]	Fe(CO)	63.9 ± 3.5[9]	CuF	-3.2 ± 2.0[1]
VO	30.5[2,5]	FeCl	49.5 ± 1.6[10]	CuF_2	-66.0[1]
VCl	37.8 ± 1.5[1]	FeO	61.1 ± 3.0[1]	CuO	76.5 ± 10.0[2]
VF	0.7 ± 15.0[1]	$FeCl_2$	32.8 ± 1.0[10]	CuS	75.1 ± 5.0[2]
CrCl	31.0 ± 0.6[6]	CoH	110.7 ± 1.0[9]	Zn_2	57.7 ± 1.5[1]
$CrCl_2$	-28.1 ± 0.4[6]	CoO	7.0 ± 5.1[1]	$Zn(CH_3)$	26.0 ± 2.5[1]
CrF	3.1 ± 2.4[7]	CoCl	50.3 ± 1.6[10]	$ZnCl_2$	-63.5 ± 0.4[1]
CrO	45.0[2,3,8]	$CoCl_2$	-22.6 ± 1.0[10]	ZnF_2	-118.9 ± 1.1[1]
CrO_2	-18.0[2,3,8]	CoF_2	-87.5[1]	ZnH	62.9 ± 0.5[1]
CrOH	18.9 ± 1.8[6]	$CoCl_3$	-39.1[2,3,8]	ZnO	52.8 ± 0.9[1]

Table 2. This table depicts the experimental values of the ionization potential (IP) for 47 different transition metal complexes estimated in this work (*eV*). These experimental IP values are taken from the different relevant literatures.

TiS	7.1 ± 0.3[3]	$MnCl_2$	11.03 ± 0.01[3]	NiO	9.5 ± 0.2[3]
TiF_2	12.2 ± 0.5[3]	MnCl	8.5 ± 0.3[1]	NiH	8.50 ± 0.10[3]
TiO	6.819 ± 0.006[3]	MnF_2	11.38 ± 0.20[3]	NiF_2	11.5 ± 0.3[3]
TiH	6[3]	MnH	7.8[3]	NiCl	9.28 ± 0.10[1]
TiF_3	10.5 ± 0.5[3]	MnO	8.65 ± 0.20[3]	$NiCl_2$	11.24 ± 0.01[3]
V2	6.357 ± 0.001[3]	MnF	8.51 ± 0.20[3]	Ni(CO)	7.30 ± 0.29[3]
VS	8.4 ± 0.3[3]	FeF_2	11.3 ± 0.3[3]	Cu2	7.9[3]
VN	8.0 ± 1.0[3]	$Fe(CO)_2$	6.68 ± 0.24[7]	CuCl	10.7 ± 0.3[3]
VO	7.2386 ± 0.0006[3]	Fe(CO)	6.66 ± 0.17[7]	CuF	10.90 ± 0.01[3]
CrCl	8.50 ± 0.10[1]	FeCl	8.08 ± 0.10[1]	CuF_2	13.18[3]
$CrCl_2$	9.9[3]	FeO	8.9 ± 0.2[3]	Zn_2	9.0 ± 0.2[3]
CrF	9.3 ± 0.4[3]	$FeCl_2$	10.63 ± 0.10[1]	$ZnCH_3$	7.2[3]
CrO	8.16 ± 0.01[3]	CoH	7.86 ± 0.07[3]	$ZnCl_2$	11.80 ± 0.005[3]
CrO_2	10.3 ± 0.5[3]	CoO	8.9 ± 0.2[3]	ZnF_2	13.91 ± 0.03[3]
CrOH	7.54 ± 0.05[10]	CoCl	8.71 ± 0.10[1]	ZnH	9.4[3]
		$CoCl_2$	10.75 ± 0.10[1]	ZnO	9.34 ± 0.02[12]

In Table 1 and Table 2 the numerical superscripts denote the respective references from where the HOF and IP values are taken. These references are given below-

1. Yungman, V. S., Ed. Thermal Constants of Substances; Wiley: New York, 1999; Vol. 4-6.
2. Barin, I. VCH: Weinheim 1989.
3. Mallard, W. G.; Linstrom, P. J. NIST Chemistry WebBook; NIST Standard Reference Database Number 69; National Institute of Standards and Technology: Gaitherburg, MD, 2000.
4. Chen, Y. M.; Clemmer, D. E.; Armentrout, P. B. *J. Chem. Phys.* **1991**, *95*, 1228.
5. Chase, M. W.; Davies, C. A.; Downey, J. R.; Frurip, D.; J.; McDonald, R. A.; Syverud, A. N. JANAF Thermochemical Tables, 3rd ed.; 1985; Vol. 14, Supp. No. 1.
6. Ebbinghaus, B. B. *Combust. Flame* **1995**, *101*, 311.
7. Espelid, O.; Borve, K. J. *J. Phys. Chem. A* **1997**, *101*, 9449.
8. Binnewies, M.; Milke, E. Wiley-VCH: Weinheim, Germany, 1999.
9. Sunderlin, L. S.; Wang, D. N.; Squires, R. R. *J. Am. Chem. Soc.* **1992**, *114*, 2788.
10. Hildenbrand, D. L.; LAU, K. H. *J. Chem. Phys.* **1995**, *102*, 3769.
11. Morse, M. D. *Chem. Rev.* **1986**, *86*, 1049.
12. Rohlfing, E. A.; Cox, D. M.; Kaldor, A.; Johnson, K. H. *J. Chem. Phys.* **1984**, *81*, 3846.

Table 3: The group of tables show the ground state gas phase energy of 16 different atoms which are used to form the 54 different TM complexes calculated with 8 different M0X functionals with LANL2DZ basis set along with their respective multiplicities. The energy has the unit a.u.

M05

Atoms	Multiplicity	Energy
H	2	−0.49
C	3	−37.82
N	4	−54.59
O	3	−75.05
F	2	−99.72
S	3	−10.00
Cl	2	−14.85
Ti	3	−57.88
V	6	−71.15
Cr	7	−86.21
Mn	4	−103.81
Fe	3	−123.36
Co	4	−145.02
Ni	3	−169.30
Cu	2	−196.23
Zn	1	−65.74

M05-2X

Atoms	Multiplicity	Energy
H	2	−0.50
C	3	−37.85
N	4	−54.59
O	3	−75.07
F	2	−99.74
S	3	−10.01
Cl	2	−14.86
Ti	3	− 57.90
V	4	−71.16
Cr	5	−86.19
Mn	4	−103.76
Fe	3	−123.30
Co	4	−145.95
Ni	3	−169.21
Cu	2	−196.09
Zn	1	−65.34

M06-L

Atoms	Multiplicity	Energy
H	2	−0.50
C	3	−37.84
N	4	−54.59
O	3	−75.07
F	2	−99.74
S	3	−10.02
Cl	2	−14.89
Ti	3	− 57.95
V	4	−71.21
Cr	7	−86.25
Mn	6	−103.83
Fe	5	−123.38
Co	4	−145.02
Ni	3	−169.25
Cu	2	−196.12
Zn	1	−65.10

M06

Atoms	Multiplicity	Energy
H	2	−0.50
C	3	−37.82
N	4	−54.57
O	3	−75.05
F	2	−99.71
S	3	−10.00
Cl	2	−14.86
Ti	3	−57.91
V	6	−71.18
Cr	7	−86.24
Mn	6	−103.81
Fe	5	−123.34
Co	4	−145.00
Ni	3	−169.26
Cu	2	−196.15
Zn	1	−65.46

M06-2X

Atoms	Multiplicity	Energy
H	2	−0.50
C	3	−37.84
N	4	−54.58
O	3	−75.06
F	2	−99.72
S	3	−9.99
Cl	2	−14.84
Ti	3	−57.89
V	6	−71.16
Cr	5	−86.22
Mn	4	−103.80
Fe	5	−123.33
Co	4	−144.99
Ni	3	−169.26
Cu	2	−196.15
Zn	1	−65.43

M06-HF

Atoms	Multiplicity	Energy
H	2	−0.49
C	3	−37.85
N	4	−54.59
O	3	−75.06
F	2	−99.73
S	3	−9.99
Cl	2	−14.82
Ti	3	−57.88
V	4	−71.13
Cr	7	−86.17
Mn	6	−103.84
Fe	5	−123.29
Co	4	−144.97
Ni	3	−169.23
Cu	2	−196.03
Zn	1	−65.60

M08-SO

Atoms	Multiplicity	Energy
H	2	−0.50
C	3	−37.82
N	4	−54.55
O	3	−75.03
F	2	−99.70
S	3	−10.03
Cl	2	−14.86
Ti	1	−57.80
V	4	−71.04
Cr	7	−86.12
Mn	6	−103.69
Fe	5	−123.20
Co	4	−144.86
Ni	3	−169.13
Cu	2	−196.02
Zn	1	−65.45

M08-HX

Atoms	Multiplicity	Energy
H	2	−0.50
C	3	−37.84
N	4	−54.58
O	3	−75.05
F	2	−99.72
S	3	−10.02
Cl	2	−14.87
Ti	1	−57.84
V	4	−71.15
Cr	7	−86.17
Mn	6	−103.73
Fe	5	−123.26
Co	4	−144.88
Ni	3	−169.11
Cu	2	−195.97
Zn	1	−65.01

Table 4: The computational HOF values of the 54 different TM complexes in 8 different M0X functionals with LANL2DZ basis set along with their respective experimental values taken from the respective literature (the references are given above) and the corresponding error (experiment–theory) values are shown in the following bunch of tables. The HOF results and the errors have the unit Kcal/mole.

Ti-Series

M05

Molecule	HOF(theo)	HOF(expt)	Error(expt–theo)
TiS	62.08	76.2	14.12
TiF_2	-129.01	-164.5	-35.49
TiO	13.39	13.7	0.31
TiH	106.74	116.4	9.66
TiF_3	-256.98	-284.1	-27.12
TiCl	32.33	24.2	-8.13

Mean Error (M E) =-7.78
Absolute Error (A E) =15.81

M05-2X

Molecule	HOF(theo)	HOF(expt)	Error(expt–theo)
TiS	93.77	76.2	-17.57
TiF_2	-107.40	-164.5	-57.10
TiO	46.28	13.7	-32.58
TiH	122.16	116.4	-5.76
TiF_3	-220.76	-284.1	-63.34
TiCl	55.27	24.2	-31.07

Mean Error (M E) =-34.57

Absolute Error (A E) =34.57

M06-L

Molecule	HOF(theo)	HOF(expt)	Error(expt–theo)
TiS	54.38	76.2	21.82
TiF_2	-123.90	-164.5	-40.60
TiO	9.36	13.7	4.34
TiH	104.97	116.4	11.43
TiF_3	-263.01	-284.1	-21.09
TiCl	37.50	24.2	-13.30

Mean Error (M E) =-6.23

Absolute Error (A E) =18.76

M06

Molecule	HOF(theo)	HOF(expt)	Error(expt–theo)
TiS	61.49	76.2	14.71
TiF_2	-122.88	-164.5	-41.62
TiO	17.32	13.7	-3.62
TiH	103.49	116.4	12.91
TiF_3	-251.42	-284.1	-32.68
TiCl	31.36	24.2	-7.16

Mean Error (M E) =-9.58

Absolute Error (A E) =18.78

M06-2X

Molecule	HOF(theo)	HOF(expt)	Error(expt–theo)
TiS	85.37	76.2	-9.17
TiF_2	-109.03	-164.5	-55.47
TiO	37.21	13.7	-23.51
TiH	112.01	116.4	4.39
TiF_3	-219.44	-284.1	-64.66
TiCl	38.42	24.2	-14.22

Mean Error (M E) =-27.11

Absolute Error (A E) =28.57

M06-HF

Molecule	HOF(theo)	HOF(expt)	Error(expt–theo)
TiS	113.45	76.2	-37.25
TiF_2	-82.16	-164.5	-82.34
TiO	72.74	13.7	-59.04
TiH	112.16	116.4	4.24
TiF_3	-176.74	-284.1	-107.36
TiCl	50.66	24.2	-26.46

Mean Error (M E) =-51.37

Absolute Error (A E) =52.78

M08-SO

Molecule	HOF(theo)	HOF(expt)	Error(expt–theo)
TiS	66.19	76.2	10.01
TiF_2	-133.07	-164.5	-31.43
TiO	4.24	13.7	9.46
TiH	76.72	116.4	39.68
TiF_3	-218.86	-284.1	-65.24
TiCl	10.39	24.2	13.81

Mean Error (M E) =-3.95

Absolute Error (A E) =28.27

M08-HX

Molecule	HOF(theo)	HOF(expt)	Error(expt–theo)
TiS	53.42	76.2	22.78
TiF_2	-152.69	-164.5	11.81
TiO	-0.06	13.7	13.76
TiH	64.29	116.4	52.12
TiF_3	-252.41	-284.1	-31.69
TiCl	4.18	24.2	20.02

Mean Error (M E) =14.7

Absolute Error (A E) =25.36

V-Series

M05

Molecule	HOF(theo)	HOF(expt)	Error(expt–theo)
V2	191.12	187.4	-3.72
VS	86.73	80.4	-6.33
VN	139.08	121	-18.08
VO	40.77	30.5	-10.27
VCl	51.31	37.8	-13.51
VF	14.21	0.7	-13.51

Mean Error (M E) =-10.90

Absolute Error (A E) =10.90

M05-2X

Molecule	HOF(theo)	HOF(expt)	Error(expt–theo)
V2	212.98	187.4	-25.58
VS	109.00	80.4	-28.60
VN	171.99	121	-50.99
VO	71.14	30.5	-40.64
VCl	60.51	37.8	-22.71
VF	26.81	0.7	-26.11

Mean Error (M E) =-32.43

Absolute Error (A E) =32.43

M06-L

Molecule	HOF(theo)	HOF(expt)	Error(expt–theo)
V2	154.07	187.4	33.33
VS	72.22	80.4	8.18
VN	120.75	121	0.25
VO	29.92	30.5	0.58
VCl	46.88	37.8	-9.08
VF	10.73	0.7	-10.03

Mean Error (M E) =3.86

Absolute Error (A E) =10.24

M06

Molecule	HOF(theo)	HOF(expt)	Error(expt–theo)
V2	170.28	187.4	17.12
VS	81.18	80.4	-0.78
VN	141.72	121	-20.72
VO	39.27	30.5	-8.77
VCl	47.35	37.8	-9.55
VF	14.57	0.7	-13.87

Mean Error (M E) =-6.10

Absolute Error (A E) =11.80

M06-2X

Molecule	HOF(theo)	HOF(expt)	Error(expt–theo)
V2	260.17	187.4	-72.77
VS	104.40	80.4	-24.00
VN	167.45	121	-46.45
VO	65.00	30.5	-34.50
VCl	49.30	37.8	-11.50
VF	22.60	0.7	-21.90

Mean Error (M E) =-35.19

Absolute Error (A E) =35.19

M06-HF

Molecule	HOF(theo)	HOF(expt)	Error(expt–theo)
V2	317.70	187.4	-130.30
VS	122.81	80.4	-42.41
VN	198.03	121	-77.03
VO	96.22	30.5	-65.72
VCl	56.51	37.8	-18.71
VF	31.35	0.7	-30.65

Mean Error (M E) =-60.80

Absolute Error (A E) =60.80

M08-SO

Molecule	HOF(theo)	HOF(expt)	Error(expt–theo)
V2	22.90	187.4	14.90
VS	92.23	80.4	-11.83
VN	120.96	121	0.041
VO	-16.31	30.5	46.81
VCl	22.90	37.8	14.90
VF	6.13	0.7	-5.43

Mean Error (M E) = 9.90

Absolute Error (A E) = 15.65

M08-HX

Molecule	HOF(theo)	HOF(expt)	Error(expt–theo)
V2	48.57	187.4	-10.77
VS	117.41	80.4	-37.01
VN	179.19	121	-58.19
VO	102.95	30.5	-72.45
VCl	48.57	37.8	-10.77
VF	27.03	0.7	-26.33

Mean Error (M E) = -35.92

Absolute Error (A E) = 35.92

Cr-Series

M05

Molecule	HOF(theo)	HOF(expt)	Error(expt–theo)
CrCl	35.50	31	-4.50
$CrCl_2$	-11.12	-28.1	-16.98
CrF	6.12	3.1	-3.02
CrO	70.93	45	-25.93
CrO_2	25.95	-18	-43.95
CrOH	35.61	18.9	-16.71

Mean Error (M E) =-18.52
Absolute Error (A E) =18.52

M05-2X

Molecule	HOF(theo)	HOF(expt)	Error(expt–theo)
CrCl	37.26	31	-6.26
$CrCl_2$	15.66	-28.1	-43.76
CrF	12.51	3.1	-9.41
CrO	87.38	45	-42.38
CrO_2	97.09	-18	-115.09
CrOH	39.19	18.9	-20.29

Mean Error (M E) =-39.54
Absolute Error (A E) =39.54

M06-L

Molecule	HOF(theo)	HOF(expt)	Error(expt–theo)
CrCl	31.50	31	-0.50
$CrCl_2$	-18.59	-28.1	-9.51
CrF	1.11	3.1	1.99
CrO	55.10	45	-10.10
CrO_2	-1.71	-18	-16.29
CrOH	32.43	18.9	-13.53

Mean Error (M E) =-7.99
Absolute Error (A E) =8.65

M06

Molecule	HOF(theo)	HOF(expt)	Error(expt–theo)
CrCl	34.41	31	-3.41
$CrCl_2$	-13.53	-28.1	-14.57
CrF	8.85	3.1	-5.75
CrO	72.19	45	-27.19
CrO_2	31.79	-18	-49.79
CrOH	37.40	18.9	-18.50

Mean Error (M E) =-19.87

Absolute Error (A E) =19.87

M06-2X

Molecule	HOF(theo)	HOF(expt)	Error(expt–theo)
CrCl	33.76	31	-2.76
$CrCl_2$	14.06	-28.1	-42.16
CrF	15.08	3.1	-11.98
CrO	88.94	45	-43.94
CrO_2	105.01	-18	-123.01
CrOH	41.29	18.9	-22.39

Mean Error (M E) =-41.04

Absolute Error (A E) =41.04

M06-HF

Molecule	HOF(theo)	HOF(expt)	Error(expt–theo)
CrCl	26.87	31	4.13
$CrCl_2$	-7.97	-28.1	-20.13
CrF	15.26	3.1	-12.16
CrO	92.30	45	-47.30
CrO_2	129.08	-18	-147.08
CrOH	37.11	18.9	-18.21

Mean Error (M E) =-40.13

Absolute Error (A E) =41.50

M08-SO

Molecule	HOF(theo)	HOF(expt)	Error(expt–theo)
CrCl	34.58	31	-3.58
$CrCl_2$	-7.03	-28.1	-21.07
CrF	14.59	3.1	-11.49
CrO	80.28	45	-35.28
CrO_2	84.19	-18	-102.19
CrOH	23.44	18.9	-4.54

Mean Error (M E) = -29.69

Absolute Error (A E) =29.69

M08-HX

Molecule	HOF(theo)	HOF(expt)	Error(expt–theo)
CrCl	30.47	31	0.53
$CrCl_2$	-19.67	-28.1	-8.43
CrF	4.02	3.1	-0.92
CrO	92.72	45	-47.72
CrO_2	94.88	-18	-112.88
CrOH	18.59	18.9	0.31

Mean Error (M E) = -28.19

Absolute Error (A E) =28.47

Mn Series

M05

Molecule	HOF(theo)	HOF(expt)	Error(expt–theo)
$MnCl_2$	-84.04	-63	21.04
MnCl	-16.31	11.3	27.61
MnF_2	-148.18	-126.2	21.98
MnH	64.16	64.2	0.04
MnO	16.93	29.6	12.67
MnF	-34.82	-19.9	14.92

Mean Error (M E) =16.38
Absolute Error (A E) =16.38

M05-2X

Molecule	HOF(theo)	HOF(expt)	Error(expt–theo)
$MnCl_2$	-91.09	-63	28.09
MnCl	-19.89	11.3	31.19
MnF_2	-155.48	-126.2	29.28
MnH	45.41	64.2	18.79
MnO	26.68	29.6	2.92
MnF	-45.42	-19.9	25.52

Mean Error (M E) =22.63
Absolute Error (A E) =22.63

M06-L

Molecule	HOF(theo)	HOF(expt)	Error(expt–theo)
$MnCl_2$	-98.55	-63	35.55
MnCl	-14.18	11.3	25.48
MnF_2	-163.04	-126.2	36.84
MnH	38.44	64.2	25.76
MnO	-1.83	29.6	31.43
MnF	-48.86	-19.9	28.96

Mean Error (M E) =30.67
Absolute Error (A E) =30.67

M06

Molecule	HOF(theo)	HOF(expt)	Error(expt–theo)
$MnCl_2$	-97.25	-63	34.25
MnCl	-23.12	11.3	34.42
MnF_2	-154.29	-126.2	28.09
MnH	59.03	64.2	5.17
MnO	10.34	29.6	19.26
MnF	-42.17	-19.9	22.27

Mean Error (M E) =23.91
Absolute Error (A E) =23.91

M06-2X

Molecule	HOF(theo)	HOF(expt))	Error(expt–theo)
$MnCl_2$	-100.23	-63	37.23
MnCl	-27.56	11.3	38.86
MnF_2	-153.13	-126.2	26.93
MnH	44.11	64.2	20.09
MnO	24.71	29.6	4.89
MnF	-47.76	-19.9	27.86

Mean Error (M E) =25.98
Absolute Error (A E) =25.98

M06-HF

Molecule	HOF(theo)	HOF(expt)	Error(expt–theo)
$MnCl_2$	-51.88	-63	-11.12
MnCl	9.58	11.3	1.72
MnF_2	-91.23	-126.2	-34.97
MnH	95.11	64.2	-30.91
MnO	94.15	29.6	-64.55
MnF	125.64	-19.9	-145.54

Mean Error (M E) =-47.56
Absolute Error (A E) =48.13

M08-SO

Molecule	HOF(theo)	HOF(expt)	Error(expt–theo)
$MnCl_2$	-86.76	-63	23.76
MnCl	-10.17	11.3	21.47
MnF_2	-137.60	-126.2	11.40
MnH	62.33	64.2	1.87
MnO	63.42	29.6	-33.82
MnF	-35.99	-19.9	16.09

Mean Error (M E) = 6.80
Absolute Error (A E) = 18.07

M08-HX

Molecule	HOF(theo)	HOF(expt)	Error(expt–theo)
$MnCl_2$	-107.24	-63	44.24
MnCl	-28.59	11.3	39.89
MnF_2	-168.33	-126.2	42.13
MnH	32.21	64.2	31.99
MnO	47.95	29.6	-18.35
MnF	-60.29	-19.9	40.39

Mean Error (M E) = 30.05
Absolute Error (A E) = 36.17

Fe-Series

M05

Molecule	HOF(theo)	HOF(expt)	Error(expt–theo)
FeF_2	-232.08	-93	139.08
$Fe(CO)_2$	44.34	0.2	-44.14
Fe(CO)	95.66	27.91	-67.75
FeCl	48.45	49.5	1.05
FeO	66.51	61.1	-5.41
$FeCl_2$	-184.00	-32.8	151.20

Mean Error (M E) = 29.005
Absolute Error (A E) = 68.105

M05-2X

Molecule	HOF(theo)	HOF(expt)	Error(expt–theo)
FeF_2	-234.32	-93	141.32
$Fe(CO)_2$	92.76	0.2	-92.56
Fe(CO)	117.33	27.91	-89.42
FeCl	44.80	49.5	4.70
FeO	78.03	61.1	-16.93
$FeCl_2$	-186.12	-32.8	153.32

Mean Error (M E) = 16.738
Absolute Error (A E) = 83.042

M06-L

Molecule	HOF(theo)	HOF(expt)	Error(expt–theo)
FeF_2	-235.79	-93	142.79
$Fe(CO)_2$	33.82	0.2	-33.62
Fe(CO)	74.25	27.91	-46.34
FeCl	33.39	49.5	16.11
FeO	54.64	61.1	6.46
$FeCl_2$	-188.56	-32.8	155.76

Mean Error (M E) =40.19
Absolute Error (A E) =66.85

M06

Molecule	HOF(theo)	HOF(expt)	Error(expt–theo)
FeF_2	-235.57	-93	142.57
$Fe(CO)_2$	29.34	0.2	-29.14
Fe(CO)	87.34	27.91	-59.43
FeCl	44.11	49.5	5.39
FeO	60.69	61.1	0.41
$FeCl_2$	-196.11	-32.8	163.31

Mean Error (M E) =37.19
Absolute Error (A E) =66.71

M06-2X

Molecule	HOF(theo)	HOF(expt)	Error(expt–theo)
FeF_2	-231.67	-93	138.67
$Fe(CO)_2$	88.94	0.2	-88.74
Fe(CO)	116.36	27.91	-88.45
FeCl	35.64	49.5	13.86
FeO	78.48	61.1	-17.38
$FeCl_2$	-194.83	-32.8	162.03

Mean Error (M E) =20
Absolute Error (A E) =84.67

M06-HF

Molecule	HOF(theo)	HOF(expt)	Error(expt–theo)
FeF_2	-223.00	-93	130.00
$Fe(CO)_2$	121.27	0.2	-121.07
Fe(CO)	141.49	27.91	-113.58
FeCl	30.86	49.5	18.64
FeO	106.79	61.1	-45.69
$FeCl_2$	-198.36	-32.8	165.56

Mean Error (M E) =5.64
Absolute Error (A E) =99.09

M08-SO

Molecule	HOF(theo)	HOF(expt)	Error(expt–theo)
FeF_2	-226.93	-93	133.93
$Fe(CO)_2$	93.74	0.2	-93.54
Fe(CO)	133.87	27.91	-105.96
FeCl	21.96	49.5	27.54
FeO	74.80	61.1	-13.70
$FeCl_2$	-193.05	-32.8	160.25

Mean Error (M E) = 18.09
Absolute Error (A E) = 89.15

M08-HX

Molecule	HOF(theo)	HOF(expt)	Error(expt–theo)
FeF_2	-230.88	-93	137.88
$Fe(CO)_2$	138.92	0.2	-138.72
Fe(CO)	147.43	27.91	-119.52
FeCl	47.96	49.5	1.54
FeO	97.32	61.1	-36.22
$FeCl_2$	-182.71	-32.8	149.91

Mean Error (M E) = -0.86
Absolute Error (A E) = 97.30

Co-Complexes

M05

Molecule	HOF(theo)	HOF(expt)	Error(expt–theo)
CoH	93.01	110.7	17.69
CoO	65.07	74	8.93
CoCl	43.69	50.3	6.61
$CoCl_2$	-23.10	-22.6	0.50
CoF_2	-92.91	-87.5	5.41
$CoCl_3$	-24.70	-39.1	-14.40

Mean Error (M E) =4.12
Absolute Error (A E) =8.92

M05-2X

Molecule	HOF(theo)	HOF(expt)	Error(expt–theo)
CoH	95.55	110.7	15.15
CoO	99.79	74	-25.79
CoCl	40.84	50.3	9.46
$CoCl_2$	-1.33	-22.6	-21.27
CoF_2	-74.83	-87.5	-12.67
$CoCl_3$	3.54	-39.1	-42.64

Mean Error (M E) =-12.96
Absolute Error (A E) =21.16

M06-L

Molecule	HOF(theo)	HOF(expt)	Error(expt–theo)
CoH	90.70	110.7	20.00
CoO	75.52	74	-1.52
CoCl	36.56	50.3	13.74
$CoCl_2$	-18.58	-22.6	-4.02
CoF_2	-77.69	-87.5	-9.81
$CoCl_3$	-38.21	-39.1	-0.89

Mean Error (M E) =2.92
Absolute Error (A E) =8.33

M06

Molecule	HOF(theo)	HOF(expt)	Error(expt–theo)
CoH	93.23	110.7	17.47
CoO	72.15	74	1.85
CoCl	47.81	50.3	2.49
$CoCl_2$	-23.31	-22.6	0.71
CoF_2	-84.45	-87.5	-3.05
$CoCl_3$	-35.96	-39.1	-3.14

Mean Error (M E) =2.73
Absolute Error (A E) =4.79

M06-2X

Molecule	HOF(theo)	HOF(expt)	Error(expt–theo)
CoH	99.80	110.7	10.90
CoO	102.10	74	-28.10
CoCl	41.05	50.3	9.25
$CoCl_2$	-10.59	-22.6	-12.01
CoF_2	-71.59	-87.5	-15.91
$CoCl_3$	-4.92	-39.1	-34.18

Mean Error (M E) =-11.68
Absolute Error (A E) =18.39

M06-HF

Molecule	HOF(theo)	HOF(expt)	Error(expt–theo)
CoH	105.70	110.7	5.00
CoO	136.94	74	-62.94
CoCl	44.46	50.3	5.84
$CoCl_2$	-5.93	-22.6	-16.67
CoF_2	-57.08	-87.5	-30.42
$CoCl_3$	-61.43	-39.1	22.33

Mean Error (M E) = -12.81
Absolute Error (A E) = 23.87

M08-SO

Molecule	HOF(theo)	HOF(expt)	Error(expt–theo)
CoH	65.02	110.7	45.68
CoO	76.01	74	-2.01
CoCl	35.76	50.3	14.54
$CoCl_2$	-29.80	-22.6	7.20
CoF_2	-88.07	-87.5	0.57

Mean Error (M E) = 13.20
Absolute Error (A E) = 14.0

M08-HX

Molecule	HOF(theo)	HOF(expt)	Error(expt–theo)
CoH	76.88	110.7	33.82
CoO	102.82	74	-28.82
CoCl	42.21	50.3	8.09
$CoCl_2$	-12.16	-22.6	-10.44
CoF_2	-82.35	-87.5	-5.15

Mean Error (M E) = -0.5
Absolute Error (A E) = 17.26

Ni-Series

M05

Molecule	HOF(theo)	HOF(expt)	Error(expt–theo)
NiO	84.26	75	-9.26
NiH	92.35	85.6	-6.75
NiF_2	-45.81	-77.8	-31.99
NiCl	45.15	41.7	-3.45
$NiCl_2$	9.85	-17.4	-27.25
NiCO	72.57	35.1	-37.47

Mean Error (M E) = -19.36
Absolute Error (A E) = 19.36

M05-2X

Molecule	HOF(theo)	HOF(expt)	Error(expt–theo)
NiO	107.18	75	-32.18
NiH	97.49	85.6	-11.89
NiF_2	-53.06	-77.8	-24.74
NiCl	45.80	41.7	-4.10
$NiCl_2$	8.34	-17.4	-25.74
NiCO	112.08	35.1	-76.98

Mean Error (M E) = -29.27
Absolute Error (A E) = 29.27

M06-L

Molecule	HOF(theo)	HOF(expt)	Error(expt–theo)
NiO	69.32	75	5.68
NiH	93.73	85.6	-8.13
NiF_2	-65.36	-77.8	-12.44
NiCl	42.41	41.7	-0.71
$NiCl_2$	-9.01	-17.4	-8.39
NiCO	57.13	35.1	-22.03

Mean Error (M E) = -7.67
Absolute Error (A E) = 9.56

M06

Molecule	HOF(theo)	HOF(expt)	Error(expt–theo)
NiO	87.64	75	-12.64
NiH	94.12	85.6	-8.52
NiF_2	-43.82	-77.8	-33.98
NiCl	44.49	41.7	-2.79
$NiCl_2$	2.98	-17.4	-20.38
NiCO	71.87	35.1	-36.77

Mean Error (M E) = -19.18
Absolute Error (A E) = 19.18

M06-2X

Molecule	HOF(theo)	HOF(expt)	Error(expt–theo)
NiO	116.15	75	-41.15
NiH	101.97	85.6	-16.37
NiF_2	-39.78	-77.8	-38.02
NiCl	46.41	41.7	-4.71
$NiCl_2$	9.04	-17.4	-26.44
NiCO	115.22	35.1	-80.12

Mean Error (M E) = -34.47
Absolute Error (A E) = 34.47

M06-HF

Molecule	HOF(theo)	HOF(expt)	Error(expt–theo)
NiO	150.45	75	-75.45
NiH	111.96	85.6	-26.36
NiF_2	-30.39	-77.8	-47.41
NiCl	51.89	41.7	-10.19
$NiCl_2$	50.28	-17.4	-67.68
NiCO	133.79	35.1	-98.69

Mean Error (M E) = -54.30
Absolute Error (A E) = 54.30

M08-SO

Molecule	HOF(theo)	HOF(expt)	Error(expt–theo)
NiO	100.25	75	-25.25
NiH	90.56	85.6	-4.96
NiF_2	-40.75	-77.8	-32.05
NiCl	42.96	41.7	-1.26
$NiCl_2$	20.46	-17.4	-37.86

Mean Error (M E) = -19.68
Absolute Error (A E) = 19.68

M08-HX

Molecule	HOF(theo)	HOF(expt)	Error(expt–theo)
NiO	99.49	75	-24.49
NiH	91.22	85.6	-5.62
NiF_2	-61.79	-77.8	-11.01
NiCl	39.32	41.7	2.38
$NiCl_2$	1.53	-17.4	-18.93

Mean Error (M E) = -11.53
Absolute Error (A E) = 12.49

Cu-Complexes

M05

Molecule	HOF(theo)	HOF(expt)	Error(expt–theo)
Cu2	115.20	113.8	-1.40
CuCl	26.14	19.3	-6.84
CuF	9.33	-3.2	-12.53
CuF_2	-27.39	-66	-38.61
CuO	85.22	76.5	-8.72
CuS	87.09	75.1	-11.99

Mean Error (M E) = -13.35
Absolute Error (A E) = 13.35

M05-2X

Molecule	HOF(theo)	HOF(expt)	Error(expt–theo)
Cu2	110.12	113.8	3.68
CuCl	24.37	19.3	-5.07
CuF	8.14	-3.2	-11.34
CuF_2	-30.39	-66	-35.61
CuO	84.14	76.5	-7.64
CuS	87.33	75.1	-12.23

Mean Error (M E) = -11.37
Absolute Error (A E) = 12.60

M06-L

Molecule	HOF(theo)	HOF(expt)	Error(expt–theo)
Cu2	101.09	113.8	12.71
CuCl	19.70	19.3	-0.40
CuF	0.17	-3.2	-3.37
CuF_2	-53.05	-66	-12.95
CuO	71.49	76.5	5.01
CuS	73.81	75.1	1.29

Mean Error (M E) = 0.38
Absolute Error (A E) = 5.96

M06

Molecule	HOF(theo)	HOF(expt)	Error(expt–theo)
Cu2	109.32	113.8	4.48
CuCl	23.30	19.3	-4.00
CuF	10.44	-3.2	-13.64
CuF_2	-26.95	-66	-39.05
CuO	84.65	76.5	-8.15
CuS	82.86	75.1	-7.76

Mean Error (M E) = -11.35
Absolute Error (A E) = 12.85

M06-2X

Molecule	HOF(theo)	HOF(expt)	Error(expt–theo)
Cu2	118.90	113.8	-5.10
CuCl	24.47	19.3	-5.17
CuF	13.70	-3.2	-16.90
CuF_2	-20.93	-66	-45.07
CuO	89.02	76.5	-12.52
CuS	93.28	75.1	-18.18

Mean Error (M E) = -17.16
Absolute Error (A E) = 17.16

M06-HF

Molecule	HOF(theo)	HOF(expt)	Error(expt–theo)
Cu2	55.18	113.8	58.62
CuCl	-14.14	19.3	33.44
CuF	-17.93	-3.2	14.73
CuF_2	-60.16	-66	-5.84
CuO	59.19	76.5	17.31
CuS	64.03	75.1	11.07

Mean Error (M E) = 21.56
Absolute Error (A E) = 23.50

M08-SO

Molecule	HOF(theo)	HOF(expt)	Error(expt–theo)
Cu2	114.35	113.8	-0.55
CuCl	21.01	19.3	-1.71
CuF	12.27	-3.2	-15.47
CuF_2	-21.48	-66	-44.52
CuO	84.01	76.5	-7.51
CuS	94.65	75.1	-19.55

Mean Error (M E) = -14.89
Absolute Error (A E) = 14.89

M08-HX

Molecule	HOF(theo)	HOF(expt)	Error(expt–theo)
Cu2	115.47	113.8	-1.66
CuCl	18.44	19.3	0.86
CuF	3.13	-3.2	-6.33
CuF_2	-53.82	-66	-12.18
CuO	81.86	76.5	-5.36
CuS	90.82	75.1	-15.72

Mean Error (M E) = -6.73
Absolute Error (A E) = 7.02

Zn-Complexes

M05

Molecule	HOF(theo)	HOF(expt)	Error(expt–theo)
Zn_2	60.37	57.7	-2.67
$ZnCH_3$	-98.29	26	124.29
$ZnCl_2$	-45.93	-63.5	-17.57
ZnF_2	-104.52	-118.9	-14.38
ZnH	68.51	62.9	-5.61
ZnO	76.21	52.8	-23.41

Mean Error (M E) = 10.11
Absolute Error (A E) = 31.32

M05-2X

Molecule	HOF(theo)	HOF(expt)	Error(expt–theo)
Zn_2	61.38	57.7	-3.68
$ZnCH_3$	-92.99	26	118.99
$ZnCl_2$	-41.99	-63.5	-21.51
ZnF_2	-100.47	-118.9	-18.43
ZnH	70.35	62.9	-7.45
ZnO	70.82	52.8	-18.02

Mean Error (M E) = 8.32
Absolute Error (A E) = 49.9

M06-L

Molecule	HOF(theo)	HOF(expt)	Error(expt–theo)
Zn_2	60.11	57.7	-2.41
$ZnCH_3$	-93.68	26	119.68
$ZnCl_2$	-47.47	-63.5	-16.03
ZnF_2	-107.11	-118.9	-11.79
ZnH	68.52	62.9	-5.62
ZnO	63.91	52.8	-11.11

Mean Error (M E) = 12.12
Absolute Error (A E) = 27.77

M06

Molecule	HOF(theo)	HOF(expt)	Error(expt–theo)
Zn_2	58.41	57.7	-0.71
$ZnCH_3$	-94.37	26	120.37
$ZnCl_2$	-46.54	-63.5	-16.96
ZnF_2	-96.29	-118.9	-22.61
ZnH	71.15	62.9	-8.25
ZnO	72.28	52.8	-19.48

Mean Error (M E) = 8.73
Absolute Error (A E) = 31.40

M06-2X

Molecule	HOF(theo)	HOF(expt)	Error(expt–theo)
Zn_2	61.41	57.7	-3.71
$ZnCH_3$	-98.31	26	124.31
$ZnCl_2$	-51.92	-63.5	-11.58
ZnF_2	-98.84	-118.9	-20.06
ZnH	65.30	62.9	-2.40
ZnO	65.09	52.8	-12.29

Mean Error (M E) = 12.38
Absolute Error (A E) = 29.06

M06-HF

Molecule	HOF(theo)	HOF(expt)	Error(expt–theo)
Zn_2	61.70	57.7	-4.00
$ZnCH_3$	-111.41	26	137.41
$ZnCl_2$	-65.37	-63.5	1.87
ZnF_2	-100.82	-118.9	-18.08
ZnH	51.59	62.9	11.31
ZnO	55.89	52.8	-3.09

Mean Error (M E) = 20.90
Absolute Error (A E) = 29.29

M08-SO

Molecule	HOF(theo)	HOF(expt)	Error(expt–theo)
Zn_2	56.70	57.7	1.00
$ZnCH_3$	-146.55	26	172.55
$ZnCl_2$	-55.21	-63.5	-8.29
ZnF_2	-102.23	-118.9	-16.67
ZnH	57.35	62.9	5.55
ZnO	62.10	52.8	-9.30

Mean Error (M E) = 24.15
Absolute Error (A E) = 35.56

M08-HX

Molecule	HOF(theo)	HOF(expt)	Error(expt–theo)
Zn_2	58.03	57.7	-0.33
$ZnCH_3$	-148.22	26	174.22
$ZnCl_2$	-61.80	-63.5	-1.70
ZnF_2	-121.61	-118.9	2.71
ZnH	55.11	62.9	7.79
ZnO	59.77	52.8	-6.97

Mean Error (M E) = 29.29
Absolute Error (A E) = 32.29

Table 5: The IP values of the 47 TM complexes in 6 different M0X functionals with LANL2DZ basis set along with their experimental and the respective error (experiment–theory) values are depicted in the following group of tables. In these following tables the columns heading neural and cation represent the zero point corrected energy of these TM complexes of these states respectively. The multiplicities (M) of these neutral and cationic states are shown in the bracket. The neutral and the cationic energy of a molecule are expressed in a.u., whereas the errors are expressed in eV.

Ti-Series

M05

Molecule	Neutral(M)	Cation(M)	I.P(Theo)/I.P(Expt)	Error(Expt–Theo)
TiS	–68.06213(3)	–67.77894(2)	7.71/7.10	–0.61
TiF_2	–257.76095(3)	–257.26933(4)	13.38/12.20	–1.18
TiO	–133.18073(3)	–132.94747(2)	6.35/6.82	0.47
TiH	–58.46101(2)	–58.23630(3)	6.15/6.00	–0.15
TiF_3	–357.71429(2)	–357.34169(1)	10.14/10.50	0.36

Mean Error (M E) = –0.348
Absolute Error (A E) = 0.680

M05-2X

Molecule	Neutral(M)	Cation(M)	I.P(Theo)/I.P(Expt)	Error(Expt–Theo)
TiS	–68.04347(3)	–67.72918(2)	8.55/7.10	–1.45
TiF_2	–257.78965(3)	–257.36568(2)	11.54/12.20	0.66
TiO	–133.17410(3)	–132.84271(2)	9.02/6.82	–2.20
TiH	–58.46508(4)	–58.23916(3)	6.15/6.00	–0.15
TiF_3	–357.73983(2)	–357.31342(1)	11.60/10.50	–1.10

Mean Error (M E) = –0.848

Absolute Error (A E) = 1.112

M06-L

Molecule	Neutral(M)	Cation(M)	I.P(Theo)/I.P(Expt)	Error(Expt–Theo)
TiS	–68.17238(3)	–67.92358(2)	6.77/7.10	0.33
TiF_2	–257.85950(3)	–257.40021(4)	12.14/12.20	0.06
TiO	–133.28499(3)	–133.05625(2)	6.22/6.82	0.60
TiH	–58.54990(2)	–58.31764(3)	6.33/6.00	–0.33
TiF_3	–357.84531(2)	–357.49433(1)	9.55/10.50	0.95

Mean Error (M E) = 0.322
Absolute Error (A E) = 0.454

M06

Molecule	Neutral(M)	Cation(M)	I.P(Theo)/I.P(Expt)	Error(Expt–Theo)
TiS	–68.09658(3)	–67.81250(2)	7.73/7.10	–0.63
TiF_2	–257.76899(3)	–257.30774(4)	12.55/12.20	–0.35
TiO	–133.20142(3)	–132.96337(2)	6.48/6.82	0.34
TiH	–58.50154(2)	–58.25807(3)	6.63/6.00	–0.63
TiF_3	–357.71623(2)	–357.34856(1)	10.01/10.50	0.49

Mean Error (M E) = –0.156
Absolute Error (A E) = 0.488

M06-2X

Molecule	Neutral(M)	Cation(M)	I.P(Theo)/I.P(Expt)	Error(Expt–Theo)
TiS	–68.03129(3)	–67.72224(2)	8.41/7.10	–1.31
TiF_2	–257.73941(3)	–257.31580(2)	11.53/12.20	0.67
TiO	–133.158801(3)	–132.82922(2)	8.97/6.82	–2.15
TiH	–58.46698(4)	–58.18975(3)	7.54/6.00	–1.54
TiF_3	–357.66313(2)	–357.24670(1)	11.33/10.50	–0.83

Mean Error (M E) = –1.032
Absolute Error (A E) = 1.30

M06-HF

Molecule	Neutral(M)	Cation(M)	I.P(Theo)/I.P(Expt)	Error(Expt–Theo)
TiS	–67.96414(3)	–67.64195(4)	8.76/7.10	–1.66
TiF_2	–257.69695(3)	–257.25506(2)	12.03/12.20	0.17
TiO	–133.09595(3)	–132.75148(2)	9.37/6.82	–2.55
TiH	–58.44952(2)	–58.19113(3)	7.03/6.00	–1.03
TiF_3	–357.60408(2)	–357.12900(1)	12.93/10.50	–2.43

Mean Error (M E) = –1.50
Absolute Error (A E) = 1.568

M08-SO

Molecule	Neutral(M)	Cation(M)	I.P(Theo)/I.P(Expt)	Error(Expt–Theo)
TiS	-67.99357 (3)	-67.68630 (2)	8.36/7.10	-1.26
TiF_2	-257.66622 (3)	-257.31846 (2)	9.46/12.20	2.74
TiO	-133.08429 (3)	-132.82884(2)	6.95/6.82	-0.13
TiH	-58.42186 (2)	-58.17636 (3)	6.68/6.00	-0.68
TiF_3	-357.54128 (2)	-357.15061 (1)	10.63/10.50	-0.13

Mean Error (M E) = 0.108
Absolute Error (A E) = 0.988

M08-HX

Molecule	Neutral(M)	Cation(M)	I.P(Theo)/I.P(Expt)	Error(Expt–Theo)
TiS	-68.0594(3)	-67.78051 (2)	7.59/7.10	-0.49
TiF_2	-257.75535 (3)	-257.41704(2)	9.21/12.20	2.99
TiO	-133.15922 (3)	-132.90480 (2)	6.92/6.82	-0.10
TiH	-58.49120 (4)	-58.24747(3)	6.63/6.00	-0.63
TiF_3	-357.65811 (2)	-357.25556(1)	10.95/10.50	-0.45

Mean Error (M E) = 0.264
Absolute Error (A E) = 0.932

V-Series
M05

Molecule	Neutral(M)	Cation(M)	I.P(Theo)/I.P(Expt)	Error(Expt–Theo)
V2	–142.39054(3)	–142.18723(4)	5.36/6.36	0.83
VS	–81.31479(4)	–81.01502(3)	8.16/8.40	0.24
VN	–125.87598(3)	–125.58023(4)	8.05/8.00	–0.05
VO	–146.42902(4)	–146.18137(3)	6.74/7.24	0.50

Mean Error (M E) = 0.380
Absolute Error (A E) = 0.405

M05-2X

Molecule	Neutral(M)	Cation(M)	I.P(Theo)/I.P(Expt)	Error(Expt–Theo)
V2	–142.35868(7)	–142.1310(4)	6.19/6.36	0.17
VS	–81.28662(4)	–80.94635(3)	9.26/8.40	–0.86
VN	–125.84760(3)	–125.59635(2)	6.84/8.00	1.16
VO	–146.40192(4)	–146.07208(3)	8.98/7.24	–1.74

Mean Error (M E) = –0.318
Absolute Error (A E) = 0.983

M06-L

Molecule	Neutral(M)	Cation(M)	I.P(Theo)/I.P(Expt)	Error(Expt–Theo)
V2	–142.56242(3)	–142.33801(4)	6.11/6.36	0.25
VS	–81.41437(4)	–81.13793(3)	7.52/8.40	0.88
VN	–125.98490(3)	–125.73963(2)	6.67/8.00	1.33
VO	–146.52263(4)	–146.26489(3)	7.01/7.24	0.23

Mean Error (M E) = 0.673
Absolute Error (A E) = 0.673

M06

Molecule	Neutral(M)	Cation(M)	I.P(Theo)/I.P(Expt)	Error(Expt–Theo)
V2	–142.47364(3)	–142.23179(4)	6.58/6.36	0.58
VS	–81.35009(4)	–81.03831(3)	8.48/8.40	–0.08
VN	–125.89482(3)	–125.64537(2)	6.79/8.00	–0.27
VO	–146.45132(4)	–146.19158(3)	7.07/7.24	0.17

Mean Error (M E) = 0.10
Absolute Error (A E) = 0.275

M06-2X

Molecule	Neutral(M)	Cation(M)	I.P(Theo)/I.P(Expt)	Error(Expt–Theo)
V2	–142.29239(7)	–142.07824(8)	5.82/6.36	0.54
VS	–81.28589(4)	–80.97817(3)	8.37/8.40	0.03
VN	–125.84787(3)	–125.58766(2)	7.08/8.00	0.92
VO	–146.39945(4)	–146.07116(1)	8.93/7.24	–1.69

Mean Error (M E) = – 0.05
Absolute Error (A E) = 0.795

M06-HF

Molecule	Neutral(M)	Cation(M)	I.P(Theo)/I.P(Expt)	Error(Expt–Theo)
V2	–142.15559(7)	–141.95538(8)	5.45/6.36	0.91
VS	–81.22480(4)	–80.90518(5)	8.70/8.40	–0.30
VN	–125.78190(3)	–125.46374(2)	8.65/8.00	–0.65
VO	–146.33410(4)	–145.99436(3)	9.24/7.24	–2.00

Mean Error (M E) = –0.51
Absolute Error (A E) = 0.965

M08-SO

Molecule	Neutral(M)	Cation(M)	I.P(Theo)/I.P(Expt)	Error(Expt–Theo)
V2	-142.16396(1)	-141.93424(4)	6.25/6.36	0.11
VS	-81.21290(4)	-80.94070(3)	7.41/8.40	0.99
VN	-125.76396(3)	-125.45015(4)	8.54/8.00	-0.54
VO	-146.38493(4)	-146.10981(3)	7.49/7.24	-0.25

Mean Error (M E) = 0.078
Absolute Error (A E) = 0.473

M08-HX

Molecule	Neutral(M)	Cation(M)	I.P(Theo)/I.P(Expt)	Error(Expt–Theo)
V2	-142.21024(1)	-142.0088(4)	5.48/6.36	0.88
VS	-81.27824(4)	-80.98257(3)	8.05/8.40	0.35
VN	-125.80643(3)	-125.51519(4)	7.92/8.00	0.08
VO	-146.32273(4)	-146.04761(3)	7.49/7.24	-0.25

Mean Error (M E) = 0.265
Absolute Error (A E) = 0.39

Cr-Series

M05

Molecule	Neutral(M)	Cation(M)	I.P(Theo)/I.P(Expt)	Error(Expt–Theo)
CrCl	–101.20560(6)	–100.89935(5)	8.33/8.50	0.17
$CrCl_2$	–116.17603(5)	–115.77705(4)	10.86/9.90	–0.96
CrF	–186.10261(6)	–185.81227(5)	7.90/9.30	1.40
CrO	–161.39602(5)	–161.11832(4)	7.56/8.16	0.60
CrO_2	–236.61280(3)	–236.22768(2)	10.48/10.30	–0.18
CrOH	–162.02722(6)	–161.75490(5)	7.41/7.54	0.13

Mean Error (M E) = 0.193
Absolute Error (A E) = 0.573

M05-2X

Molecule	Neutral(M)	Cation(M)	I.P(Theo)/I.P(Expt)	Error(Expt–Theo)
CrCl	–101.19015(6)	–100.82929(5)	9.82/8.50	–1.32
$CrCl_2$	–116.12818(5)	–115.70593(4)	11.49/9.90	–1.59
CrF	–186.09065(6)	–185.76705(5)	8.81/9.30	0.49
CrO	–161.36900(5)	–161.06997(4)	8.14/8.16	0.02
CrO_2	–236.52012(5)	–236.05300(2)	12.71/10.30	–2.41
CrOH	–162.02360(6)	–161.74374(5)	7.62/7.54	–0.08

Mean Error (M E) = –0.815

Absolute Error (A E) = 0.985

M06-L

Molecule	Neutral(M)	Cation(M)	I.P(Theo)/I.P(Expt)	Error(Expt–Theo)
CrCl	–101.28768(6)	–100.97753(5)	8.44/8.50	0.06
$CrCl_2$	–116.30232(5)	–115.94268(4)	9.79/9.90	0.11
CrF	–186.16204(6)	–185.87004(5)	7.95/9.30	1.35
CrO	–161.47803(5)	–161.19095(4)	7.81/8.16	0.35
CrO_2	–236.73353(3)	–236.32495(2)	11.19/10.30	–0.89
CrOH	–162.09710(6)	–161.82976(5)	7.28/7.54	0.26

Mean Error (M E) = 0.207
Absolute Error (A E) = 0.503

M06

Molecule	Neutral(M)	Cation(M)	I.P(Theo)/I.P(Expt)	Error(Expt–Theo)
CrCl	–101.24026(6)	–100.91847(5)	8.76/8.50	–0.26
$CrCl_2$	–116.22236(5)	–115.81287(4)	11.14/9.90	–1.24
CrF	–186.11430(6)	–185.81054(5)	8.27/9.30	1.03
CrO	–161.41191(5)	–161.11840(4)	7.99/8.16	0.17
CrO_2	–236.61604(3)	–236.22574(2)	10.62/10.30	–0.32
CrOH	–162.04534(6)	–161.76330(5)	7.68/7.54	–0.14

Mean Error (M E) = –0.127
Absolute Error (A E) = 0.527

M06-2X

Molecule	Neutral(M)	Cation(M)	I.P(Theo)/I.P(Expt)	Error(Expt–Theo)
CrCl	–101.20783(6)	–100.83224(5)	10.22/8.50	–1.72
$CrCl_2$	–116.12464(5)	–115.75010(4)	10.19/9.90	–0.29
CrF	–186.09718(6)	–185.76146(5)	9.14/9.30	0.16
CrO	–161.38083(5)	–161.07764(4)	8.25/8.16	–0.09
CrO_2	–236.50468(5)	–236.05836(6)	12.14/10.30	–1.84
CrOH	–162.03302(6)	–161.74384(5)	7.87/7.54	–0.33

Mean Error (M E) = –0.685
Absolute Error (A E) = 0.738

M06-HF

Molecule	Neutral(M)	Cation(M)	I.P(Theo)/I.P(Expt)	Error(Expt–Theo)
CrCl	–101.14248(6)	–100.76304(5)	9.72/8.50	–1.18
$CrCl_2$	–116.06271(5)	–115.61589(6)	12.15/9.90	–2.25
CrF	–186.04902(6)	–185.72680(5)	8.77/9.30	0.53
CrO	–161.32715(5)	–160.99854(6)	8.94/8.16	–0.78
CrO_2	–236.42523(5)	–235.99254(6)	11.77/10.30	–1.47
CrOH	–161.98755(6)	–161.70440(5)	7.71/7.54	–0.17

Mean Error (M E) = –1.128

Absolute Error (A E) = 1.063

M08-SO

Molecule	Neutral(M)	Cation(M)	I.P(Theo)/I.P(Expt)	Error(Expt–Theo)
CrCl	-101.11260(6)	-100.77343(5)	9.23/8.50	-0.73
$CrCl_2$	-116.07634(5)	-115.64768(4)	11.66/9.90	-1.76
CrF	-185.98527(6)	-185.67754(5)	8.37/9.30	0.93
CrO	-161.25885(5)	-160.96230(4)	8.07/8.16	0.09
CrO_2	-236.37573(5)	-235.94612(8)	11.69/10.30	-1.39
CrOH	-161.90945(6)	-161.63013(5)	7.6/7.54	-0.06

Mean Error (M E) = –0.487
Absolute Error (A E) = 0.827

M08-HX

Molecule	Neutral(M)	Cation(M)	I.P(Theo)/I.P(Expt)	Error(Expt–Theo)
CrCl	-101.18510(6)	-100.85293(5)	9.04/8.50	-0.54
$CrCl_2$	-116.17204(5)	-115.73415(4)	11.92/9.90	-2.02
CrF	-186.06204(6)	-185.76687(5)	8.03/9.30	1.27
CrO	-161.31378(5)	-161.04311(4)	7.37/8.16	0.79
CrO_2	-236.45201(5)	-236.033(8)	11.4/10.30	-1.10
CrOH	-161.99146(6)	-161.72585(5)	7.52/7.54	0.02

Mean Error (M E) = –0.263
Absolute Error (A E) = 0.957

Mn-Series

M05

Molecule	Neutral(M)	Cation(M)	I.P(Theo)/I.P(Expt)	Error(Expt–Theo)
$MnCl_2$	–133.84734(6)	–133.44409(5)	10.97/11.03	0.06
MnCl	–118.84234(5)	–118.55901(6)	7.71/8.50	0.79
MnF_2	–303.65422(6)	–303.21135(5)	12.05/11.38	–0.67
MnH	–104.39165(5)	–104.15779(6)	6.36/7.80	1.44
MnO	–179.03790(6)	–178.72627(5)	8.48/8.65	0.17
MnF	–203.72374(7)	–203.46117(6)	7.15/8.51	1.36

Mean Error (M E) = 0.525
Absolute Error (A E) = 0.748

M05-2X

Molecule	Neutral(M)	Cation(M)	I.P(Theo)/I.P(Expt)	Error(Expt–Theo)
$MnCl_2$	–133.82815(6)	–133.40428(5)	11.53/11.03	–0.50
MnCl	–118.80858(5)	–118.51330(6)	8.04/8.50	0.46
MnF_2	–303.65641(6)	–303.17590(5)	13.08/11.38	–1.70
MnH	–104.37663(7)	–104.11759(6)	7.05/7.80	0.75
MnO	–178.99462(6)	–178.62020(5)	10.18/8.65	–1.53
MnF	–203.71100(7)	–203.42537(6)	7.77/8.51	0.74

Mean Error (M E) = –0.297
Absolute Error (A E) = 0.947

M06-L

Molecule	Neutral(M)	Cation(M)	I.P(Theo)/I.P(Expt)	Error(Expt–Theo)
$MnCl_2$	–133.96468(6)	–133.56618(5)	10.84/11.03	0.19
MnCl	–118.79842(5)	–118.45070(8)	9.46/8.50	0.96
MnF_2	–303.72264(6)	–303.31761(5)	11.02/11.38	0.36
MnH	–104.45650(5)	–104.18610(6)	7.36/7.80	0.44
MnO	–179.10353(6)	–178.78553(5)	8.65/8.65	0.00
MnF	–203.77634(5)	–203.49784(6)	7.58/8.51	–0.07

Mean Error (M E) = 0.313
Absolute Error (A E) = 0.337

M06

Molecule	Neutral(M)	Cation(M)	I.P(Theo)/I.P(Expt)	Error(Expt–Theo)
$MnCl_2$	–133.88871(6)	–133.47583(5)	11.24/11.30	–0.21
MnCl	–118.86434(5)	–118.57298(6)	7.93/8.50	0.57
MnF_2	–303.64977(6)	–303.19774(5)	12.30/11.38	–0.92
MnH	–104.40442(7)	–104.15965(6)	6.66/7.80	1.14
MnO	–179.04459(6)	–178.72451(5)	8.71/8.65	–0.06
MnF	–203.72979(7)	–203.45158(6)	7.57/8.51	0.94

Mean Error (M E) = 0.243
Absolute Error (A E) = 0.640

M06-2X

Molecule	Neutral(M)	Cation(M)	I.P(Theo)/I.P(Expt)	Error(Expt–Theo)
$MnCl_2$	–133.84101(6)	–133.41339(5)	11.64/11.03	–0.61
MnCl	–118.83792(5)	–118.53510(6)	8.24/8.50	0.26
MnF_2	–303.64780(6)	–303.16924(5)	13.02/11.38	–1.64
MnH	–104.41349(7)	–104.15099(6)	7.14/7.80	0.66
MnO	–179.01711(6)	–178.71127(5)	8.32/8.65	0.33
MnF	–203.73139(7)	–203.43479(6)	8.07/8.51	0.44

Mean Error (M E) = –0.093
Absolute Error (A E) = 0.657

M06-HF

Molecule	Neutral(M)	Cation(M)	I.P(Theo)/I.P(Expt)	Error(Expt–Theo)
$MnCl_2$	–133.76475(6)	–133.31654(5)	12.20/11.03	–1.17
MnCl	–118.80056(5)	–118.47298(6)	8.90/8.50	–0.40
MnF_2	–303.60698(6)	–303.09217(5)	14.01/11.38	–2.63
MnH	–104.37118(7)	–104.11075(6)	7.09/7.80	0.71
MnO	–178.95652(4)	–178.66967(5)	7.81/8.65	–0.16
MnF	–203.50530(7)	–203.21518(8)	7.89/8.51	–0.62

Mean Error (M E) = –0.712
Absolute Error (A E) = 0.948

M08-SO

Molecule	Neutral(M)	Cation(M)	I.P(Theo)/I.P(Expt)	Error(Expt–Theo)
$MnCl_2$	-133.73428(6)	-133.28663(7)	12.18/11.03	-1.15
MnCl	-118.71340(7)	-118.42489(6)	7.85/8.50	0.65
MnF_2	-303.49917(6)	-303.04255(5)	12.43/11.38	-1.05
MnH	-104.27061(5)	-104.03271(6)	6.47/7.80	1.33
MnO	-178.81785(8)	-178.53766(7)	7.62/8.65	1.03
MnF	-203.59679(7)	-203.30549(6)	7.93/8.51	0.58

Mean Error (M E) = 0.232
Absolute Error (A E) = 0.965

M08-HX

Molecule	Neutral(M)	Cation(M)	I.P(Theo)/I.P(Expt)	Error(Expt–Theo)
$MnCl_2$	-133.82113(6)	-133.39587(5)	11.57/11.03	-0.54
MnCl	-118.78722(7)	-118.49836(6)	7.86/8.50	0.64
MnF_2	-303.59147(6)	-303.13692(5)	12.37/11.38	-0.99
MnH	-104.35302(5)	-104.09524(6)	7.01/7.80	0.79
MnO	-178.89544(8)	-178.6118(7)	7.72/8.65	0.93
MnF	-203.67416(7)	-203.38442(6)	7.88/8.51	0.63

Mean Error (M E) = 0.243
Absolute Error (A E) = 0.753

Fe-Series

M05

Molecule	Neutral(M)	Cation(M)	I.P.(Theo)/I.P.(Expt)	Error(Expt–Theo)
FeF_2	–323.17464(5)	–322.7560(6)	11.39/11.30	–0.09
$Fe(CO)_2$	–349.92686(3)	–349.64031(4)	7.80/6.68	–1.12
Fe(CO)	–236.60356(3)	–236.36637(4)	6.45/6.66	0.21
FeCl	–138.33650(4)	–138.06096(5)	7.50/8.08	0.58
FeO	–198.55624(5)	–198.25594(6)	8.17/8.90	0.73
$FeCl_2$	–153.36239(5)	–152.97253(6)	10.61/10.63	0.02

Mean Error (M E) = 0.055
Absolute Error (A E) = 0.458

M05-2X

Molecule	Neutral(M)	Cation(M)	I.P(Theo)/I.P(Expt)	Error(Expt–Theo)
FeF_2	–323.15660(5)	–322.68585(6)	12.81/11.30	–1.51
$Fe(CO)_2$	–349.88156(3)	–349.648123(4)	6.35/6.68	0.38
Fe(CO)	–236.55729(3)	–236.32935(4)	6.16/6.66	0.50
FeCl	–138.29076(6)	–137.99462(5)	8.06/8.08	0.02
FeO	–198.49805(6)	–198.17188(6)	8.88/8.90	0.02
$FeCl_2$	–153.32240(5)	–152.88989(4)	11.76/10.63	–1.13

Mean Error (M E) = –0.287
Absolute Error (A E) = 0.593

M06-L

Molecule	Neutral(M)	Cation(M)	I.P(Theo)/I.P(Expt)	Error(Expt–Theo)
FeF_2	–323.22768(5)	–322.81445(6)	11.25/11.30	0.05
$Fe(CO)_2$	–350.03896(3)	–349.77287(4)	7.25/6.68	–0.56
Fe(CO)	–236.69488(3)	–236.43441(4)	7.09/6.66	–0.43
FeCl	–138.41747(4)	–138.11276(5)	8.29/8.08	–0.21
FeO	–198.61331(5)	–198.29543(6)	8.65/8.90	0.25
$FeCl_2$	–153.46522(5)	–153.07825(6)	10.53/10.63	0.10

Mean Error (M E) = –0.133
Absolute Error (A E) = –0.267

M06

Molecule	Neutral(M)	Cation(M)	I.P(Theo)/I.P(Expt)	Error(Expt–Theo)
FeF_2	–323.14989(5)	–322.72976(6)	11.43/11.30	–0.13
$Fe(CO)_2$	–349.92134(3)	–349.62914(4)	7.95/6.68	–1.27
Fe(CO)	–236.59464(3)	–236.34582(4)	6.77/6.66	–0.11
FeCl	–138.33712(6)	–138.05367(5)	7.71/8.08	0.37
FeO	–198.54425(5)	–198.23517(6)	8.41/8.90	0.49
$FeCl_2$	–153.38501(5)	–152.99294(6)	10.67/10.63	–0.04

Mean Error (M E) = –0.115
Absolute Error (A E) = 0.402

M06-2X

Molecule	Neutral(M)	Cation(M)	I.P(Theo)/I.P(Expt)	Error(Expt–Theo)
FeF_2	–323.14347(5)	–322.68328(6)	12.52/11.30	–1.22
$Fe(CO)_2$	–349.86512(3)	–349.63597(4)	6.24/6.68	0.44
Fe(CO)	–236.56190(3)	–236.331979(4)	6.26/6.66	0.40
FeCl	–138.31843(6)	–138.01244(5)	8.33/ 8.08	0.25
FeO	–198.51263(5)	–198.19274(6)	8.71/8.90	0.19
$FeCl_2$	–153.33025(5)	–152.89777(6)	11.77/10.63	–1.14

Mean Error (M E) = –0.18
Absolute Error (A E) = 0.607

M06-HF

Molecule	Neutral(M)	Cation(M)	I.P(Theo)/I.P(Expt)	Error(Expt–Theo)
FeF_2	–323.10426(5)	–322.59831(6)	13.77/11.30	–2.47
$Fe(CO)_2$	–349.81303(5)	–349.59754(4)	5.86/6.68	082
Fe(CO)	–236.50153(7)	–236.31722(4)	5.02/6.66	1.64
FeCl	–138.26482(6)	–137.95164(5)	8.52/8.08	–0.44
FeO	–198.43447(5)	–198.13905(6)	8.04/8.90	0.86
$FeCl_2$	–153.25359(5)	–152.76533(6)	13.29/10.63	–2.66

Mean Error (M E) = –0.375
Absolute Error (A E) = 1.482

M08-SO

Molecule	Neutral(M)	Cation(M)	I.P(Theo)/I.P(Expt)	Error(Expt–Theo)
FeF_2	-322.98566(5)	-322.32397(8)	18.01/11.30	-6.71
$Fe(CO)_2$	-349.60638(1)	-349.37589(2)	6.27/6.68	0.41
Fe(CO)	-236.34235(1)	-236.18822(4)	4.19/6.66	2.47
FeCl	-138.21711(4)	-137.89732(5)	8.70/8.08	-0.62
FeO	-198.35345(3)	-197.95282(2)	10.90/8.90	-2.00
$FeCl_2$	-153.21581(5)	-152.69099(2)	14.28/10.63	-3.65

Mean Error (M E) = 1.683
Absolute Error (A E) = 2.643

M08-HX

Molecule	Neutral(M)	Cation(M)	I.P(Theo)/I.P(Expt)	Error(Expt–Theo)
FeF_2	-323.06130(5)	-322.39615(8)	18.10/11.30	-6.80
$Fe(CO)_2$	-349.67467(1)	-349.49725(2)	4.83/6.68	1.85
Fe(CO)	-236.41939(3)	-236.26486(4)	4.21/6.66	2.45
FeCl	-138.24618(6)	-137.95115(5)	8.03/8.08	0.05
FeO	-198.39894(3)	-197.98698(2)	11.21/8.90	-2.31
$FeCl_2$	-153.27947(5)	-152.86001(6)	11.41/10.63	-0.78

Mean Error (M E) = –0.923
Absolute Error (A E) = 2.373

Co-Complexes

M05

Molecule	Neutral(M)	Cation(M)	I.P(Theo)/I.P(Expt)	Error(Expt–Theo)
CoH	–145.60625(3)	–145.29226(2)	8.54/7.86	–0.68
CoO	–220.22177(4)	–219.89630(5)	8.86/8.90	0.04
CoCl	–160.00731(3)	–159.70661(4)	8.18/8.71	0.53
$CoCl_2$	–175.01184(4)	–174.60302(5)	11.12/10.75	–0.37

Mean Error (M E) = –0.120
Absolute Error (A E) = 0.405

M05-2X

Molecule	Neutral(M)	Cation(M)	I.P(Theo)/I.P(Expt)	Error(Expt–Theo)
CoH	–145.53921(3)	–145.22497(4)	8.55/7.86	–0.69
CoO	–220.12058(4)	–219.80796(5)	8.51/8.90	0.39
CoCl	–159.95430(3)	–159.59780(4)	9.71/8.71	–1.00
$CoCl_2$	–174.92784(4)	–174.50328(5)	11.55/10.75	–0.80

Mean Error (M E) = –0.525

Absolute Error (A E) = 0.720

M06-L

Molecule	Neutral(M)	Cation(M)	I.P(Theo)/I.P(Expt)	Error(Expt–Theo)
CoH	–145.61831(3)	–145.29588(2)	8.77/7.86	–0.91
CoO	–220.22529(4)	–219.92950(5)	8.05/8.90	0.85
CoCl	–160.05764(3)	–159.73119(4)	8.88/8.71	–0.17
$CoCl_2$	–175.08236(4)	–174.70091(5)	10.38/10.75	0.37

Mean Error (M E) = 0.035
Absolute Error (A E) = 0.575

M06

Molecule	Neutral(M)	Cation(M)	I.P(Theo)/I.P(Expt)	Error(Expt–Theo)
CoH	–145.58906(3)	–145.27053(4)	8.67/7.86	–0.81
CoO	–220.18524(4)	–219.85295(5)	9.04/8.90	–0.14
CoCl	–159.99046(3)	–159.67737(4)	8.52/8.71	0.19
$CoCl_2$	–175.01157(4)	–174.60055(5)	11.18/10.75	–0.43

Mean Error (M E) = –0.298
Absolute Error (A E) = 0.393

M06-2X

Molecule	Neutral(M)	Cation(M)	I.P(Theo)/I.P(Expt)	Error(Expt–Theo)
CoH	–145.57214(3)	–145.25930(4)	8.51/7.86	–0.65
CoO	–220.14113(4)	–219.82586(5)	8.58/8.90	0.32
CoCl	–159.97596(3)	–159.62490(4)	9.55/8.71	–0.84
$CoCl_2$	–174.94551(4)	–174.51315(5)	11.77/10.75	–1.02

Mean Error (M E) = –0.548
Absolute Error (A E) = 0.708

M06-HF

Molecule	Neutral(M)	Cation(M)	I.P(Theo)/I.P(Expt)	Error(Expt–Theo)
CoH	–145.53179(2)	–145.23423(4)	8.10/7.86	–0.24
CoO	–220.06575(4)	–219.78416(5)	7.66/8.90	1.24
CoCl	–159.92249(3)	–159.56212(4)	9.81/8.71	–1.10
$CoCl_2$	–174.86898(4)	–174.38120(5)	13.27/10.75	–2.52

Mean Error (M E) = 0.655
Absolute Error (A E) = 1.275

M08-SO

Molecule	Neutral(M)	Cation(M)	I.P(Theo)/I.P(Expt)	Error(Expt–Theo)
CoH	-145.45154(3)	-145.15417(4)	8.09/7.86	-0.23
CoO	-220.01236(4)	-219.63150(3)	10.36/8.90	-1.46
CoCl	-159.85585(3)	-159.53574(4)	8.71/8.71	0.00
$CoCl_2$	-174.85906(4)	-174.40189(3)	12.44/10.75	-1.69

Mean Error (M E) = –0.845
Absolute Error (A E) = 0.845

M08-HX

Molecule	Neutral(M)	Cation(M)	I.P(Theo)/I.P(Expt)	Error(Expt–Theo)
CoH	-145.45880(3)	-145.16520(4)	7.99/7.86	-0.13
CoO	-220.01655(4)	219.63180(3)	10.47/8.90	-1.57
CoCl	-159.88413(3)	-159.54137(4)	9.33/8.71	-0.62
$CoCl_2$	-174.87904(4)	-174.44221(3)	11.89/10.75	-1.14

Mean Error (M E) = –0.865
Absolute Error (A E) = 0.865

Ni-Series

M05

Molecule	Neutral(M)	Cation(M)	I.P(Theo)/I.P(Expt)	Error(Expt–Theo)
NiO	–244.47808(3)	–244.16127(4)	8.62/9.50	0.88
NiH	–169.8941792)	–169.56710(3)	8.90/8.50	–0.40
NiF_2	–369.03858(3)	–368.61511(4)	11.52/11.50	–0.02
NiCl	–184.29184(2)	–183.85512(3)	11.02/9.28	–1.74
$NiCl_2$	–199.24630(3)	–198.82214(4)	11.54/11.24	–0.30
NiCO	–282.59610(1)	–282.29501(2)	8.19/7.30	0.89

Mean Error (M E) = –0.115
Absolute Error (A E) = 0.705

M05-2X

Molecule	Neutral(M)	Cation(M)	I.P(Theo)/I.P(Expt)	Error(Expt–Theo)
NiO	–244.36405(3)	–244.01205(4)	9.58/9.50	–0.08
NiH	–169.79136(2)	–169.46740(3)	8.82/8.50	–0.32
NiF_2	–368.99062(3)	–368.47946(4)	13.91/11.50	–2.41
NiCl	–184.20161(2)	–183.75973(3)	12.02/9.28	–2.74
$NiCl_2$	–199.16772(3)	–198.73267(4)	11.84/11.24	–0.60
NiCO	–282.48160(1)	–282.22624(2)	6.94/7.30	0.36

Mean Error (M E) = –0.965
Absolute Error (A E) = 1.085

M06-L

Molecule	Neutral(M)	Cation(M)	I.P(Theo)/I.P(Expt)	Error(Expt–Theo)
NiO	–244.46808(3)	–244.13818(4)	8.98/9.50	0.52
NiH	–169.84639(2)	–169.53818(3)	8.39/8.50	0.11
NiF_2	–369.04480	–368.61324(4)	11.74/11.50	–0.24
NiCl	–184.28120(2)	–183.94821(3)	9.06/9.28	0.22
$NiCl_2$	–199.29999(3)	–198.88208(4)	11.37/11.24	–0.13
NiCO	–282.60548	–282.30513(2)	8.17/7.30	–0.87

Mean Error (M E) = –0.065
Absolute Error (A E) = 0.552

M06

Molecule	Neutral(M)	Cation(M)	I.P(Theo)/I.P(Expt)	Error(Expt–Theo)
NiO	–244.42051(3)	–244.08761(4)	9.06/9.50	0.44
NiH	–169.84758(2)	–169.51249(3)	9.12/8.50	–0.62
NiF_2	–368.97402(3)	–368.53409(4)	11.97/11.50	–0.47
NiCl	–184.25567(2)	–183.83903(1)	11.33/9.28	–2.05
$NiCl_2$	–199.22962(3)	–198.79485(4)	11.83/11.24	–0.59
NiCO	–282.54369(1)	–282.23473(2)	8.41/7.30	–1.11

Mean Error (M E) = –0.733
Absolute Error (A E) = 0.88

M06-2X

Molecule	Neutral(M)	Cation(M)	I.P(Theo)/I.P(Expt)	Error(Expt–Theo)
NiO	–244.38381(3)	–244.06510(4)	8.67/9.50	0.83
NiH	–169.83374(2)	–169.50897(3)	8.84/8.50	–0.34
NiF_2	–368.97930(3)	–368.47952(4)	13.60/11.50	–2.10
NiCl	–184.23247(2)	–183.78927(3)	12.06/9.28	–2.78
$NiCl_2$	–199.17932(3)	–198.73846(4)	12.00/11.24	–0.76
NiCO	–282.50018(1)	–282.24600(2)	6.92/7.30	0.38

Mean Error (M E) = –0.795
Absolute Error (A E) = 1.198

M06-HF

Molecule	Neutral(M)	Cation(M)	I.P(Theo)/I.P(Expt)	Error(Expt–Theo)
NiO	–244.30688(3)	–243.92367(4)	10.43/9.50	–0.93
NiH	–169.78455(2)	–169.45866(3)	8.87/8.50	–0.37
NiF_2	–368.94976(3)	–368.39010(4)	15.23/11.50	–3.73
NiCl	–184.17336(2)	–183.74873(3)	11.56/9.28	–2.28
$NiCl_2$	–199.04228(3)	–198.64213(4)	10.89/11.24	0.35
NiCO	–282.46233(3)	–282.20172(2)	7.09/7.30	0.21

Mean Error (M E) = – 1.125
Absolute Error (A E) = 1.312

M08-SO

Molecule	Neutral(M)	Cation(M)	I.P(Theo)/I.P(Expt)	Error(Expt–Theo)
NiO	-244.24743(3)	-243.92533(4)	8.76/9.50	0.74
NiH	-169.71266(2)	-169.38010(3)	9.05/8.50	-0.55
NiF_2	-368.83140(3)	-368.30351(2)	14.36/11.50	-2.86
NiCl	-184.11626(2)	-183.72908(3)	10.54/9.28	-1.26
$NiCl_2$	-199.04865(3)	-198.61061(4)	11.92/11.24	-0.68

Mean Error (M E) = –0.922
Absolute Error (A E) = 1.218

M08-HX

Molecule	Neutral(M)	Cation(M)	I.P(Theo)/I.P(Expt)	Error(Expt–Theo)
NiO	-244.25453(3)	-243.93265(4)	8.76/9.50	0.74
NiH	-169.69905(2)	-169.38188(3)	8.63/8.50	-0.13
NiF_2	-368.86150(3)	-368.30389(2)	15.17/11.50	-3.67
NiCl	-184.11985(2)	-183.75262(3)	9.99/9.28	-0.71
$NiCl_2$	-199.08872(3)	-198.61061(4)	13.01/11.24	-1.77

Mean Error (M E) = –1.108
Absolute Error (A E) = 1.404

Cu-Complexes

M05

Molecule	Neutral(M)	Cation(M)	I.P(Theo)/I.P(Expt)	Error(Expt–Theo)
Cu2	–392.52365(1)	–392.24986(2)	7.45/7.90	0.45
CuCl	–211.20999(1)	–210.84353(2)	9.97/10.70	0.73
CuF	–296.08868(1)	–295.70459(2)	10.45/10.90	0.45
CuF_2	–395.89882(2)	–395.42547(3)	12.88/13.18	0.30

Mean Error (M E) = 0.483
Absolute Error (A E) = 0.483

M05-2X

Molecule	Neutral(M)	Cation(M)	I.P(Theo)/I.P(Expt)	Error(Expt–Theo)
Cu2	–392.26378(1)	–391.98220(2)	7.66/7.90	0.24
CuCl	–211.08707(1)	–210.71418(2)	10.15/10.70	0.55
CuF	–295.97569(1)	–295.57584(2)	10.88/10.90	0.02
CuF_2	–395.80827(2)	–395.28317(3)	14.29/13.18	–1.11

Mean Error (M E) = -0.075
Absolute Error (A E) = 0.48

M06-L

Molecule	Neutral(M)	Cation(M)	I.P(Theo)/I.P(Expt)	Error(Expt–Theo)
Cu2	–392.32527(1)	–392.04287(2)	7.69/7.90	0.21
CuCl	–211.14849(1)	–210.78163(2)	9.98/10.70	0.72
CuF	–296.00731(1)	–295.62593(2)	10.38/10.90	0.52
CuF_2	–395.85876(2)	–395.40228(3)	12.42/13.18	0.76

Mean Error (M E) = 0.553
Absolute Error (A E) = 0.553

M06

Molecule	Neutral(M)	Cation(M)	I.P(Theo)/I.P(Expt)	Error(Expt–Theo)
Cu2	–392.37541(1)	–392.08044(2)	8.03/7.90	–0.13
CuCl	–211.14535(1)	–210.76129(2)	10.45/10.70	0.25
CuF	–296.00093(1)	–295.60046(2)	10.90/10.90	0.00
CuF_2	–395.80561(2)	–395.31909(3)	13.24/13.18	–0.06

Mean Error (M E) = -0.015
Absolute Error (A E) = 0.11

M06-2X

Molecule	Neutral(M)	Cation(M)	I.P(Theo)/I.P(Expt)	Error(Expt–Theo)
Cu2	–392.36500(1)	–392.08944(2)	7.50/7.90	0.40
CuCl	–211.12544(1)	–210.74606(2)	10.32/10.70	0.38
CuF	–296.00387(1)	–295.60496(2)	10.86/10.90	0.04
CuF_2	–395.80971(2)	–395.28820(3)	14.19/13.18	–1.01

Mean Error (M E) = -0.048
Absolute Error (A E) = 0.458

M06-HF

Molecule	Neutral(M)	Cation(M)	I.P(Theo)/I.P(Expt)	Error(Expt–Theo)
Cu2	–392.22573(1)	–391.98291(2)	6.61/7.90	1.29
CuCl	– 211.04551(1)	–210.66928(2)	10.24/10.70	0.46
CuF	–295.94129(1)	–295.52292(2)	11.38/10.90	–0.48
CuF_2	–395.76656(2)	–395.17660(3)	16.05/13.18	–2.87

Mean Error (M E) = -0.4
Absolute Error (A E) = 1.275

M08-SO

Molecule	Neutral(M)	Cation(M)	I.P(Theo)/I.P(Expt)	Error(Expt–Theo)
Cu2	-392.09953(1)	-391.82578(2)	7.45/7.90	0.45
CuCl	-211.00595(1)	-210.62906(2)	10.26/10.70	0.44
CuF	-295.86248(1)	-295.46030(2)	10.94/10.90	-0.04
CuF_2	-395.65778(2)	-395.20424(1)	12.34/13.18	0.84

Mean Error (M E) = 0.423
Absolute Error (A E) = 0.443

M08-HX

Molecule	Neutral(M)	Cation(M)	I.P(Theo)/I.P(Expt)	Error(Expt–Theo)
Cu2	-391.99845(1)	-391.72784(2)	7.36/7.90	0.54
CuCl	-210.97084(1)	-210.13573(2)	22.72/10.70	-12.02
CuF	-295.83194(1)	-295.44143(2)	10.63/10.90	0.27
CuF_2	-395.66947(2)	-395.18926(1)	13.07/13.18	0.11

Mean Error (M E) = –2.775
Absolute Error (A E) = 3.235

Zn-Complexes

M05

Molecule	Neutral(M)	Cation(M)	I.P(Theo)/I.P(Expt)	Error(Expt–Theo)
Zn_2	–131.48769(1)	–131.21171(2)	7.51/9.00	1.49
$ZnCH_3$	–105.51983(2)	–105.27486(1)	6.67/7.20	0.53
$ZnCl_2$	–95.66124(1)	–95.24782(2)	11.25/11.80	0.55
ZnF_2	–265.45820(1)	–264.98826(2)	12.79/13.91	1.12
ZnH	–66.25818(2)	–65.99196(1)	7.24/9.40	2.16
ZnO	–140.81694(1)	–140.51711(2)	8.16/9.34	1.18

Mean Error (M E) = 1.172
Absolute Error (A E) = 1.172

M05-2X

Molecule	Neutral(M)	Cation(M)	I.P(Theo)/I.P(Expt)	Error(Expt–Theo)
Zn_2	–130.68995(1)	–130.40313(2)	7.81/9.00	1.19
$ZnCH_3$	–105.14762(2)	–104.88942(1)	7.03/7.20	0.17
$ZnCl_2$	–95.27331(1)	–94.84012(2)	11.79/11.80	0.01
ZnF_2	–265.09180(1)	–264.58855(2)	13.69/13.91	0.22
ZnH	–65.85998(2)	–65.57990(1)	7.62/9.40	1.78
ZnO	–140.44756(1)	–140.12187(2)	8.86/9.34	0.48

Mean Error (M E) = 0.642
Absolute Error (A E) = 0.642

M06-L

Molecule	Neutral(M)	Cation(M)	I.P(Theo)/I.P(Expt)	Error(Expt–Theo)
Zn_2	–130.20734(1)	–129.93107(2)	7.52/9.00	1.48
$ZnCH_3$	–104.91490(2)	–104.66198(1)	6.88/7.20	0.32
$ZnCl_2$	–95.10063(1)	–94.69195(2)	11.12/11.80	0.68
ZnF_2	–265.32264(1)	–264.79053(2)	14.48/13.91	–0.57
ZnH	–65.62252(2)	–65.35193(1)	7.63/9.40	1.77
ZnO	–140.21614(1)	–139.90115(2)	8.57/9.34	0.77

Mean Error (M E) = 0.742
Absolute Error (A E) = 0.932

M06

Molecule	Neutral(M)	Cation(M)	I.P(Theo)/I.P(Expt)	Error(Expt–Theo)
Zn_2	–130.92934(1)	–130.63692(2)	7.96/9.00	1.24
$ZnCH_3$	–105.24085(2)	–104.98174(1)	7.05/7.20	0.15
$ZnCl_2$	–95.40075(1)	–94.97627(2)	11.55/11.80	0.25
ZnF_2	–265.14999(1)	–264.67371(2)	12.96/13.91	0.95
ZnH	–65.97630(2)	–65.69488(1)	7.66/9.40	1.74
ZnO	–140.53731(1)	–140.21115(2)	8.88/9.34	0.46

Mean Error (M E) = 0.798
Absolute Error (A E) = 0.798

M06-2X

Molecule	Neutral(M)	Cation(M)	I.P(Theo)/I.P(Expt)	Error(Expt–Theo)
Zn_2	–130.86416(1)	–130.59157(2)	7.42/9.00	1.58
$ZnCH_3$	–105.22848(2)	–104.96699(1)	7.12/7.20	0.08
$ZnCl_2$	–95.33812(1)	–94.90339(2)	11.83/11.80	–0.03
ZnF_2	–265.13526(1)	–264.64046(2)	13.46/13.91	0.45
ZnH	–65.95377(2)	–65.66963(1)	7.73/9.40	1.67
ZnO	–140.52693(1)	–140.19692(2)	8.98/9.34	0.36

Mean Error (M E) = 0.685
Absolute Error (A E) = 0.695

M06-HF

Molecule	Neutral(M)	Cation(M)	I.P(Theo)/I.P(Expt)	Error(Expt–Theo)
Zn_2	–131.20259(1)	–130.95452(2)	6.75/9.00	2.25
$ZnCH_3$	–105.41959(2)	–105.15215(1)	7.28/7.20	–0.08
$ZnCl_2$	–95.48692(1)	–95.03112(2)	12.40/11.80	–0.60
ZnF_2	–265.32264(1)	–264.79053(2)	14.48/13.91	–0.57
ZnH	–66.14115(2)	–65.85066(1)	7.91/9.40	1.49
ZnO	–140.71806(1)	–140.38462(2)	9.07/9.34	0.27

Mean Error (M E) = 0.46
Absolute Error (A E) = 0.877

M08-SO

Molecule	Neutral(M)	Cation(M)	I.P(Theo)/I.P(Expt)	Error(Expt–Theo)
Zn_2	-130.90932(1)	-130.63109(2)	7.57/9.00	1.43
$ZnCH_3$	-105.24509(2)	-104.98641(1)	7.04/7.20	0.16
$ZnCl_2$	-95.38503(1)	-94.91956(2)	12.67/11.80	-0.87
ZnF_2	-265.14278(1)	-264.57646(2)	15.41/13.91	-1.50
ZnH	-65.97973(2)	-65.70251(1)	7.54/9.40	1.86
ZnO	-140.52146(3)	-140.19968(2)	8.76/9.34	0.58

Mean Error (M E) = 0.277
Absolute Error (A E) = 1.067

M08-HX

Molecule	Neutral(M)	Cation(M)	I.P(Theo)/I.P(Expt)	Error(Expt–Theo)
Zn_2	-130.01575(1)	-129.74383(2)	7.40/9.00	1.60
$ZnCH_3$	-104.82281(2)	-104.56793(1)	6.94/7.20	0.26
$ZnCl_2$	-94.96992(1)	-54.50502(2)	12.65/11.80	-0.85
ZnF_2	-264.73854(1)	-264.18503(2)	15.06/13.91	-1.15
ZnH	-65.53737(2)	-65.26244(1)	7.48/9.40	1.92
ZnO	-140.09833(3)	-139.78189(2)	8.61/9.34	0.73

Mean Error (M E) = 0.418
Absolute Error (A E) = 1.085

Acknowledgements

During my research work, I have been supported and persuaded by many peoples. Today I am very much pleased to express my gratitude to all of them.

First and foremost I want to express my deepest gratitude to my honorable advisor, Dr. Anirban Misra for his constant advice, guidance, inspiration, insight and sharing his extensive knowledge throughout the work. I feel lucky being associated with his research group and begin research work under his prudent and affable supervision. His enthusiasm and constant encouragement have been of the utmost importance for the progress of this work.

I take this opportunity to show deep reverence to all my teachers, Department of chemistry, North Bengal University for their help in different ways.

I am especially thankful to my lab mates (Rakesh da and Debojit da Satadal, Manoj, Tamal and Suranjan) for their kind cooperation and friendly demeanor.

I express my sincere gratitude to my family for all their unconditional love and encouragement. My father has raised me with a love of science and supported me in all my pursuits. Most of all, for my loving, supportive, encouraging, and patient husband whose faithful support during my Ph.D. work is also appreciated.

I would also like to give my thanks to my colleagues at Nand Prasad High School for their help and encouragement in pursuing my research work.

Sonali Sarkar
Sonali Sarkar